

## Durham E-Theses

---

### *The interpretation of magnetic anomalies North of the dartmoor granite*

Green, Frances W.

#### How to cite:

---

Green, Frances W. (1979) *The interpretation of magnetic anomalies North of the dartmoor granite*, Durham theses, Durham University. Available at Durham E-Theses Online:  
<http://etheses.dur.ac.uk/9149/>

#### Use policy

---

The full-text may be used and/or reproduced, and given to third parties in any format or medium, without prior permission or charge, for personal research or study, educational, or not-for-profit purposes provided that:

- a full bibliographic reference is made to the original source
- a [link](#) is made to the metadata record in Durham E-Theses
- the full-text is not changed in any way

The full-text must not be sold in any format or medium without the formal permission of the copyright holders.

Please consult the [full Durham E-Theses policy](#) for further details.

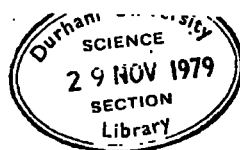
"THE INTERPRETATION OF MAGNETIC ANOMALIES  
NORTH OF THE DARTMOOR GRANITE"

This thesis is submitted for the  
degree of Master of Science

1979

Frances W. Green, B.Sc.  
Graduate Society  
University of Durham

The copyright of this thesis rests with the author.  
No quotation from it should be published without  
his prior written consent and information derived  
from it should be acknowledged.



## ABSTRACT

The large negative magnetic Okchampton Anomaly, northwest of the Dartmoor granite, and rock samples from the same locality, were studied to determine the cause of the magnetic disturbances in this area. Mineralogical examination revealed that the ferromagnetic mineral pyrrhotite ( $Fe_7S_8$ ) has been developed in rocks within, and probably beyond, the metamorphic aureole. Magnetic measurements of the rock samples suggested that the Carboniferous sediments, notably shales, have a mean Q value of 3.57, and that the direction of magnetisation is near horizontal and reversed.

Models made to define the profiles across the Okchampton Anomaly suggested that the causal body was composite, dipped north at  $30^\circ$  and had an undulating surface. This could be interpreted as faulted and folded Lower Carboniferous rocks which disappear north from the exposed Meldon inlier under overlying Upper Carboniferous sediments. The  $30^\circ$  dip of the slabs of magnetised rock is the same as the dip of the edge of the Permian-Carboniferous granite from which mineralising fluids emanated to deposit pyrrhotite in the Lower Carboniferous sediments. The directions of magnetisation used in the models correspond to typical early Permian directions suggesting that the magnetic properties of the rock could be attributed to pyrrhotite emplaced at the time of the granite intrusion.

Comparison with other magnetic anomalies found around the northern edge of the Dartmoor granite, where it abuts against Carboniferous sediments, showed that this explanation is tenable elsewhere. It was also noted that where pyroclastics are interbedded with the Carboniferous sediments the anomaly was the most pronounced. This was attributed to the abundant supply of sulphur and iron in the volcanics which could be a source for pyrrhotite development.

LIST OF CONTENTS

	<u>Page</u>
Abstract	i
List of Contents	ii
List of Figures	v
List of Tables	vi
Acknowledgements	vii
Chapter 1: INTRODUCTION AND PREVIOUS WORK	1
1.1 Introduction	1
1.2 The General Geology of the Field Area	3
(i) Igneous Rocks	10
1.3 Metamorphism, mineral- isation and magnetisation of the Culm Measures at Meldon	12
1.4 Structure	17
1.5 Previous geophysical investigation	23
Chapter 2: DATA ACQUISITION AND REDUCTION	32
2.1 Introduction	32
2.2 Data Acquisition	32
2.3 Data Reduction	34

	Page
Chapter 3: THE MAGNETIC PROPERTIES OF THE ROCK SAMPLES	39
3.1 Introduction	39
3.2 Spinner Magnetometer	41
3.3 Susceptibility Bridge	45
3.4 Initial Data Assimilation	45
3.5 The Results	46
3.6 Petrographic Description of the rock samples	55
(i) Rocks from sites outside the meta- morphic aureole	56
(ii) Rocks from Meldon Quarry	57
3.7 Discussion of the results of the magnetic measure- ments and the mineral- ogical investigation	59
Chapter 4: INTERPRETATION	67
4.1 Introduction	67
4.2 Depth Estimates	67
4.3 The Aeromagnetic Map and Geology	68
4.4 The Profiles and Geology	70
(i) The Okehampton Anomaly	70
(ii) The local magnetic disturbances	79
4.5 Discussion of the Observations	81
(i) Local magnetic dis- turbances	81
(ii) Okehampton Anomaly	82

	Page
4.6 Graphical Interpretation	82
4.7 Computer Modelling	87
(i) Introduction	87
(ii) Mathematical Limitations	88
(iii) Geological Limitations	89
(iv) The models	92
(v) The directions of magnetisation	99
4.8 Assessment of the models	100
4.9 Conclusions	108
Chapter 5: DISCUSSION OF THE RESULTS	111
5.1 Introduction	111
5.2 The models	111
5.3 Comparison with anomalies elsewhere in Cornubia	115
5.4 Conclusions	120
References	I
Appendix A: Derivations	V
Appendix B: Listings of Computer Programs	XI
Appendix C: Data describing the ground and aerial profiles	XVI

LIST OF FIGURES

	Page
1.1 Geological Map of Devon, and overlay showing the Aeromagnetic Map	2
1.2 Geological Map of N-W Dartmoor	5
1.3 Geological Cross-Sections through the Meldon Inlier	18
1.4 Possible structures in the Okehampton area	19
2.1 The corrected and uncorrected ground profile along Line 3	36
3.1 Map of Meldon Quarry	40
3.2 Spinner Magnetometer	43
3.3 Susceptibility Bridge	44
3.4) Stereographic Projections showing the directions of magnetisation of rock samples	53,54
3.5)	
4.1 Geological Map of N-W Dartmoor showing ground profiles, and overlay showing the Aeromagnetic map	69
4.2 ) Magnetic Profiles and cross-sections of near surface geology	71-77
4.7)	
4.8 ) Observed and calculated Profiles and the models	4.8:90 4.9-4.14:93-98
4.14)	
5.1 Magnetic Profile and geological cross-section along a line down the north-west side of the Dartmoor granite	117

LIST OF TABLES

	Page
1.1 Lithostratigraphic sequence of rocks in the Meldon Area	6
1.2 Measurements of magnetic susceptibility of rock samples taken from the Okehampton area	27
3.1 Results of measurements made on samples collected in October 1977 from Meldon Quarry	47
3.2 Results of measurements made on samples collected in April 1978 from Meldon Quarry	48
3.3 Table of remanent and resultant magnetic directions for samples taken in April 1978	49



### ACKNOWLEDGEMENTS

Acknowledgements often appear as a list of indigestible names and I fear that this passage will be the same as so many people have given me help and encouragement.

In particular I want to thank my supervisor, Professor K. H. P. Bott, who offered me much constructive criticism, especially in the final stages of this work. The other members of the Geology Department at Durham University to whom I should like to extend my thanks are Mr. Roy Phillips, Dr. G. K. Westbrook, and Dr. G. A. L. Johnson, together with fellow students Tom Armstrong, Karl Gunnarsson and Alan Nunns. Dr. Brian Lander in the Computing Department kindly helped me digitise the data from Hartland Magnetic Observatory which was provided for me by Mr. Allen. Other data took the form of rock samples mostly collected from Meldon and Aggetts Quarries, Okehampton, Devon, with the generous permission of the managers. The magnetic properties of these samples were measured at the School of Physics, Newcastle University, with the assistance of Dr. Don Tarling with whom I also discussed various of my ideas.

I feel indebted to Drs. Scrivenor and Beer at the Institute of Geological Sciences in Exeter who gave up a great deal of their time to explain the vagaries of the mineralisation in the north-west Dartmoor area, and to Dr. Dave Sanderson at Queen's University, Belfast, who made the geologic structure of this region more comprehensible.

Like all research this project required financial backing and I should like to thank Conoco and my parents for providing this support.

CHAPTER 1

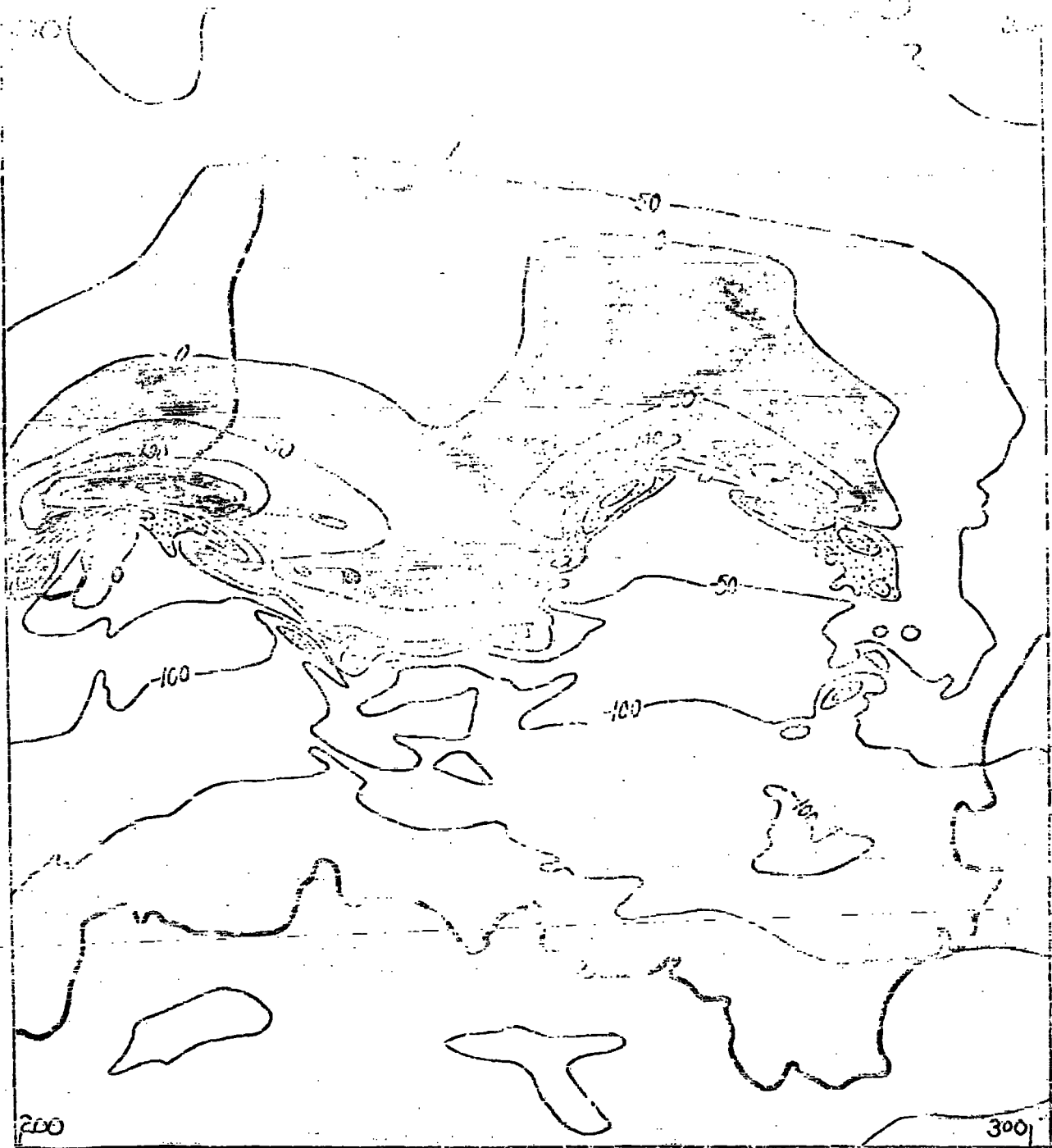
INTRODUCTION AND PREVIOUS WORK

1.1 Introduction

The area of study is a locality in the south-west of England where there is an extensive magnetic anomaly lying just to the north of the Dartmoor and Bodmin Moor granites. This anomaly occurs over the southern half of the mid Devon syncline where carboniferous rocks are exposed (see Fig. 1.1). The anomaly is elongate with its long axis running approximately west-east. Its southern margin, like the southern limit of the carboniferous rocks, is deflected northwards by the two granite masses: Bodmin Moor granite to the west and the larger Dartmoor granite to the east. As the overlay to Fig. 1.1 shows, large local positive anomalies are found along this southern boundary and even larger negative anomalies flank them to the south. One of these pairs of anomalies is studied here. It is that found north-west of the Dartmoor granite, and centred 2 km. south-west of Okehampton (see Fig. 1.1).

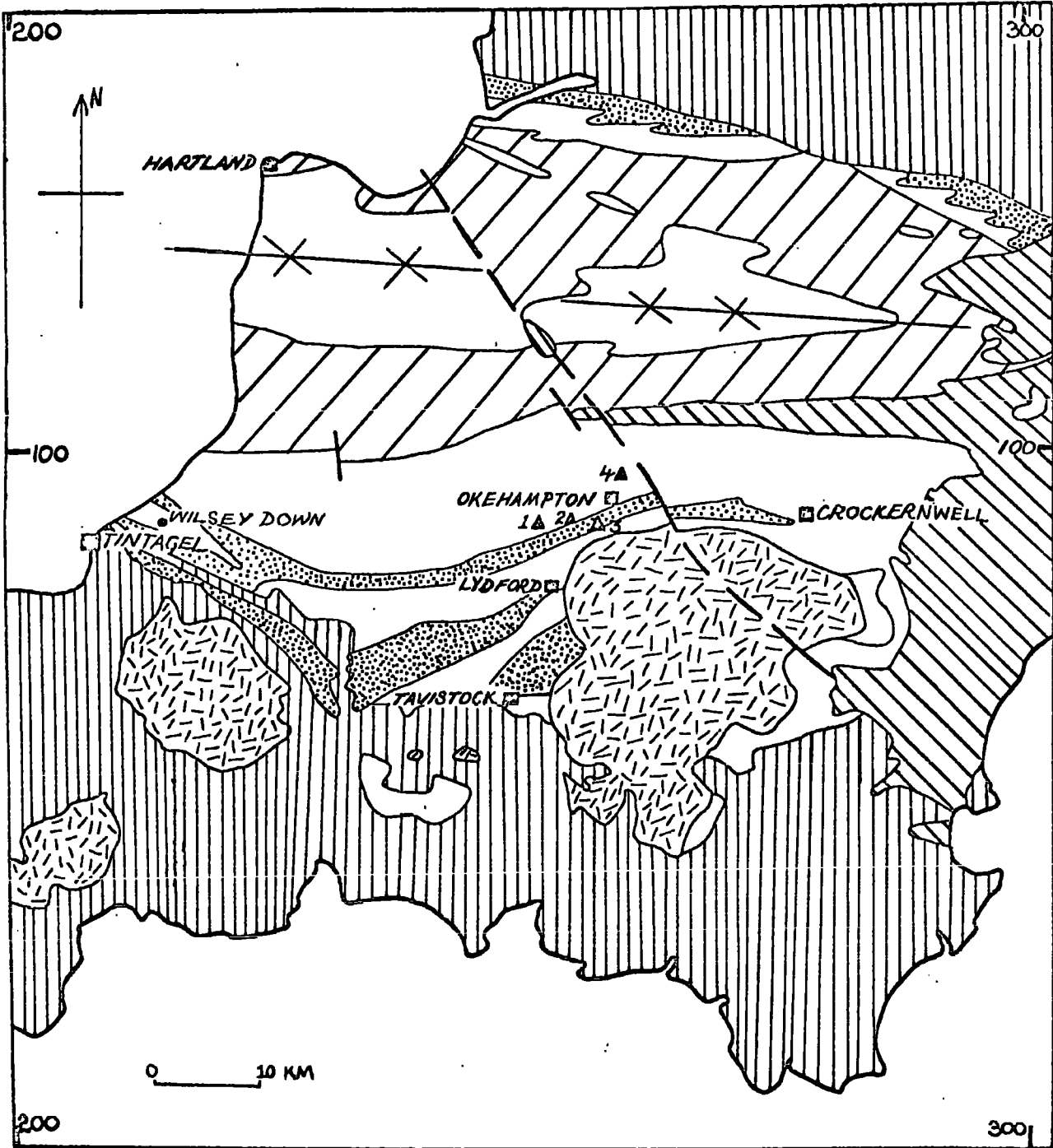
The Okehampton anomaly, as it is called, was first located by Bott, Day and Masson-Smith (1958) and it was







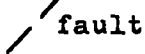







PART OF THE ORDNANCE SURVEY AEROMAGNETIC MAP (1:525,000) FOR GREAT BRITAIN - MID DEVON AND EAST CORNWALL - PRODUCED FOR THE I.G.S.

Contours at 50 $\gamma$  intervals  
Stippled enclosures are negative anomalies  
Shaded area is a positive anomaly



-  Permian and later deposits
-  Bude Formation (Westphalian)
-  Crackington Formation (Namurian)
-  Lower Carboniferous
-  Devonian
-  granite
-  fault
-  axis of syncline
-  Sample Site
- \*1 Bridestowe, near A30
- \*2 Near Meldon Village
- 3 Meldon Quarry
- \*4 Aggetts Quarry
-  town
- \*outside metamorphic aureole

**Fig.1.1.** THE GEOLOGY OF MID DEVON AND EAST CORNWALL - showing towns and collection sites (after Edmonds et al, 1975)

fully defined during the period 1958-59 when the 1:625,000 aeromagnetic map of south-west England was being made for the Geological Survey. As the overlay to Fig. 1.1 shows it is a negative anomaly roughly 6 km. by 1.5 km. in size, and peaking at about 2.5 km. from the granite contact. The positive peak, which flanks it approximately 2 km. to the north, is smaller in amplitude. The axes of both anomalies run approximately parallel to the granite contact, and, in this aerial survey, the peak to peak amplitude of these two related anomalies was measured as 550 $\gamma$ . As Fig. 1.1 shows the negative Okehampton Anomaly occurs partly over the Lower Carboniferous inlier found in that locality.

This thesis describes the work done to determine a possible explanation of this major anomaly and the minor disturbances to its south-west in terms of the geology and mineralogy of the area. Four traverses were made using a proton precession magnetometer. Rock samples were taken from various sites in the area (see Fig. 1.1), and their magnetic and mineralogical properties were studied.

## 1.2 The general geology of the field area

The regional setting of the field area is shown on Fig. 1.1; namely the region south-west of Okehampton in which sites 1, 2 and 3 are found (site 4 is beyond the main study area). It is located on the southern

flank of the mid Devon syncline where the older rocks are exposed as inliers in the Upper Culm Measure sediments (Culm Measure is a local term synonymous with Carboniferous). There are a series of these inliers along the southern margin of the Culm Measures. They comprise rocks of Upper Devonian and Lower Carboniferous age. The inlier, known as the Meldon inlier, and situated 2 km. south-west of Okehampton, is of special interest here as it roughly coincides with the Okehampton Anomaly. The Meldon inlier is shown in more detail in Fig. 1.2. It is the northernmost inlier, running from the Sticklepath fault, through Meldon, to Bridestowe.

Even though early workers (De la Beche, 1839, Sedgwick and Murchison, 1840, Ussher, 1893, 1900, 1901) made great contributions to the study of the Culm Measures and introduced their own classifications, the lithostratigraphic succession used here will be that described by Dearman and Butcher (1959), but the nomenclature is that used by the I.G.S. (Edmonds et al, 1968)(see Table 1.1).

The oldest of these formations is the Meldon Slate-with-lenticles Formation. This formation is a member of the Transition Series which straddles the boundary between Devonian and Carboniferous being part Famennian and part Tournaisian in age. The formation consists of alternations of dark brown slates and

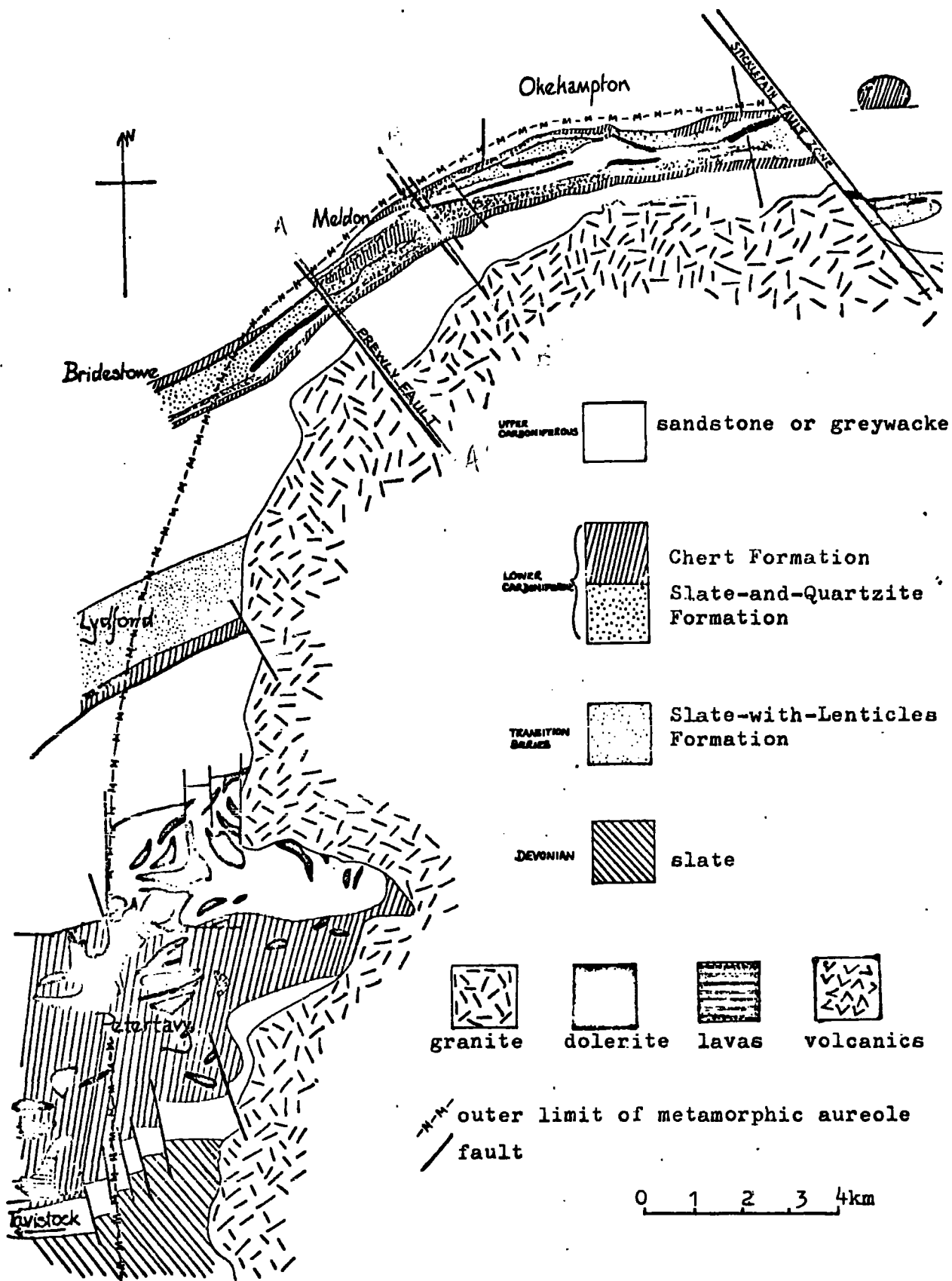
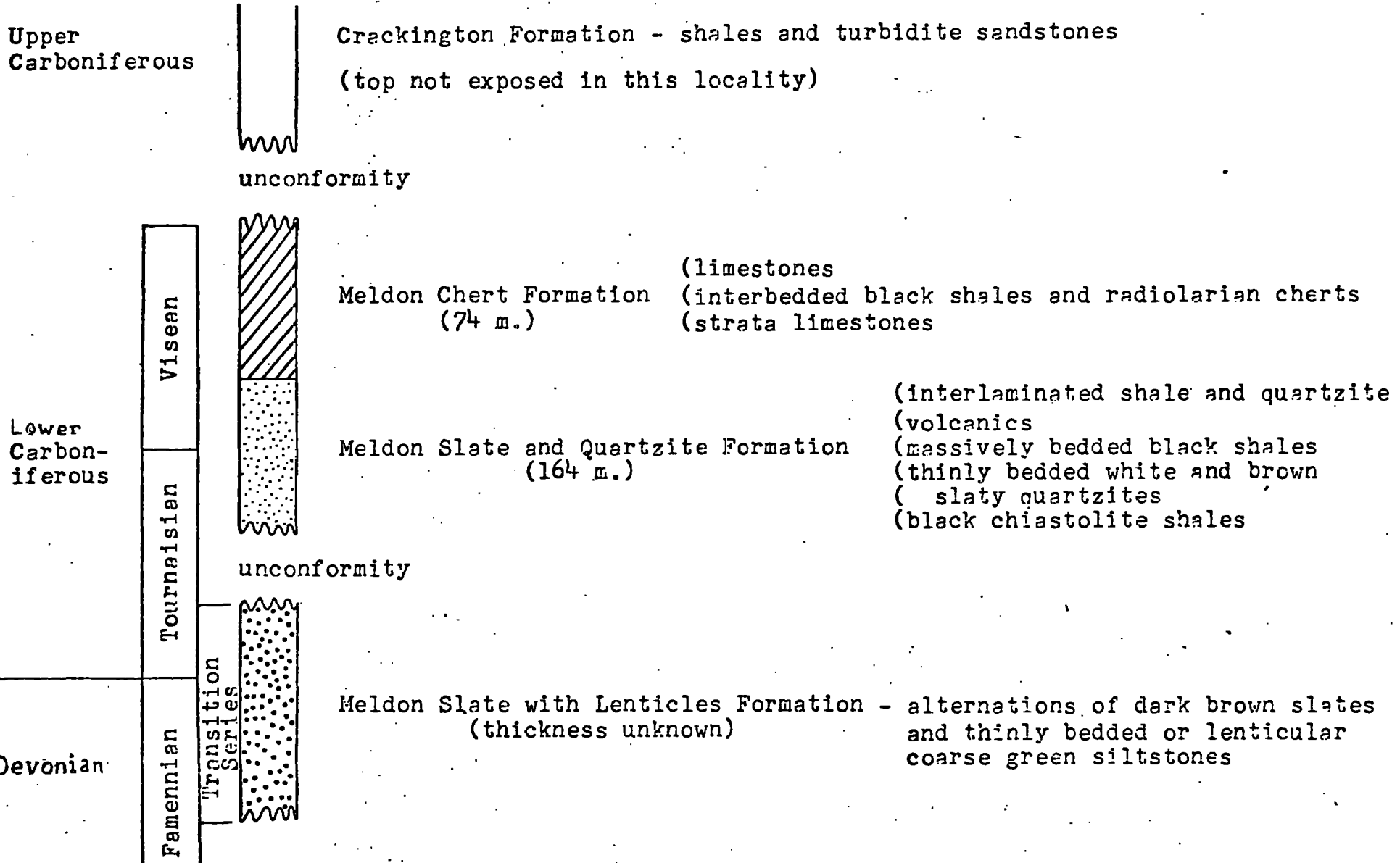


Fig. 1.2. Geology of north-west Dartmoor (Dearman and Butcher, 1959)



Table 1.1: Lithostratigraphic Sequence of the Rocks in Meldon Area  
 (Stratigraphy after Dearman and Butcher, 1959,  
 nomenclature after Edmonds et al, 1968)



thinly bedded or lenticular coarse green siltstones.

Overlying these rocks are the Meldon Slate-and-Quartzite and Meldon Chert Formations which are both Lower Carboniferous in age; the latter being the younger.

The Meldon Slate-and-Quartzite Formation can be divided into five main units, listed below, with the youngest bed at the top:-

- 70' (22 m.) interlaminated shales and Quartzites
- 200' (62 m.) volcanics
- 130' (40 m.) massively bedded black shales
- 45' (14 m.) thinly bedded white and brown slaty quartzites
- 85' (26 m.) black chiascolite shales

Of particular note is the volcanic group, as it forms a prominent horizon and is known to be magnetic (Beer and Fenning, 1976). It consists of pyroclastic rocks, notably tuffs and spilitic agglomerates. They were all laid down under marine conditions and may be graded or cross laminated. The volcanic group decreases in thickness in all directions from the Meldon centre.

There are three divisions in the Meldon Chert Formation making up a total thickness of 240' (74 m.). The list below puts the youngest rock at the top:-

- 20' (6 m.) limestones
- 120' (37 m.) interbedded black shales and radiolarian cherts
- 100' (31 m.) strata limestones

The strata limestones can pass laterally into cherts and the radiolarian cherts into black calcareous shales. This suggests that the various rocks are lenticular deposits as does the fact that there is a sporadic distribution of limestone in the area.

The inlier is surrounded by rocks which are Upper Carboniferous in age. They are the shales and turbidite sandstones of the Crackington Formation. They are fairly uniform in composition, although zones of iron nodules have been found. One such zone was exposed during house constructions near the A30 at Bridestowe (site 1 on Fig. 1.1). As Table 1.1 shows there is a gap in the stratigraphic sequence between these rocks and the underlying Lower Carboniferous and Transition Series sediments which make up the Meldon inlier.

Fig. 1.2 shows a more detailed map of north-west Dartmoor, compiled by Dearman and Butcher (1959). The field area is in the north-west quarter and the Meldon inlier is that stretching from the Sticklepath fault west, through Meldon, to Bridestowe. Further south there are two other inliers; the Lydford inlier and the Petertavy inlier. The stratigraphy of these inliers is similar to that of the Meldon inlier, except that volcanics can be found in horizons other than the Slate-and-Quartzite Formation. As Fig. 1.2 shows, volcanics are found in the Chert Formation near Petertavy.

The outcrop at Meldon is the most complicated but this is a structural feature and not related to any major differences in lithology. In fact, all the inliers of Transition Series and Lower Carboniferous rocks which outcrop along the southern margin of the Culm Measures (see Fig. 1.1) have a similar lithology. Edmonds (1974) compared several inliers and noted the following sequence:-

Stratigraphic Age	General name of formation in the region N-W of the Dartmoor granite	Rock Type
Middle and Upper Viséan	Chert Formation	Shale and cherts (limestones, volcanics)
Tournaisian-Viséan	Slate-and-Quartzite Formation	Shales (volcanics, quartzites)
Femennian-Tournaisian	Slate-with-Lenticles Formation	Shales (siltstones and siliceous, earthy or calcareous lenses)
The rocks in brackets are not ubiquitous		

The names of the three formations change from inlier to inlier. Usually only the place name changes such as the Meldon Chert Formation becoming the Watervale Chert Formation when it is exposed in the Lydford inlier (see Fig. 1.2), and, similarly, rocks of comparable age,

exposed north of the Bodmin Moor granite are known as rocks of the Fire Beacon Chert Formation.

The table above shows that the predominant rock type is shale and that the sediments become more calcareous up the sequence. It also shows that volcanics are found throughout the Upper Tournaisian and Viséan.

### 1.2(i) Igneous Rocks

The most prominent igneous rock in the Meldon district is the Dartmoor granite which is the largest and most eastern batholith of a chain which stretches across Devon and Cornwall. It consists of two main types of granite; a highly porphyritic variety referred to as giant granite (Brammall and Harwood, 1923), 'G' (Osman, 1924) or big feldspar granite (Edmonds et al, 1968), and a non porphyritic rock known as blue granite (Brammall and Harwood, 1923), 'G1' (Osmond, 1924) or poorly megacrystic granite (Edmonds et al, 1968).

The blue granite is a medium grained, hypidiorhombic quartz-feldspar-biotite rock which contains scattered crystals of feldspar and quartz which make up less than 5% of the rock and are normally less than 25 mm. in length. This granite is overlain by the big feldspar granite which is considered to be a marginal facies and shows abundant evidence of contamination by country rocks. It has a similar composition to the underlying granite but the feldspar

megacrysts are better developed, being over 25 mm. in length and taking up more than 5% of the rock. In the Okehampton area 70% of the granite is the big feldspar variety. Fine grained variants of this rock occur as minor intrusions as do a variety of aplites. These cut across both types of granite and belong to a distinct and later period of intrusive activity.

Many authors, of whom Ussher (1888) was the first, suggested that the Dartmoor granite was an asymmetrical laccolith with a flat body intruded northwards from a feeder further south. The gravity survey, conducted by Bott, Day and Masson-Smith (1958), also suggested this mode of intrusion. Interpretations based on this gravity survey indicated that the granite contact is steep along its southern, eastern and northern contacts while there is a more gentle dip along the western margin. Field evidence shows that the contact dips outwards at  $20^{\circ}$ - $30^{\circ}$  in the Okehampton region, and becomes steeper to the east (Edmonds et al, 1968). Field evidence also indicates that the granite is post Culm Measure but pre Permian red beds (Edmonds et al, 1968). This was confirmed using K-Ar age dating (Miller and Mohr, 1964) which put its age of intrusion at about 280 M.Y., which is early Permian.

Dolerites and volcanics are the other igneous rocks found in the area. The pyroclastics, marked as volcanics on Fig. 1.2, mainly comprise the tuffs and

agglomerates of Shale-and-Quartzite Formation, although they can be found in association with Chert Formation rocks in the Petertavy inlier (see Fig. 1.2). The dolerites are only found in the Lower Culm Measure rocks in the Meldon district while, further south, near Petertavy, they are found as intrusions in Upper Culm Measure rocks.

### 1.3 Metamorphism, mineralisation and magnetism of the Culm Measures at Meldon

Fig. 1.2 shows that the Meldon inlier, as well as the eastern ends of those inliers further south, is within the metamorphic aureole of the Dartmoor granite, which has a maximum width of 2 km. (Geological Survey Map No. 324) although Dearman and Butcher (1959) believe that it is as narrow as 1500 ft. (462 m.).

The thermal metamorphism of the Dartmoor granite caused an internal rearrangement of constituent elements of the country rock in the presence of hydrous fluids derived from the magma. However these changes are often masked by metasomatic changes which probably occurred later (Dearman and Butcher, 1959). There is evidence of this metasomatic change in both the granite and country rocks. Stone and Austin (1961) noted that K-feldspar megacrysts were developed across the boundaries of aplites and xenoliths in the granite and suggested that this was a result of late stage potash metasomatism. In the country rock examples of late

stage metasomatism include the development of biotite (potash metasomatism) in some dolerites, and tourmaline and aximite (boron metasomatism) in some sedimentary hornfelses (Edmonds et al, 1968).

The degree of thermal metamorphism decreases away from the granite so at the outer edge of the metamorphic aureole, which corresponds to the northern contact of the Meldon inlier, the sediments only show a mild induration. Nearer to the granite they become harder and spotting occurs, while very close to the granite hornfelses are developed. These hornfelses are mainly restricted to the Upper Culm Measure sediments which outcrop between the granite and the Meldon inlier, but they do occur in the inlier itself.

Altered argillaceous rocks give rise to quartz-biotite-cordierite hornfelses in the Upper Culm Measure rocks found between the granite and the inlier. Biotite continues to be developed in shales, located further from the granite and which are not hornfelled. The shales of the Transition Series (Slate-with-lenticles Formation) can form brown biotite rich bands which simulate calc-flinta. True calc-flintas, or fine grained calc-silicate hornfelses, are the alteration product of cherts and calcareous siltstones, primarily from the Chert Formation (Dearman and Butcher, 1959).

Little or no biotite is developed in the sandstones and siltstones, but muscovite and quartz with



some chlorite, andalusite or cordierite may be found. The sandstones and siltstones of the Crackington Formation rocks adjacent to the granite are the most affected and boron metasomatism, giving rise to the development of tourmaline, has occurred in these rocks.

The cherts and limestones of the Chert Formation have been the most affected by thermal metamorphism and metasomatism. As has been mentioned above, calc-flintas are a common alteration product, though pure limestone near the southern margin of the inlier has been converted to marble (Dearman and Butcher, 1959). Pyrrhotite is a common accessory constituent and probably resulted from the alteration of pyrite originally contained in these rocks (Edmonds et al, 1968). Pyrrhotite is also found as an accessory mineral in the calc-silicate assemblages which are believed to be the alteration product of cherts. Edmonds et al (1968) suggest that during metamorphism, calcium, aluminium, iron and magnesium tended to migrate from calcareous and argillaceous horizons into the cherty bands interbedded with them. However the samples studied by Cornwell (1967) and Beer and Fenning (1976) show that pyrrhotite development is not restricted to the Chert Formation cherts and limestones as it was found in shales and sandstones. It is not uncommon for this mineral to be developed in thermally metamorphosed black shales or other rocks rich in iron and sulphur (Harbord, 1962),

but it seems that the pyrrhotite development in these shales is largely the result of metasomatism rather than the thermal metamorphic alteration of detrital iron sulphide, such as has occurred in the cherts. This metalliferous metasomatism within the metamorphic aureole was followed by later hydrothermal veining in both granite and country rock for a distance of up to 4.5 miles (7 km.) from the granite contact (Edmonds et al, 1968).

From the point of view of the present study the development of pyrrhotite is important as it is a magnetic mineral. Beer and Fenning (1976) noted that the rocks exposed along the margins of the inlier tended to have a significant magnetisation. As Fig. 1.2 shows the outermost rocks largely comprise those of the Chert Formation and it has been shown (Edmonds et al, 1968) that the magnetic mineral pyrrhotite is often developed as an accessory mineral in the metamorphosed cherts and limestones of this formation. Another group of rocks near to the margins of the Meldon inlier are the volcanics of the Slate-and-Quartzite Formation. These form a pronounced magnetic horizon, but this is probably the result of a high magnetite content, though pyrrhotite does occur (Edmonds et al, 1968).

Even though the volcanics and rocks of the Chert Formation form prominent magnetic horizons the widespread distribution of pyrrhotite ensures that many of the rocks within 7 km. of the granite contact have a

significant magnetisation. The following extract from the Okehampton Memoir (Edmonds et al, 1968) describes the distribution of this mineral:-

"Of the metalliferous minerals seen at the surface, pyrrhotite is the most widespread and also the most abundant. It occurs chiefly in finely disseminated form in calc-silicate, limestone, sandstone and argillaceous or silty argillaceous beds. Locally it may account for up to 5 or 6 per cent of these rock types. In the harder chert, dolerite and volcanic horizons, the mineral is more commonly developed in veins and along joints. Disseminated crystals of pyrrhotite do appear in these rocks, however, and in dolerites this sulphide locally replaces ilmenite."

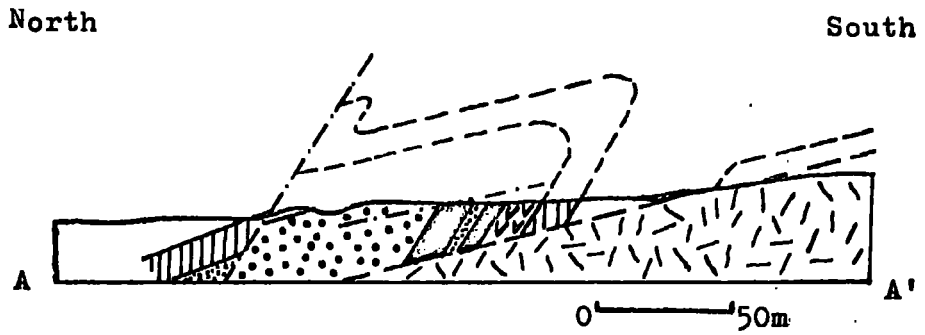
In summary it seems that pyrrhotite can be developed in one of two ways; as the thermally altered product of detrital sulphides or metasomatically emplaced as a disseminated or vein mineral. It is confined to the metamorphic aureole unless it is formed as a vein mineral when it can be found at distances as great as 7 km. from the granite contact. The significant values for the magnetisation measured in some of the Culm Measure rocks within the metamorphic aureole of the Dartmoor granite have been attributed to this mineral (Cornwell, 1967, Edmonds et al, 1968, Beer and Fenning, 1976) though it is less likely to be responsible for the magnetic properties of the volcanics and dolerites. In fact, the behaviour of the dolerites in the area is anomalous as they have a mean magnetisation less than that for dolerites found elsewhere (Creer, 1966).

#### 1.4 Structure

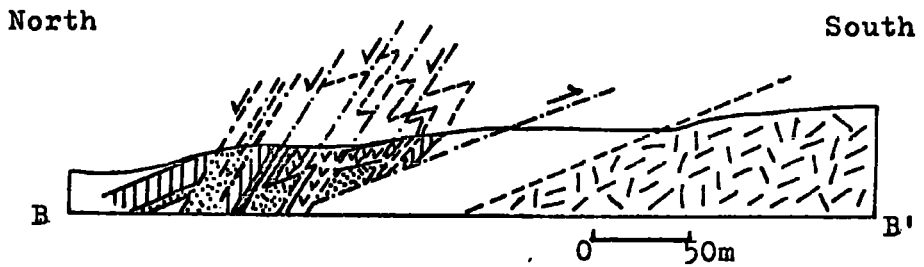
The structure in the Meldon district is illustrated in Fig. 1.3. This shows that the Meldon inlier is essentially a faulted anticlinal structure, which has a complementary syncline to the south. The fold (Fig. 1.3(a)), or folds where several have been developed (Fig. 1.3(b)) have straight limbs and turn sharply. The normal and inverted limbs of these recumbent folds dip north at  $30^{\circ}$  and  $60^{\circ}$  respectively. The axial plane faces south and dips at  $45^{\circ}$ . This structure of zig-zag folds is further complicated with various types of faulting.

The faulted anticline, or anticlines, which make up the Meldon inlier, are some of the many recumbent folds which form part of the southern flank of the mid-Devon syncline. As will be discussed later, several explanations of their formation have been suggested, such as variation in strain from north to south, or that these folds are superimposed on a major overfold formed before the granite was intruded.

The smaller folds are overturned and dip north. They are found in a belt which stretches from just east of the Sticklepath fault west-south-west to the coast at Efford Cliff (SX 2200 1060) (Sanderson and Dearman, 1973). The amplitude and wavelength of the major fold at Meldon has been shown (Dearman, 1969) to be of the same order of magnitude as the folds at Sticklepath and Efford Cliff.



(a) Profile roughly coincides with part of Line 3



(b) Profile roughly coincides with part of Line 5

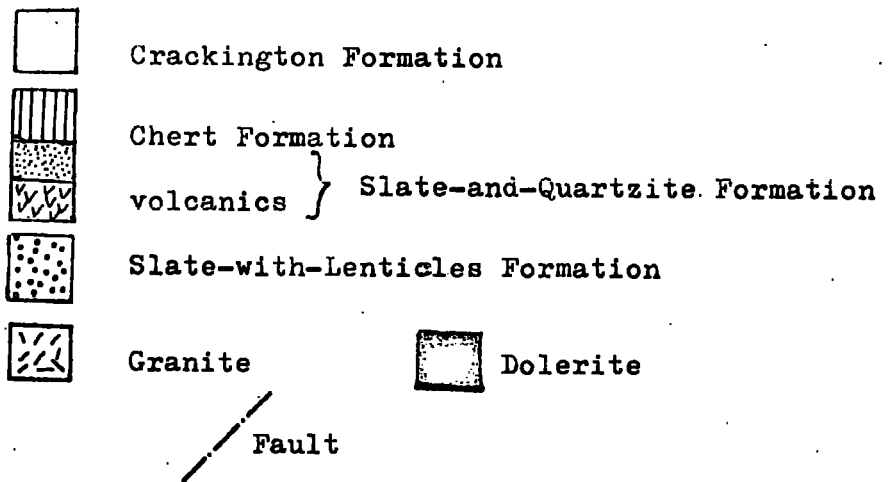
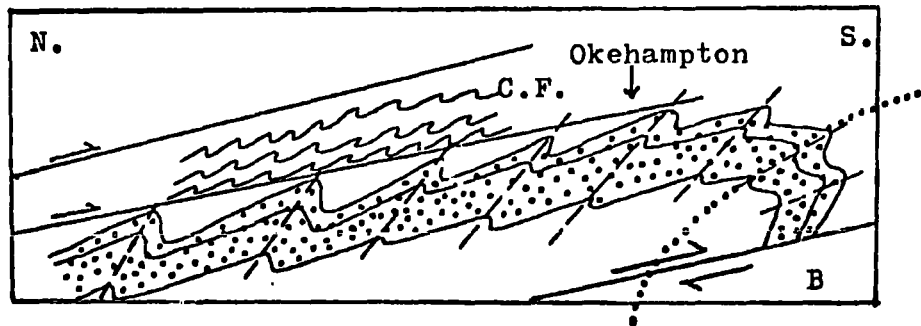
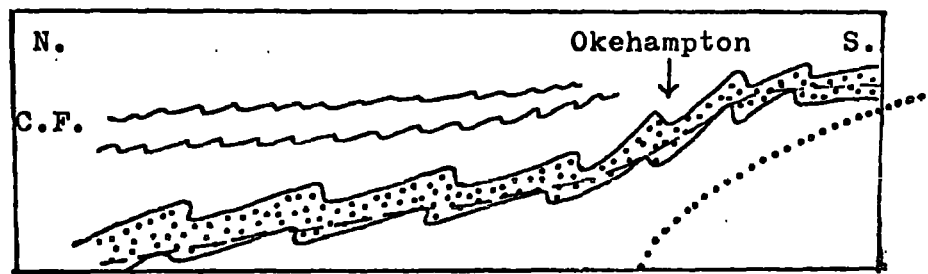


Fig. 1.3 showing cross-sections through the Meldon inlier - marked on the map on Fig. 1.2 as (a) AA' and (b) BB' (after Dearman and Butcher, 1959).



(a) Thrust model (after Edmonds et al, 1968)



(b) Northward progression into Mid-Devon Syncline



- |   |   |
|---|---|
| C.F.  | Crackington Formation                     |
|  | Lower Culm Measures (Lower Carboniferous) |
| B   | Basement                                  |
|  | Boundary of Granite (intruded later)      |

Fig. 1.4 Diagrams showing the possible structure in the Okehampton region.

	<u>Half wave length</u>	<u>amplitude</u>
Meldon	1.5 km.	0.5 km.
Sticklepath	2.5 km.	0.5 km.
Efford Cliff	variable (mean $\sim$ 2.5 km.)	0.5 km.

The easterly trending ridges of the Chert Formation between Dartmoor and Launceston (see Fig. 1.2) have similar periodicity, though no estimates of the amplitude had been made in 1969.

Further south, in a zone which stretches from Lydford to Tintagel (Fig. 1.1) the folds have a different style (Sanderson and Dearman, 1973). They still trend approximately west-east but they are recumbent rather than overturned. This change in fold inclination can be explained (Edmonds et al, 1968) in terms of a major overfold. This overfold was caused when basement rocks were thrust northwards under the southern limb of the mid-Devon syncline. As Fig. 1.4(a) shows, the Culm Measure rocks were overturned on this basement slab and minor folds were developed within them. Larger folds were developed in the Lower Carboniferous rocks than in the overlying incompetent Upper Culm Measure Crackington Formation. The north-south change in dip of the axial planes from recumbent to overturned is then explained, since their inclination is determined by the dip of the major fold on which they are superimposed. Fig. 1.4(a) illustrates this point.

However, Sanderson and Dearman (1973) suggest that this explanation is not tenable, as the transition from upright to recumbent folding can be explained in terms of strain increase from north to south. And Selwood and McCourt (1973), even though they proffer no explanation of how the Meldon anticline formed, argue that "the change from overturned to close recumbent folds observed west of Dartmoor need not be associated with underthrusting or any special mechanism: it need only signal the passage into a synclinal fold zone". This suggests that the Meldon folds form part of the southern flank of the mid-Devon syncline. As it dips more steeply to the north, so do the axial planes of the smaller folds (see Fig. 1.4(b)).

Either of these interpretations could be used to explain the geology between Bridestowe and Tavistock (see Fig. 1.2). The ridges of the Chert Formation rocks are the remains of synclines separated by anticlines which bring the older Slate-with-Lenticles Formation to be exposed (Dearman, 1969). These folds have wavelengths of the same order of magnitude as those in the zone which runs from the Sticklepath fault to the west Devon coast (Dearman, 1969).

It is worth noting that both structural interpretations suggest that a series of recumbent folds in the Lower Culm Measures continue northwards under the Crackington Formation rocks and become progressively deeper. Also, if they possess the same characteristics



as those exposed at the surface, they will have a half wave-length of 2.5 km. and an amplitude of 0.5 km.

However, to describe the structure of the Carboniferous rocks north and west of the Dartmoor granite in terms of folding alone is to oversimplify the situation. In the Meldon area three types of faulting have been observed (Dearman and Butcher, 1959):-

- (i) strike faults along the bedding
- (ii) normal faults parallel to the steep inverted bedding
- (iii) reverse faults following the angle of the bedding in the normal limbs of the folds

These faults have elongated the anticline (Dearman, 1968) giving the rocks a structure like a pack of once vertical playing cards which have been tilted to the south and slipped. The faults tend to dip at angles of  $30^{\circ}$  and  $60^{\circ}$  to the north since they follow the bedding of the normal and inverted limbs. Fig. 1.3 illustrates the way in which the faults alter the apparent shape of the anticline so that it appears to dip less steeply to the north. The normal faulting could provide another mechanism by which Lower Carboniferous rock can be found at progressively greater depths to the north under the Crackington Formation. Alternatively, reverse faulting such as that shown in Fig. 1.3(b) may ensure that Lower Carboniferous rocks are kept near to the surface.

In summary, then, the structure in the Meldon district can be described in terms of a faulted anticline flanked to the south by a syncline which is truncated by the granite (see Fig. 1.3). It is believed (Dearman and Butcher, 1959, Freshey and Taylor, 1971, Sanderson and Dearman, 1973, Hobson and Sanderson, 1975) that the rocks which form the Meldon inlier continue north under the Crackington Formation rocks as well as to the south where they outcrop as inliers (see Fig. 1.2). The concealed Lower Carboniferous rocks which continue north may form a series of ever deepening folds (see Fig. 1.4) though faulting, such as that seen at Meldon, may bring certain rocks up near the surface, or place others at greater depths.

#### 1.5 Previous geophysical investigation.

The first relevant geophysical work to be done in the Cornubian peninsula was carried out in 1936 when Bullard and Jolly made a number of pendulum gravity measurements in Devon and Cornwall using a pendulum gravimeter. Then, in 1958, Bott, Day and Masson-Smith used a Worden gravimeter to make a comprehensive gravity map of Cornubia. This shows a belt of negative anomalies which follows the line of the granite chain. The gravity lows are more marked over the exposed granites but their persistence in the intervening areas suggests that the granites are connected at depth - an idea first put forward by Murchison and Sedgewick in 1840 to explain the continuity of mineralisation between batholiths.

The Dartmoor granite is the largest and most eastern batholith. On the basis of a gravity interpretation its northern contact is thought to dip at an angle in the range  $40-75^{\circ}$  and descend to a depth of at least 10 km. This is for a density contrast of  $0.16 \text{ g.cm.}^{-3}$  between the granite and the denser Culm Measures (Bott, Day and Masson-Smith, 1958). In the Okehampton area the contact is thought to dip at  $20-30^{\circ}$  near the surface (Edmonds et al, 1968). The gravity map shows that the negative anomaly caused by the granite has a gently sloping northern edge and that no other gravity disturbances have been detected in the area.

As well as conducting a gravity survey Bott, Day and Masson-Smith (1958) made some exploratory magnetic traverses using vertical field magnetometers. The main feature observed was that the magnetic field north of the line of granites was much higher than that over the granite or the rocks to its south. Along the course delineating the northern limit of the gravity low very large local negative magnetic anomalies were found, flanked to their north by a belt of positive magnetic anomalies. It was suggested that the main positive anomaly (see overlay to Fig.1.1) was caused by highly polarised rocks beneath the Carboniferous sediments which dwindle northwards, or basement metamorphics brought nearer to the surface as a result of Hercynian thrusting in this region. No suggestions

were put forward as to the cause of the local negative anomalies.

The fact that the junction between the gravity lows and gravity highs roughly coincides with the line of granites supports the idea that the cupolas are connected at depth. It also suggests that the magnetic features found along this line are associated with the contact between the granite and the more magnetic country rock to the north. The broad regional change from persistent low to persistent high (see overlay to Fig. 1.1) suggests that the polarisation contrasts go down to great depths. No comparable contrast is found south of the granite, indicating that the magnetic properties of the rocks found in south Devon are similar to the granite.

In 1965 the Geological Survey published an aeromagnetic map of Cornubia (scale 1:625,000). An airborne fluxgate magnetometer had been used. This instrument measures the total magnetic field so the survey was the first total field survey of the area. No large scale interpretation was done but the survey did confirm the findings of Bott, Day and Masson-Smith (1958) and showed the magnetic anomalies in greater detail and extent. Part of this map is shown on the overlay to Fig. 1.1.

Using this aeromagnetic data and supplementary ground measurements, made by the Geophysical Department of the Geological Survey in 1963/64, using a proton

precession magnetometer, an interpretation of the anomalies encircling the northern edge of the Dartmoor granite was attempted (Edmonds et al, 1968). The conclusion reached was that concealed, but near surface bodies, probably igneous intrusions, situated directly under the anomaly, 2.5 km. to the north of the granite contact, caused the large negative anomalies. The Okehampton Anomaly was found to have a peak to peak anomaly of 550γ. Using the graphical method of Bruckshaw and Kunaratnam (1963), this body was estimated at being at a depth of 150-250 feet (46-81 m.), but no estimation of the width was recorded. From the fact that the negative anomaly is positioned south of the positive peak it was assumed that the causal body was reversely magnetised. The I.G.S. found that more definitive interpretation proved difficult as most methods then available assumed that magnetisation arose purely from induction in the earth's field.

To accompany this work the Geological Survey (Edmonds et al, 1968) measured the susceptibility of a number of rock samples taken from the Meldon area. The results are shown in Table 1.2. It was noted that the values of the susceptibility of the granite were low and uniform, thus accounting for the low magnetic field, and lack of relief on the aeromagnetic map, across the granite exposure. By contrast, the measurements made for the samples of Culm Measure rocks taken

Table 1.2

Showing the localities and susceptibilities  
of a number of rock samples taken by the  
Institute of Geological Sciences in order  
to measure their magnetic properties  
 (Edmonds et al, 1968)

Rock Type	Locality	Number of specimens	Range of susceptibility (K x 10 <sup>-6</sup> units)
Granite	Dartmoor	13	7-18
Albite-dolerite	Sourton Tors (near Bridestowe)	2	54
	Meldon	2	110-234
Pyrrhotite-bearing calc-silicate hornfels	Meldon	1	13500
Carboniferous (Culm Measure) sediments from within the meta-morphic aureole	Various	16	7-380

from the metamorphic aureole, were varied, ranging from  $7-380 \times 10^{-6}$  c.g.s. units. On closer examination it proved that those samples with the highest susceptibility contained the magnetic iron sulphide pyrrhotite. This mineral was also present in the sample with the highest susceptibility: the pyrrhotite-bearing calc-silicate hornfels. The twelve samples of Carboniferous sediment which did not contain pyrrhotite had a range of susceptibility of  $7-39 \times 10^{-6}$  c.g.s. ( $88-490 \times 10^{-6}$  S.I. units). Apart from the pyrrhotite bearing calc-silicate hornfels the only other rocks with high susceptibility were some of the albite dolerites.

The Geological Survey (Fenning, in Edmonds et al, 1968) concluded that the uniform nature and large areal extent of the anomalies made the possibility of their arising from mineralisation within the Culm Measure rocks extremely unlikely. He suggested that the major anomalies were caused by igneous rock such as dolerite, with the smaller features, detected only on the ground traverses, being due either to pyrrhotite mineralisation or to the dolerite intrusions in the Lower Carboniferous.

More detailed work was done on the magnetic properties of the Carboniferous rocks outcropping at Meldon (Cornwell, 1967) and at Sourton Tors, south of Bridestowe (Beer and Fenning, 1967). A similar conclusion was reached in both areas, that the large local magnetic anomalies were caused by pyrrhotite which had developed in the rocks as a result of late stage

metasomatic activity associated with the intrusion of the Dartmoor granite. Cornwell (1967) noted that even though there was considerable scatter in the direction of the magnetisation of these rocks its mean was comparable with that measured in early Permian rocks found elsewhere, again suggesting that the pyrrhotite mineralisation was the same age as the granite. Beer and Fenning (1976) describe both vein and disseminated pyrrhotite in their samples suggesting that it has developed in more than one way. The disseminated crystals could be the product of thermal metamorphism of detrital sulphides or a result of metasomatism. The vein mineral is definitely metasomatic and was probably a late stage hydrothermal emplacement (see Edmonds et al, 1968, p. 131).

Work was also done on the magnetic properties of igneous rocks of Carboniferous age which outcrop in south-west England. Creer (1966) noted that dolerites of this age tended to have a lower magnetisation, often reduced by one order of magnitude, than that for dolerites found elsewhere. The magnetisation of a highly magnetic rock such as dolerite mainly comprises the remanent component so the unusually low value for the magnetisation is probably a result of a much reduced remanent magnetisation. This was thought to have been caused by a widespread remagnetisation during the early Permian (Chalmers and Creer, 1964, Creer, 1966).



More recently, in 1969, the I.G.S. put down a borehole at Wilsey Down, located on Fig. 1.1 (borehole log unpublished and a brief account in the Boscastle and Holsworthy Memoir, McKeown et al, 1973). The object of doing this was to confirm the stratigraphy and structure deduced from surface outcrops and to discover the source of the strong negative magnetic anomaly located in that area. As the overlay to Fig. 1.1 shows, this negative anomaly is similar to the one situated at Okehampton, so the conclusions reached here may help in interpreting the Okehampton Anomaly. Beneath 250 ft. (78 m.) of shales, siltstones and turbidite sandstones of the Crackington Formation the borehole encountered shales and limestones similar to those of the Meldon Chert Formation. These beds were pyrrhotite enriched between 250 and 850 ft. (78 and 262 m.) and were thought to be the cause of at least part of the magnetic anomaly. The pyrrhotite found in the Wilsey Down borehole differs from that found by the Geological Survey (1968, 1976) or Cornwell (1967) in the Meldon samples in that it was bedded and found outside the metamorphic aureole. The pyrrhotite is thought (Beer and Scrivenor, personal communication) to have developed when the sediments were still unconsolidated. It is found in the shales but is always near a calcareous horizon (unpublished I.G.S. borehole log). Greenstone bands and tuffs are found throughout the calcareous sequence, and it has been suggested (Scrivenor, personal

communication) that these igneous rocks could have been contemporary volcanics whose solutions provided the Fe, S and possibly Ni for the pyrrhotite development.

The geophysical work to date falls into two schools of thought; that the magnetic anomalies are caused by igneous bodies such as dolerites or that mineralisation, in the form of pyrrhotite development, is the main contributing factor. However, there does seem to be one point of agreement in that the short wavelength anomalies only detectable along ground traverses, and superimposed on the major anomalies, are thought to be caused by near surface mineralisation, largely confined to the metamorphic aureole.

## CHAPTER 2

### DATA ACQUISITION AND REDUCTION

#### 2.1 Introduction

This chapter describes the acquisition and reduction of data. These include the ground magnetic readings defining six profiles across magnetic anomalies northwest of the Dartmoor granite. Rock samples for determination of magnetic and mineralogical properties were also collected but their treatment will be considered in Chapter 3.

The magnetic anomaly of particular interest is that defined on the 1:250,000 aeromagnetic map (see overlay to Fig. 4.1) as the Okehampton Anomaly - named after the principal town in that area.

#### 2.2 Data Acquisition

The data for the ground traverses were collected in October 1977. Six traverses were made across or near to the Okehampton anomaly. They ran along lines joining the following pairs of grid references:

line 1: SX 2535 0870 -- SX 2516 0905

line 2: SX 2558 0871 -- SX 2531 0922

line 3: SX 2579 0864 -- SX 2520 0953

line 4: SX 2599 0860 -- SX 2544 0930

line 5: SX 2589 0900 -- SX 2552 0969

line 6: SX 2600 0930 -- SX 2565 0970

The instrument used to make the measurements was a GeoMetrics portable precession magnetometer model G-816, which measures the total field intensity read out in gamma on a digital display.

Position fixing in the field was done in one of two ways. As 1:10,560 Ordnance Survey maps were used, it was possible, when near buildings, or in fields, to locate position relative to suitable land marks, estimating distances by pacing. This was impossible on Dartmoor so continual back bearings were made to locate position.

The time at which each reading was taken was recorded, and the height was estimated from the contour map. A local base station was established near Meldon village at SX 2565 0923. Since sections from different lines were often measured in the same day a base station reading was obtained before and after each set of readings was made. When it took an entire day to measure a section it was not always possible to take a base station reading during the day. Continuous reading magnetometers are installed at Hartland Magnetic Observatory, near Bideford, 40 km. north-east of the area (see Fig. 1.1), and the records from these instruments were obtained so that corrections for diurnal variation could be made.

### 2.3 Data Reduction

The field data were processed to remove the effects of diurnal variation. The I.G.R.F. was calculated for the area, and was then subtracted from the field data and the residual taken to be the anomaly. This was done using the program INTERPOL (see Appendix B) which calls the subroutine I.G.R.F. This subroutine was compiled by Dr. G.K. Westbrook at Durham University from a program supplied by the I.G.S. (ref. I.A.G.A. study group, 1976). The I.G.R.F. value was computed for certain points along each traverse and the values for intervening points were calculated by linear interpolation.

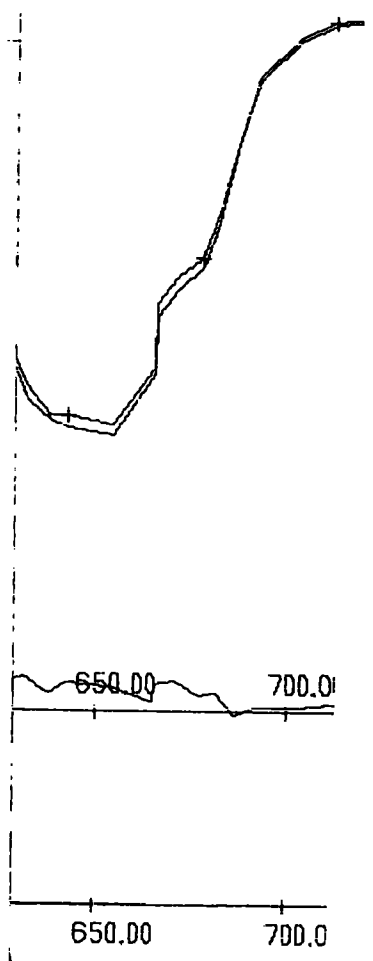
In order to calculate the diurnal variation the results from Hartland Magnetic Observatory were studied. These were digitised using a digitising table and the results fed into CREANOM (see Appendix B). This program calculates the mean value of both the vertical and horizontal components of the magnetic field, as measured at Hartland, and subtracts this value from each reading to produce the vertical and horizontal anomalies. Interpolating between these values  $dZ$  and  $dH$  were calculated for each point in time at which a reading was taken in the field. The total anomaly,  $dF$ , was then calculated:  $dF = dH \cdot \cos I + dZ \cdot \sin I$ , where  $I$  is the angle of inclination of the earth's magnetic field.  $dF$  was then subtracted from the I.G.R.F. corrected anomaly which had been computed using INTERPOL. Fig. 2.1 shows the plot of a profile before and after corrections for diurnal variation were made.

Figs. 4.2 to 4.7 show that the topography is rugged and can vary over a range as great as 421.6 m. (line 4).

The original intention had been to upward continue the ground data to a height of 500 ft. (167 m.) so that they could be directly compared with profiles along the same lines taken from the unpublished 1:25,000 I.G.S. aeromagnetic map, flown at that height. As this was not possible the ground profiles were compared with the aerial data. Figs. 4.2 to 4.7 show both types of profile as well as the terrain and geology.

Even though the ground and aerial profiles display similar features they differ in two respects. Firstly the main peaks and troughs on the ground profiles have greater amplitudes, as would be expected, but, superimposed on these are large amplitude magnetic disturbances which have too short a wavelength to enable them to be detected from the air. The fact that the two types of profile are similar, except that greater detail is displayed on the ground traverses, shows that they describe the same features, and that the major anomaly shown on the ground traverses is the Okehampton Anomaly.

FIC



## CHAPTER 3

### THE MAGNETIC PROPERTIES OF THE ROCK SAMPLES

#### 3.1 Introduction

Rock samples for determination of the magnetic and mineralogical properties were taken from four different localities; at Meldon Quarry (SX 2570 0925) and from three sites outside the metamorphic aureole - Aggetts Quarry (SX 2594 0961), a building site near the A30 (SX 2519 0900) and near Meldon village (SX 2562 0928). Samples of shale and sandstone of the Upper Carboniferous Crackington Formation were taken from the three sites outside the metamorphic aureole (Fig. 1.1). The samples from Meldon Quarry consist of a variety of Lower Carboniferous shales, cherts and meta-igneous rocks (notably baked tuffs) from the Slate-with-Lenticles, Slate-and-Quartzite and Chert Formations.

A preliminary sampling was carried out in October 1977, and a more specific collection was made in April 1978, when further samples were collected from Meldon Quarry. The sites from which the second set of samples were taken are shown in Fig. 3.1. The sampling method required that the orientation of the rocks relative to



Fig. 3.1 Table listing the sites in Meldon Quarry at which samples were taken in April 1978

<u>Collection Site</u>	<u>Sample Number</u>
New Stone Area	M601, M602, M603
Stone Area 1	M800
Stone Area 2	M101, M102, M103, M104
Stone Area 4	M901, M904, M905

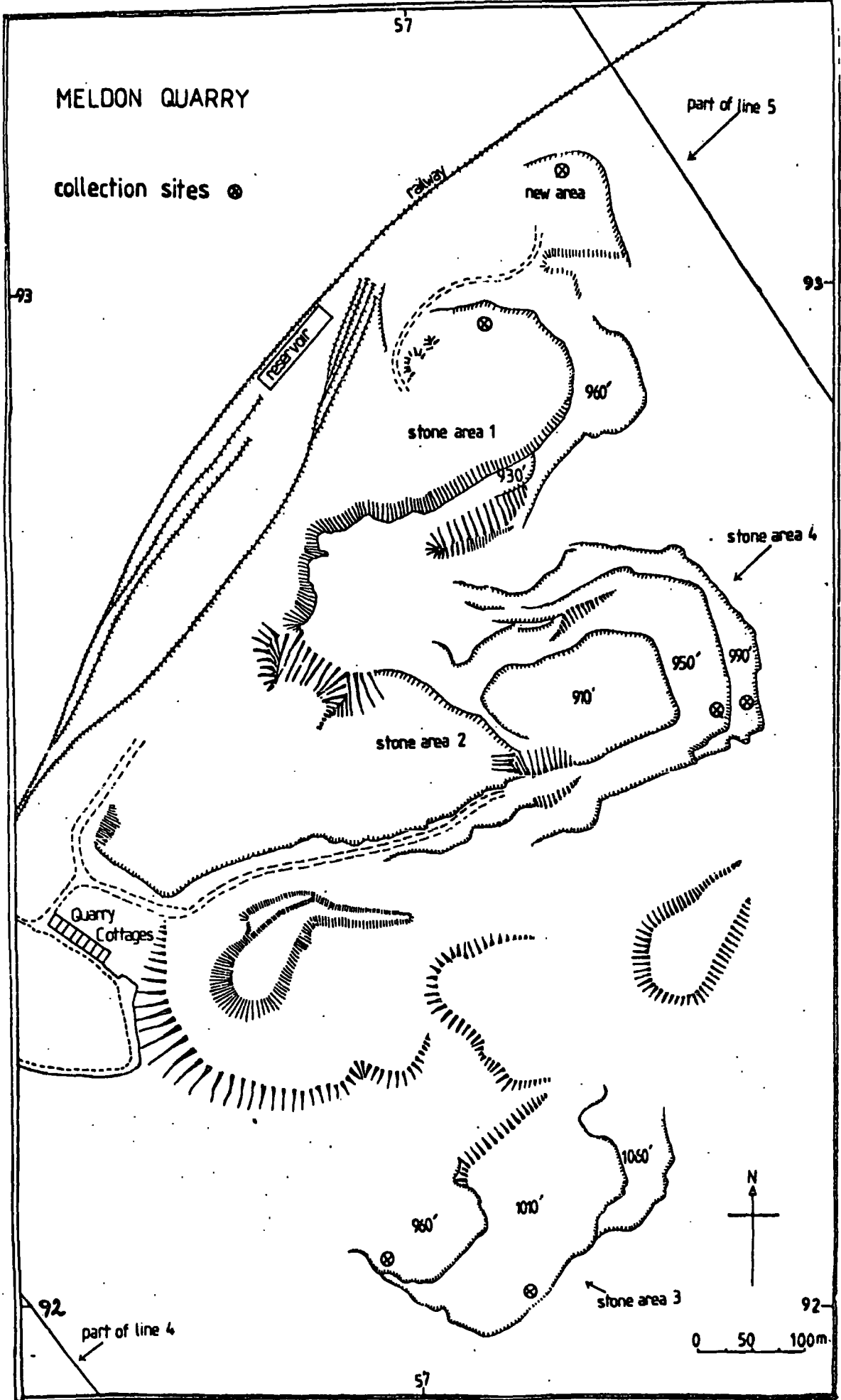


Fig. 3.1 Map showing the collection sites in Meldon Quarry

the magnetic north, and to the dip of the strata, was determined. When the samples had been suitably marked with orientated arrows they were removed, using a hammer.

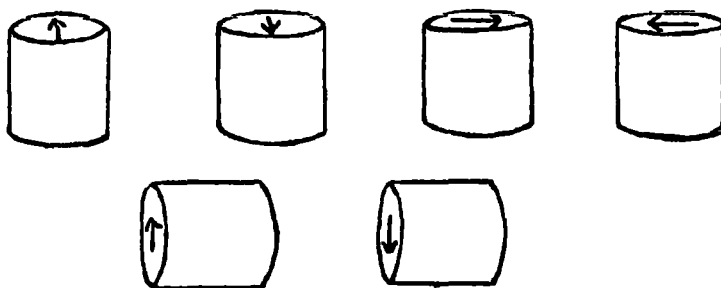
The samples were prepared at the Physics Department, Newcastle University, by drilling one or more 1" cores from each sample. These cores were then cut into 1" lengths. When a sample was too small to permit coring, a specimen was cut as near as possible to a 1" cube. Some of the 1977 collection were undersized, and the variation in specimen size produced errors when the magnetic measurements were made.

The measurement of the magnetic properties was also done at Newcastle under the supervision of Dr. D. H. Tarling. The magnetic susceptibility was measured using a susceptibility bridge (Collinson, Molyneux and Stone, 1963) and the intensity and direction of remanent magnetisation with a Digico spinner magnetometer (Molyneux, 1971). Measurements were made on up to three cores, or cubes, from each rock sample.

### 3.2 Spinner magnetometer

The Digico spinner magnetometer is a computerised system in which a spinner magnetometer is connected to a 'Digico micro 16' computer (Molyneux, 1971). The instrument employs the principle that a magnetic moment rotating within a coil about an axis in the plane of the coil will produce an alternating e.m.f. in a pick-up

coil. Because the instrument can only measure the magnetic moment perpendicular to the axis of rotation, the specimen core is placed in six different orientations. These are shown below. The arrow indicates magnetic north and it is drawn on the top side of the specimen.



The readings, taken when the specimen is in each of these positions, are stored in the computer, which is programmed to calculate the intensity and direction of magnetisation of the specimen. The results are printed out at the keyboard terminal.

The basic design of the spinner magnetometer (Fig. 3.2) relies on the fact that the current produced is proportional to the speed of specimen rotation and its magnetic moment. The speed of rotation is measured in the photocell unit. The rotating disc has a slot which permits light to pass when it comes between the lamp and the photocells. When this occurs the electronic signal generated in the flux gates by the magnetic specimen passes to the computer. This is repeated many times so that a mean value of the wave form from the rock can be gathered. The amplitude and phase of this

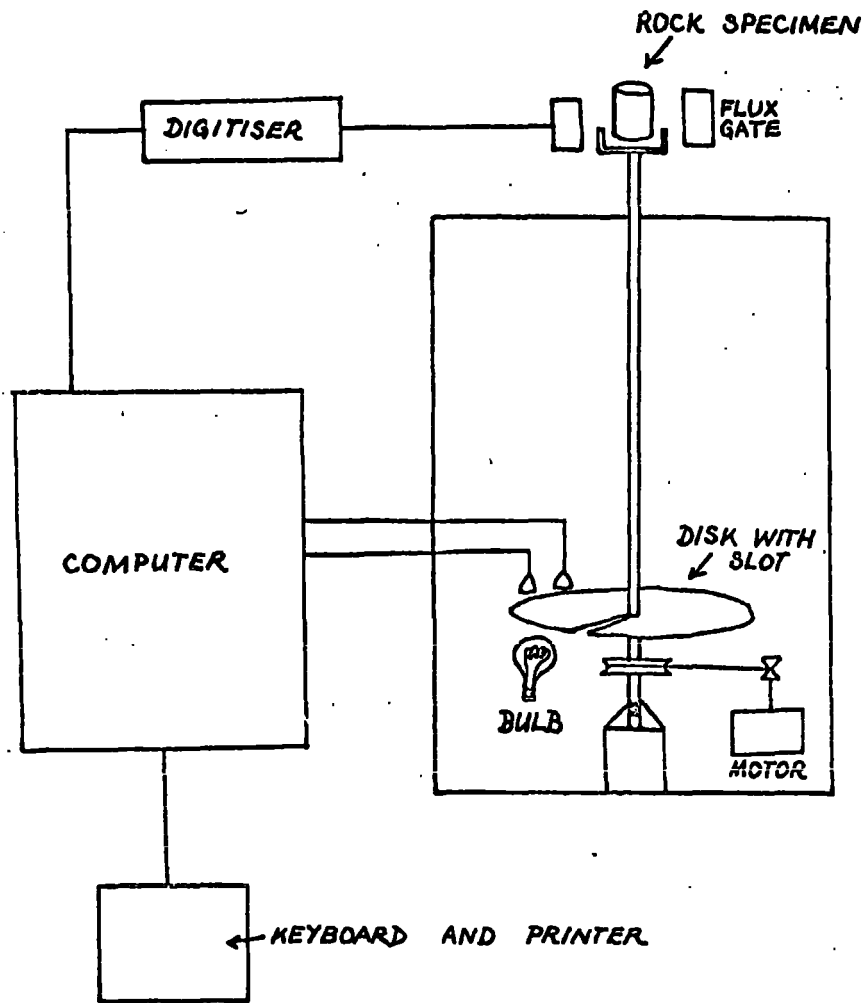
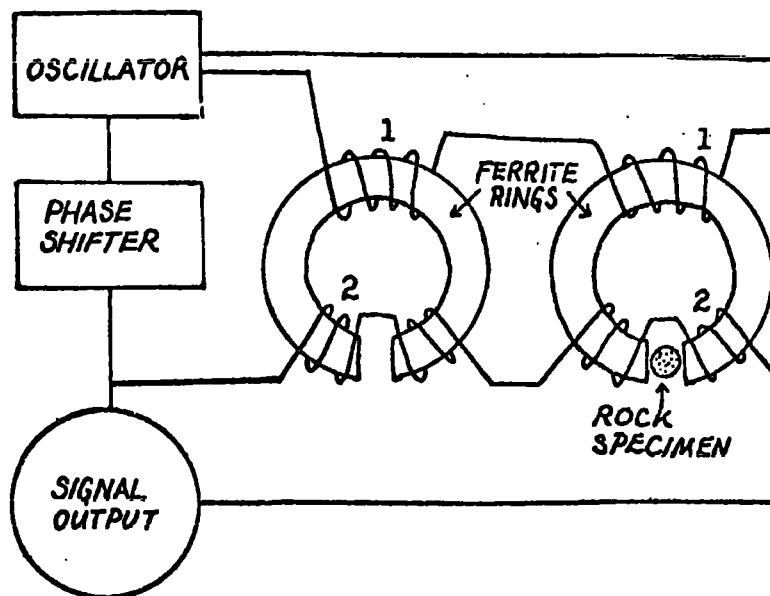


FIG 3.2 BLOCK DIAGRAM OF COMPUTERISED SPINNER MAGNETOMETER.  
(after Molyneux, 1971)



- 1 PRIMARY WINDING
- 2 SECONDARY WINDING

FIG 3.3 BLOCK DIAGRAM OF A SUSCEPTIBILITY BRIDGE  
 (Design: Collinson, Molyneux & Stone, 1963  
 Diagram: Tarling, 1971)

wave form, as compared with the photocell output, is a measure of the intensity and direction of magnetisation for the sample in that orientation.

The results for each orientation of a specimen are printed out, as is the final computation of the specimen's remanent magnetisation, *measured as magnetic moment per unit volume.*

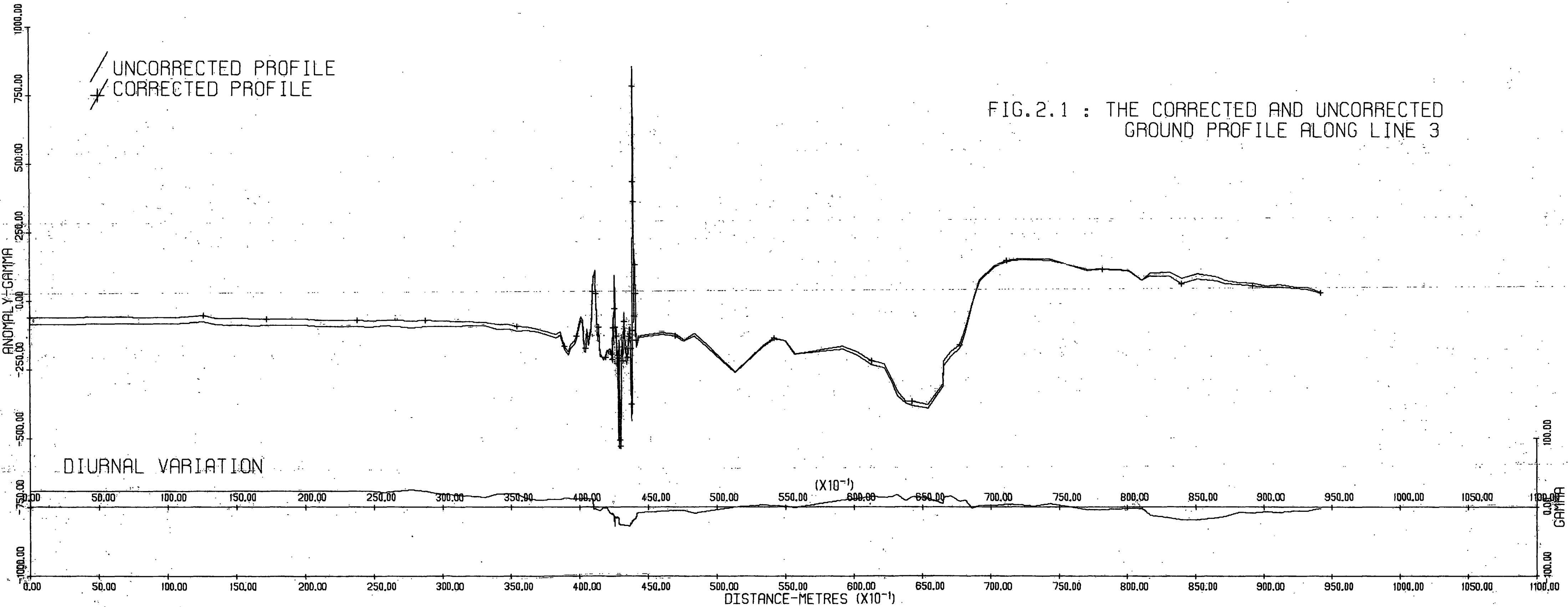
### 3.3 Susceptibility Bridge

The susceptibility bridge (Collinson, Molyneux and Stone, 1963), shown in Fig. 3.3, consists of two split ferrite rings, both of which are surrounded by a primary coil carrying an alternating current. This produces an alternating magnetic field across the gap in the rings. A standard sample, placed in one of these gaps, alters the magnetic field and the new alternating field is picked up as a current by the secondary winding about that ring. The current in the primary winding is then altered so that the outputs from both secondary windings balance. This standard sample is then removed and a rock specimen emplaced. It unbalances the secondary circuit by an amount proportional to its susceptibility.

The specimen can be tested for anistotropic susceptibility by altering its orientation in the gap. The great advantage of this instrument is that measurements can be taken quickly.

### 3.4 Initial Data Assimilation

Before the data could be studied, certain computations had to be made. These included the calculation





of the mean vector for certain sets of results. Whereas the mean value of the susceptibility could be calculated as a straight arithmetic mean, the mean remanent field could not. Its mean value was calculated by dividing the remanent field for each specimen into its x, y and z components, taking their means and from them computing the mean vector. A full description of the technique is given in Appendix A.

### 3.5 The results

Magnetic measurements were only made on the samples from Meldon Quarry. The results are listed in Tables 3.1 and 3.2.

Table 3.1 lists the measurements of those rocks collected in October 1977. They are divided into their various lithologies. The results in Table 3.1 cannot be taken as more than a general guide since the non-standard specimen sizes introduced errors. Also field orientation of the samples was not sufficiently accurate to enable the direction of the remanent magnetisation to be measured to acceptable accuracy. This meant that the weighted mean value for the remanent field could not be calculated.

With the exception of two specimens, M1 and M22, all the rocks in Table 3.1 have a Q value of less than 1. The mean value of the magnetic susceptibility for the various lithologies was calculated and it was found that the shales possessed the highest susceptibility.

Table 3.1: Showing the results of the measurements made on samples collected in October 1977 from Meldon Quarry

Specimen Name	Intensity of Remanent Magnetisation		Susceptibility x 10 <sup>-6</sup> C.g.s.		Q	Rock Type
	e.m.u./cc x 10 <sup>-8</sup>	A.M.-1 x 10 <sup>-3</sup>				
M	0.38	0.38	180.9	)	0.004	CHERT
M1	252.86	252.86	88.9	)	5.95	
M2	0.65	0.65	22.2	) mean	0.06	
M10	0.07	0.07	191.2	) = 107.56	0.0008	
M21	0.90	0.90	54.6	)	0.03	
M4	27.85	27.85	322.0	)	0.18	SHALE
M12	0.41	0.41	310.5	)	0.003	
M15	12.64	12.64	868.3	) mean	0.03	
M17	34.35	34.35	222.3	) = 438.6	0.32	
M20	0.06	0.06	158.1	)	0.0008	
M22	430.98	430.98	750.4	)	1.2	
M7	0.25	0.25	84.3	)	0.006	META- IGNECUS
M8	0.04	0.04	103.5	)	0.0008	
M9	3.16	3.16	355.7	)	0.019	
M11	0.04	0.04	144.5	) mean	0.0006	
M13	0.05	0.05	359.6	) = 204.76	0.0003	
M14	0.30	0.30	195.0	)	0.003	
M16	0.01	0.01	189.7	)	0.01	
M18	20.02	20.02	205.7	)	0.22	

Table 3.2: Showing the results of the measurements made on samples collected in April 1978 from Meldon Quarry

	Specimen Name	Remanent Magnetisation			Magnetic Susceptibility $\times 10^{-6}$ c.g.s.	Q	
		Direction		Intensity			
		Declination	Inclination	e.m.u./c.c. $\times 10^{-6}$			A.M. $-1 \times 10^{-3}$
New Area	( M601.3	61.2	-10.25	0.131	0.131	27.65	0.01
	( M601.2.2	319.1	+31.35	0.278	0.278	37.36	0.02
	( M602.2	359.5	+ 0.85	9.842	9.842	13.04	1.5
	( M603.3.2	169.85	-55.7	3.505	3.505	12.24	0.6
	( M603.2.2	178.45	-44.7	3.302	3.302	12.12	0.6
	( M603.1.1	166.2	-46.4	5.809	5.809	12.19	1.0
Stone Area 1	( M800.1.1	102.2	-41.5	1296.227	1296.227	556.97	4.9
	( M800.2.2	113.75	-39.4	996.881	996.881	416.04	5.0
	( M800.2.1	121.3	-45.3	1381.7	1381.7	519.70	5.6
Stone Area 3	( M102.1	55.15	+17.7	0.1	0.1	7.70	0.03
	( M103.2.2	73.6	-12.85	237.151	237.151	31.75	15.6
	( M103.1.2	213.95	+31.2	0.162	0.162	9.14	0.04
	( M103.2.1	91.7	-15.45	45.274	45.274	13.43	2.1
	( M104.1.1	165.5	-63.05	108.233	108.233	86.61	2.6
	( M104.1.2	174.55	-68.25	880.64	880.64	135.57	13.6
	( M101.1.1	83.45	+44.55	805.733	805.733	274.62	6.1
( M101.3	69.9	+52.05	879.295	879.295	330.08	5.6	
Stone Area 4	( M901.2	140.95	+14.6	0.092	0.092	3.37	0.06
	( M901.1	93.5	+70.25	0.156	0.156	3.69	0.1
	( M904.1	281.85	- 8.5	4.668	4.668	24.14	0.3
	( M904.28	326.65	+ 5.15	26.786	26.786	35.09	1.0
	( M905.2.2	3.55	+ 5.95	0.546	0.546	32.62	0.04
	( M905.3.2	37.7	+31.8	0.132	0.132	37.7	0.01
	( M905.3.1	176.85	+79.7	0.035	0.035	36.46	0.002

Table 3.3: Showing the direction and intensity of the remanent magnetisation and the resultant magnetisation found by resolving the remanent and induced magnetisations. The data refers to the samples collected at Meldon in April 1978

Specimen Name	Remanent Magnetisation			Resultant Magnetisation (Remanent and Induced)		
	Declination	Inclination	Intensity $\times 10^{-6}$ e.m.u./c.c.	Dec.	Inc.	Int. $\times 10^{-6}$ e.m.u./c.c.
M601.3	61.2	-10.25	0.131	0.20	64.5	10.84
M601.2.2	319.1	31.35	0.278	10.82	65.39	14.9
M602.2	359.5	0.85	9.842	357.54	25.23	2.48
M603.3.2	169.85	-55.7	3.505	351.40	5.84	0.25
M603.2.2	178.45	-44.7	3.302	176.73	87.8	2.97
M603.1.1	166.2	-46.4	5.809	160.51	33.7	0.61
M800.1.1	102.2	-41.5	1296.227	96.01	-33.4	339.44
M800.2.2	113.75	-39.4	996.881	108.42	-31.82	238.22
M800.2.1	121.3	-45.3	1381.7	116.46	-39.78	483.74
M102.1	55.15	17.7	0.1	353.29	65.5	3.08
M103.2.2	73.6	-12.85	237.151	72.08	-9.51	6.43
M103.1.2	213.95	31.2	0.162	346.72	67.46	3.75
M103.2.1	91.7	-15.45	45.274	76.51	7.97	0.86
M104.1.1	165.5	-63.05	108.233	158.74	-60.68	51.29
M104.1.2	174.55	-68.25	880.64	174.94	-68.46	705.97
M101.1.1	83.45	44.55	805.733	78.09	50.05	324.89
M101.3	69.9	52.05	879.295	63.06	56.74	699.85
M901.2	140.95	14.6	0.092	174.64	66.68	1.37
M901.1	93.5	70.25	0.156	173.48	68.18	1.64
M904.1	281.85	-8.5	4.668	134.85	60.57	12.33
M904.2	326.65	5.15	26.786	151.25	28.09	8.32
M905.2.2	3.55	5.95	0.546	168.82	63.97	12.80
M905.3.2	37.7	31.8	0.132	170.80	65.68	15.01
M905.3.1	176.85	79.7	0.035	170.13	65.86	14.5
Weighted Mean	105	-29	15.0	97	15	13

The mean shale value (438.6) is twice that of the meta-igneous rocks (204.75) and three times that of the cherts (107.56). By inspection the intensity of the remanent magnetisation of the shales seems to be at least one order of magnitude greater than either the igneous rocks or the cherts, suggesting that the shales are the greatest contributor to the magnetisation of the Lower Culm Measure rocks. Noting this, only shales were collected in April 1978 when the second set of rock samples were taken.

When the further samples were collected in April 1978 directional measurements could be made, since these samples were accurately orientated. Errors due to varying specimens size were eliminated as large samples were taken. Table 3.2 lists the magnetic properties of these shales. As this table shows they vary both in intensity and direction. Eleven of the 24 specimens had a Q value greater than unity and the weighted mean value of Q for all the April 1978 specimens is 3.57. This was calculated using the method described in Appendix A. The weighted mean remanent field for all the specimens is given by:-

$$\text{Intensity} = 190 \times 10^{-3} \text{ A.m}^{-1}$$

$$\text{Inclination} = -29^{\circ}$$

$$\text{Declination} = 105^{\circ}$$

The resultant of the induced and remanent components of the magnetisation was calculated for each specimen, and

the weighted mean of these resultant fields is:-

$$\text{Intensity} = 164 \times 10^{-3} \text{ A.m.}^{-1}$$

$$\text{Inclination} = +15^{\circ}$$

$$\text{Declination} = 97^{\circ}$$

These data are listed in Table 3.3.

Table 3.2 illustrates the extent to which the magnetic properties vary within a rock sample. For example, the Q value for M103 ranges from 0.0 to 15.6. Similarly the direction of its remanent magnetisation is variable, with the direction ranging from  $73.6^{\circ}$  to  $213.95^{\circ}$  and inclinations of  $-15.45^{\circ}$ ,  $-12.85^{\circ}$  and  $+31.2^{\circ}$ . This variation meant that each specimen had to be treated separately; so, for instance, M103 had to be considered as three samples rather than as three specimens of the same sample.

The directions of the remanent magnetisation, defined by the declination and inclination, were plotted on a stereographic projection (Fig. 3.4(a)). This diagram shows that there is no significant variation between the collection sites. It also indicates that when the remanent magnetisation has a northerly azimuth it is likely to dip down and when the magnetisation has a south-easterly azimuth it tends to dip upwards. Most of the results plot in the eastern section of the diagram.

A similar plot was drawn to show the direction of total magnetisation, that is, the resultant of the induced and remanent components (Fig. 4.4(b)). These

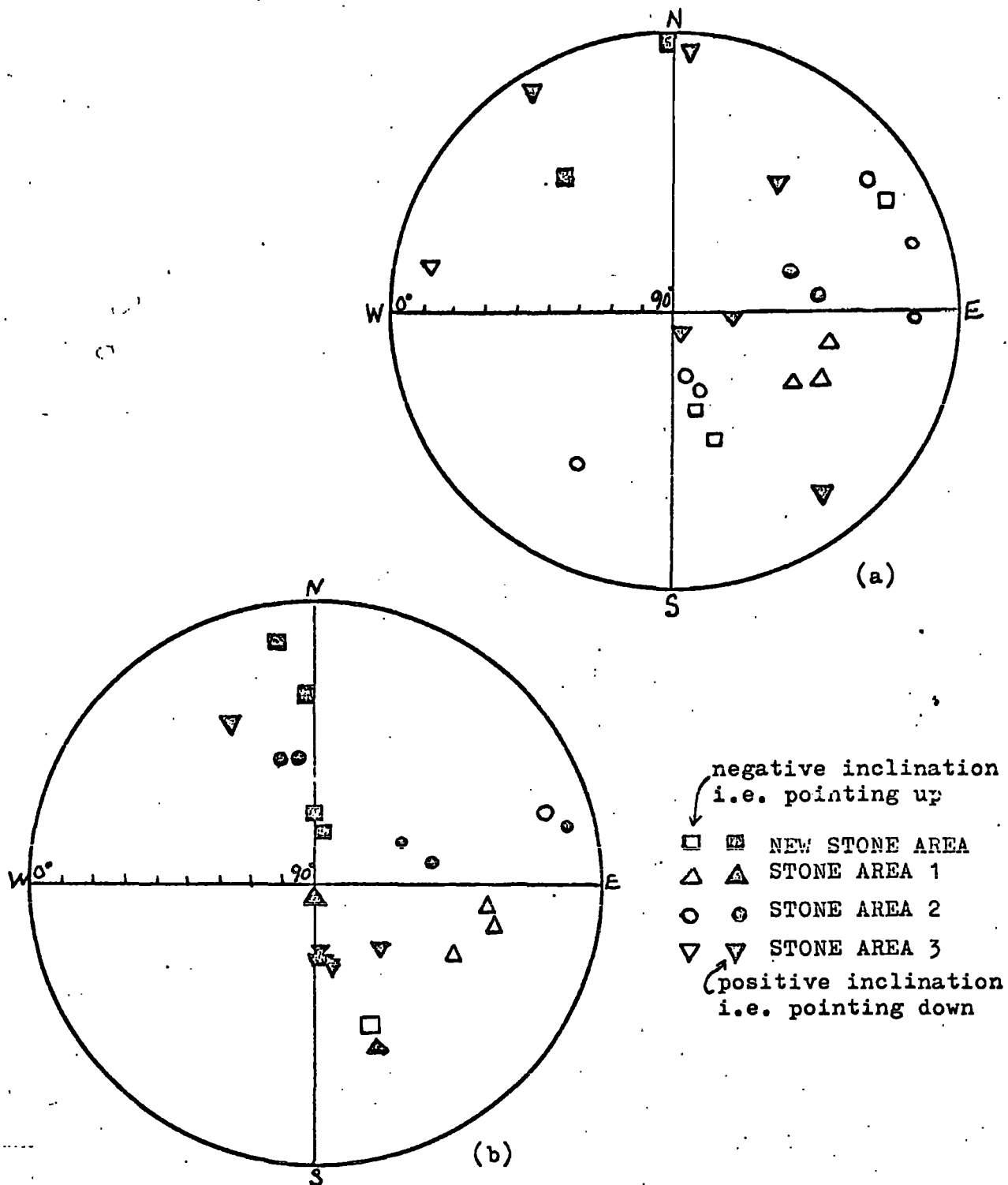
directions are less scattered than those for the remanent field and a greater number have a positive inclination. The declinations tend to be NNW or SE. None plotted in the south-west sector of the diagram. Despite their comparative clustering about the NNW-SE axis the plots have a low precision parameter,  $K = 1.85$ . This low value suggests that the results are well scattered since  $K = 0$  indicates a perfectly random distribution and  $K = \infty$  identical directions. When  $K$  is less than 10 the reliability of statistical estimates becomes uncertain. Such estimates include  $\alpha_{95}$  which is a measure of the accuracy,  $\theta_{63}$  (the circular standard deviation) which is a measure of the scatter of directions about that mean, and c.s.e. (the circular standard error). For all the 1978 results the mean direction of the total rock magnetisation is  $97^\circ$ ,  $+15^\circ$  (declination, inclination). For the total rock magnetisation:-

$$\begin{aligned} k &= 1.85 \\ \alpha_{95} &= 31.7^\circ \\ \theta_{63} &= 59.55^\circ \\ \text{c.s.e.} &= 13^\circ \end{aligned}$$

(for calculations see  
Appendix A)

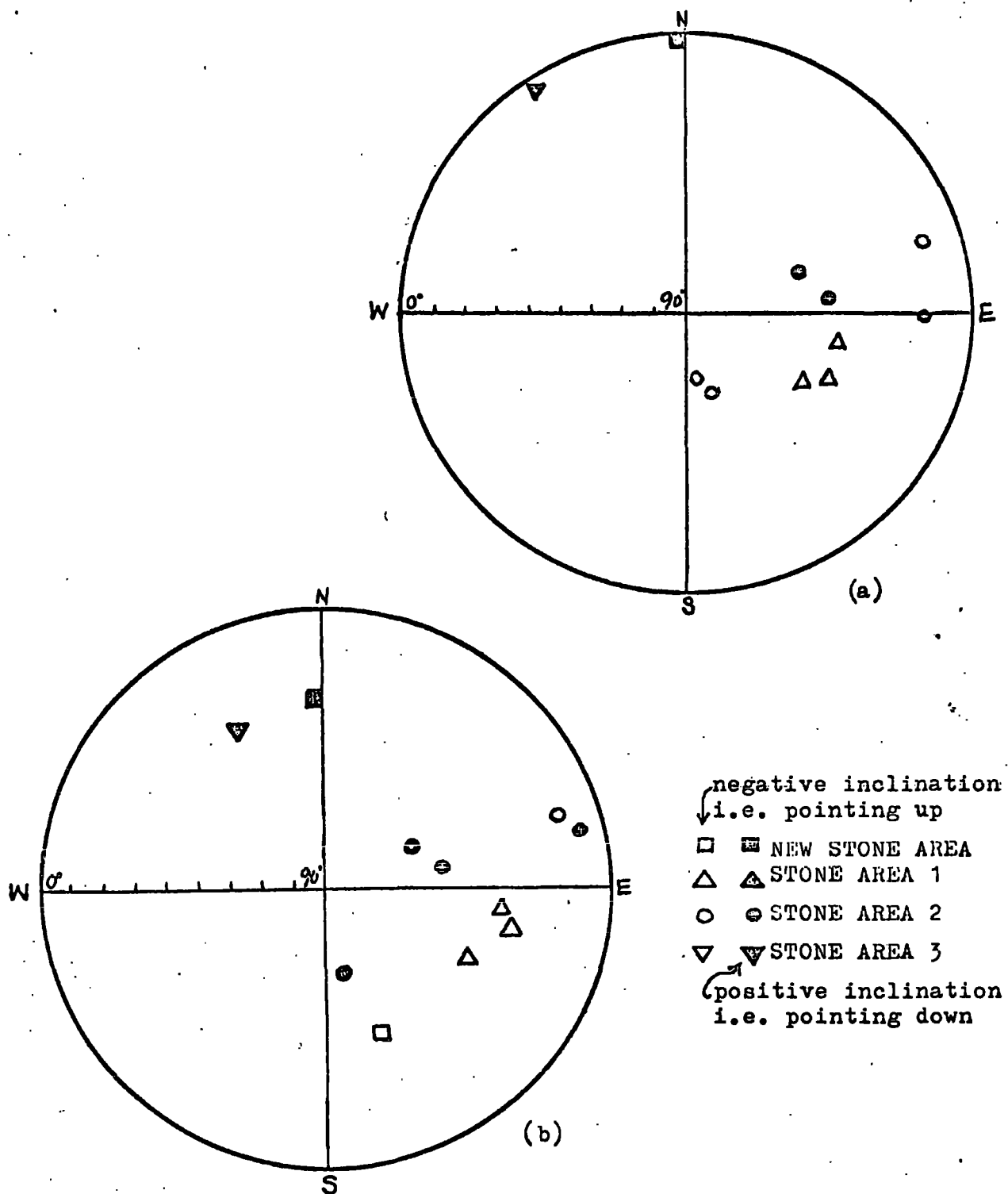
The large values of  $\alpha_{95}$  and  $\theta_{63}$  also suggest scatter.

When  $N$ , the number of samples, or  $K$  are small the other statistical parameters become unreliable (Tarling, 1971, pg. 79). In this case  $K = 1.85$  and the value of  $\alpha_{95}$  which is normally similar to that of c.s.e. is twice



**Fig. 3.4** Stereographic projections showing the directions of (a) Remanent magnetisation and (b) Total magnetisation (the resultant of the induced and remanent components) for samples taken from Meldon Quarry in April 1978.





**Fig. 3.5** Stereographic projections showing the directions of (a) Remanent and (b) Total Magnetisation for the Meldon Shale samples which have a Q value greater than 1.

that amount. This suggests that the statistical analysis done here is unreliable.

Fig. 3.5 shows stereographic projections on which the directions of remanent and total magnetisation for samples with  $Q$  values greater than 1 are plotted. These show the same trends as are described for the total rock, except that the results are more clustered in the eastern quadrant.

In conclusion, the results show that the directions of the remanent and total magnetisations are well scattered although there is some clustering about a roughly NNW-SE axis, especially for the total magnetisation. The degree of scatter does not significantly decrease when the directions for only those specimens with a  $Q$  value greater than 1 are plotted. The mean remanent and total magnetisations are both reversed and near horizontal; at  $105^\circ$ ,  $-29^\circ$  and  $97^\circ$ ,  $+15^\circ$  respectively, with a maximum error of  $30^\circ$ .

### 3.6 Petrographic Description of the rock samples

Polished sections of seven samples from Meldon Quarry and six from outside the metamorphic aureole were studied with the assistance of Mr. Roy Phillips. The object was to determine which minerals were responsible for the pronounced magnetic properties of some shales from Meldon Quarry, and to see if rocks from outside the metamorphic aureole contained similar minerals.

3.6.(1) Rocks from sites outside the metamorphic aureole

The shale and sandstone samples came from three different sites within the Crackington Formation (see Fig. 1.1);

Site 4: Aggetts Quarry (SX 2594 0961) A1, A2

Site 1: Building site near A30 (SX 2519 0900) S1

Site 2: Near Meldon village (SX 2562 0928)

H1, H2, H3

H1 and H2 are silty shales containing no coloured minerals except for a brownish tinge in some bands. The sandstone, H3, was similarly featureless.

The sandstone, A1, and the shale, A2, from Aggetts Quarry north of Okehampton contained no detrital or disseminated sulphides, though a veinlet was observed in A1. It mainly contained goethite ( $\alpha$  FeO.OH), the normal alteration product of pyrite.

S1 was more interesting because it is an iron nodule found in Crackington Formation shale. Pyrite crystals were seen in the centre of the nodule but they had been weathered to goethite around the perimeter.

From the point of view of the magnetic properties of the rock it is interesting that there are no ferromagnetic minerals in the rocks of the Crackington Formation outside the metamorphic aureole. Pyrite is sometimes present though often weathered to goethite. There are no indications that it has been thermally altered to, say, pyrrhotite. This confirms the findings

of others (Edmonds et al, 1968) that pyrrhotite is only found exposed at the surface in the Upper Culm Measures inside the metamorphic aureole. Beyond it pyrite, or its weathered derivative, is found. It is worth noting that pyrrhotite is believed to exist at depth beyond the metamorphic aureole, to a distance of 7 km. from the granite contact (Edmonds et al, 1968) and it has been found in bedded form in Lower Culm Measure rocks in the Wilsey Down borehole (Freshney in McKeown et al, 1973).

### 3.6.(ii) Rocks from Meldon Quarry

Polished sections of the following seven samples were made from rocks collected in October 1977: M2, M4, M12, M15, M17, M20, M22. The ferromagnetic mineral pyrrhotite was present in all seven samples, and, except for the rare occurrence of magnetite, it was the only magnetic mineral present. In all the specimens it was found disseminated through the ground mass. In this form it is probably thermally altered detrital pyrite. Other iron ores found as small crystals in the shales are also likely to have been altered from detrital minerals. However, the magnetite (M17) mentioned above is one of the rare minerals to have remained unchanged; similarly the pyrite in M4.

There is a second form of pyrrhotite present in some samples. Here it is a vein mineral often associated with chalcopyrite and pentlandite. The crystals tend

to be larger than those in the ground mass and were probably hydrothermally emplaced rather than being the alteration product of pre-existing minerals.

The veinlets are similar to those described by the I.G.S. (Beer and Fenning, 1976) in the boreholes at Sourton Tors, but they differ in detail. In their work no chalcopyrite was found in contact with the pyrrhotite; yet these intergrowths are common in M15, M17, M20 and M22. Another feature peculiar to the samples studied here is that the pyrrhotite contains exsolved pentlandite. This mineral is a Ni, Fe sulphide and it is exsolved from pyrrhotite as this mineral cools down through 300°C and can no longer contain much nickel in the lattice. The presence of pentlandite, then, indicates two things; firstly, that the pyrrhotite must have been at a temperature greater than 300°C, and, secondly, that it must have come from a source other than detrital pyrite which contains insufficient nickel. This indicates that the Meldon shales were near to a supply of nickel, such as from the volcanic tuffs with which some shales were deposited. By contrast the source for the Sourton Tors pyrrhotite was the detrital pyrite, in the shales of the Crackington Formation, which had been altered to pyrrhotite by the hydrothermal fluids associated with the granite intrusion.

In conclusion, therefore, it seems that two types of pyrrhotite have been developed in the Meldon shales,

probably as a result of those shales being metamorphosed by the Dartmoor granite. There is an almost ubiquitous development of disseminated pyrrhotite probably derived from detrital pyrite. The second form is the vein mineral, found in association with chalcopyrite and exsolved pentlandite. These vein minerals are believed to have derived their nickel from volcanic horizons, and been transported by hot solutions emanating from the granite.

### 3.7 Discussion of the results of the magnetic measurements and the mineralogical investigation

The results of the magnetic measurements indicate that sedimentary rocks, notably shales, have the most pronounced magnetic properties, and the mineralogical examination indicates that pyrrhotite is the mineral responsible for the ferromagnetic character of the rock. This confirms the findings of the I.G.S. (Edmonds et al, 1968, Beer and Fenning, 1976) that pyrrhotite bearing sediments have pronounced magnetic properties. Of the three lithologies studied the shales were the most magnetic and the igneous rocks less so. The magnetic susceptibilities listed in the Okehampton Memoir (Edmonds et al, 1968) also suggests that the sedimentary rocks can be more magnetic than the igneous rocks (see Table 1.2). The susceptibility for the non-hornfelsed Culm Measures ranges from 7-380 x 10<sup>-6</sup> (16 samples) whereas the igneous rocks (including

dolerite) cover the range  $7-234 \times 10^{-6}$  (20 samples) (c.g.s. units). Creer (1966) noted that the dolerites and volcanics of S. W. England have a magnetic intensity at least one order of magnitude less than those from elsewhere; the Whin Sill, for instance, at  $2-4 \times 10^{-3}$  A.m.<sup>-1</sup>. He suggested that this is because they have been remagnetised, probably when they were heated by the granite. However, it has been suggested (Creer and Chalmanaun, 1964) that there was widespread remagnetisation of the Laurasian continent during the early Permian, and this could have affected the igneous rocks.

Table 3.2 lists the magnetic properties of the samples taken in April 1978. It is apparent that there is considerable scatter between samples and within samples. This agrees with the findings of Cornwell (1967) who explained the variation in magnetic direction in terms of the anisotropic nature of pyrrhotite, and the variation in magnetic intensity to the sporadic distribution of this mineral. Pyrrhotite forms a Fe-S solid solution of which  $\text{Fe}_7\text{S}_8$  is the most abundant composition. All forms display magnetic anisotropy and when they freeze in a magnetic direction it will be aligned somewhere on the great circle between the direction of maximum susceptibility and the ambient field. It is noteworthy that the maximum susceptibility of the most

common form of pyrrhotite,  $\text{Fe}_7\text{S}_8$ , is the greatest for all forms. One result, however, which does not fit in with this picture is the tests for anisotropy done using the susceptibility bridge. When the specimen was rotated in the gap no appreciable change in reading was noted. However, this may be explained in terms of the random distribution of pyrrhotite crystals within each rock specimen.

When Cornwell (1967) plotted the directions of the remanent magnetisation for his Meldon samples on a stereographic net he found that rocks from Stone Area 1 and Stone Area 2 fell in the western half of his diagram whereas S.E. declinations were recorded for rocks from Stone Area 4. By contrast, the results shown here in Fig. 3.4 show no areal distribution, but are scattered throughout the eastern quadrants and are almost totally absent from the south-western area.

The weighted mean value for the remanent magnetisation was computed as  $105^\circ, -29^\circ$ . This does not agree well with Cornwell's result of  $189^\circ, -21^\circ$  except to confirm that the overall remanent magnetisation for the Lower Culm Measures in the Meldon area is reversed and near horizontal.

The shales collected in April 1978 have a mean susceptibility of  $13 \times 10^{-3}$  (c.g.s.) which is an order of magnitude greater than that for dolerite suggesting that the shales are capable of producing the magnetic



disturbances observed near Okehampton. The direction of the total magnetisation, taking account of both the remanent and induced components, is  $97^{\circ}, 15^{\circ}$ , which is a near horizontal east pointing field and would be expected to produce a negative anomaly, flanked to the north by a positive anomaly, similar to the Okehampton anomaly.

Before discussing the results of the mineralogical study it is worth considering the findings of the Wilsey Down borehole (unpublished I.G.S. log). This borehole was situated at SX 1797 8890 (220 090 on Fig. 1.1) north of the Bodmin Moor granite and beyond its metamorphic aureole. The Carboniferous rocks exposed at the surface on Wilsey Down contain pyrite, not pyrrhotite (Scrivenor, personal communication). In the borehole, beneath the drift, rocks of the Crackington Formation were encountered, below them Lower Carboniferous, Devonian and Lower Carboniferous again. In the Lower Carboniferous Fire Beacon Chert Formation, found beneath the Crackington Formation rocks, and equivalent to the Meldon Chert Formation bedded pyrrhotite was found. It was common at depths of 250 ft. (78 m.) and 850 ft. (262 m.).

This discovery of pyrrhotite was unexpected in view of its absence elsewhere beyond the aureole. Its form also differs from that found in the Meldon samples, described earlier in the chapter, in which the pyrrhotite was disseminated or concentrated in small veins. These forms are probably a direct result of contact metamorphism when the

Dartmoor granite was intruded. Detrital pyrite was altered to pyrrhotite, and enough Fe and S was dissolved in hot solutions emanating from the granite to produce vein pyrrhotite. By contrast, the bedded pyrrhotite found in the Wilsey Down borehole is thought (Beer, personal communication) to have been formed when the shales were still wet and they reacted with volcanic solutions rich in iron and sulphur. There are a number of greenstone, ash and tuff horizons in the Fire Beacon Chert Formation and these are thought to have been injected into the unconsolidated sediments and been the source of both the iron and sulphur and the hot solutions which transported these elements. Even though no pentlandite has been recorded it is thought that it is mineralogically possible for it to exist as these volcanic solutions are likely to be rich in nickel. The Fire Beacon Chert Formation contains a variety of rock types but the pyrrhotite is always developed in the shale horizons.

As in the Wilsey Down case it was the shale samples from Meldon which contained pyrrhotite. In these samples pyrrhotite was found disseminated through the shale horizons or concentrated in veins. The former is probably thermally altered detrital pyrite, and could only be developed within the metamorphic aureole of the Dartmoor granite. The vein pyrrhotite was deposited by hot solutions rich in iron and sulphur. These solutions probably emanated

from the granite but the elements which make up the pyrrhotite could not have come solely from detrital pyrite as it contains insufficient Ni to produce exsolved pentlandite such as that described in the polished sections. It seems likely that the nickel and much of the Fe and S came from the volcanic horizons in the Lower Culm Measures. If this were the case they could have provided the hot solutions which mobilised the Fe, Ni and S instead of solutions from the granite. This would then provide another mechanism by which pyrrhotite could be developed beyond the metamorphic aureole. Solution movement of this kind would be greatly facilitated by the complex fault system (Dearman and Butcher, 1959). The development of pyrrhotite in shales would depend on the ease with which a metasomatising fluid could get from an area rich in S, Fe, and Ni, such as a volcanic horizon, to the host rock. As a result the distribution of ferromagnetic rock seems sporadic.

From what has been described it seems that there are two possible modes of pyrrhotite emplacement outside the metamorphic aureole; bedded pyrrhotite such as at Wilsey Down, or the vein mineral similar to that seen within the aureole at Meldon and believed (Edmonds et al, 1968) to extend beyond it. Edmonds et al (1968) suggest that the injection temperature of the Dartmoor granite was 600-700°C and that vein pyrrhotite could exist up to a distance of 4½ miles (7 km) from the granite contact.

In the Meldon district pyrrhotite is found, at the surface, exclusively in the metamorphic aureole. However, this may be explained by the lithology. The outer limit of the metamorphic aureole coincides with the northernmost extreme of the Lower Culm Measure outcrop, so pyrrhotite mineralisation is contained within the Lower Carboniferous rocks and those Upper Culm Measures near to the granite where mineralising fluids were most active. It seems likely that further from the granite batholith hydrothermal fluids may only leave their mark in the more chemically active Lower Carboniferous rocks. Alternatively, banded pyrrhotite may be found at depth in the older Culm Measures.

The occurrence of pyrrhotite in the Meldon samples confirms the findings of Cornwall (1967) and the I.G.S. (Beer and Fenning, 1976) that near surface developments of this iron sulphide in the metamorphic aureole are responsible for the large high frequency anomalies measured on ground traverses.

In conclusion, it seems that pyrrhotite developed in the Lower Culm Measures could be found beyond the metamorphic aureole, and as Freshney (Boscastle and Holsworthy Memoir, 1973) suggests in his Wilsey Down borehole report:-

"A line of aeromagnetic anomalies of near-surface origin extends westwards (from Wilsey Down) to the coast at Boscastle, and eastwards towards Okehampton. These anomalies are probably due mainly to the presence of pyrrhotite ... this mineral is largely confined to the Fire Beacon Chert Formation ... it breaks surface (at Tregeare Down, SX 2250 0864) and the Meldon Chert Formation crops out thence almost continuously to Drewsteignton."

## CHAPTER 4

### INTERPRETATION

#### 4.1 Introduction

The interpretation of the magnetic anomalies was done in three steps. *Rough* depth estimates were made using Peter's Length and Solokov Length (Åm, 1972). Then, having shown that both the Okehampton Anomaly and the local disturbances are near surface, the aeromagnetic map and profiles were compared with the known geology to see if any deductions could be made about the causal body or bodies.

Attempts were made to assess the dimensions of the body, and its direction of magnetisation, using the graphical methods of Bruckshaw and Kunaratnam (1963) and Åm (1972), but they were not wholly successful. Finally computer models were devised and their feasibility assessed in the light of known geology.

#### 4.2 Depth Estimates

An estimate of the depth **to a body (if near vertical)** causing the Okehampton Anomaly can be obtained by direct measurement from the drawn profile. Peter's Length (PL)




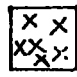
and Solokov Length (SL) are two such parameters ( $\dot{A}_m$ , 1972). Peter's Length is the horizontal distance between two points on the anomaly at which the tangent has half the maximum slope and the Solokov Length is the horizontal length of the inflection tangent as it rises from the minimum to the maximum value of the anomaly. These lengths are based on the mathematical expression for the vertical component of the anomalous field produced by a vertically magnetised dyke with vertical sides extending to infinity. The relationship between these lengths and the depth to body, depends on the ratio of the depth,  $z$ , to the width,  $t$ , of the body. For  $t/z = 2.2$ ,  $PL = 1.6z$  and  $SL = 2z$ . For a greater value of  $t/z$  the measured lengths are a larger multiple of the depth.

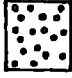
Measurements made on the traverses along lines 3, 4 and 5 gave the depth to the body causing the Okehampton Anomaly to be in the range 41-128 m. This is the same order of magnitude as the depth estimate of 46-81m. made by the I.G.S. (Edmonds et al, 1968) and this shows that the body is near surface, so study of the surface geology may have direct relevance to assessing the nature of the body. Also, when a body is near surface, the areal extent of the magnetic anomaly is often comparable to the size of the body.

#### 4.3 The Aeromagnetic Map and Geology

The overlay to Fig. 4.1 is part of the unpublished 1:25,000 aeromagnetic map made for the I.G.S. The

Key for Fig. 4.1

Carboniferous:	Upper	Crackington Formation	{ mainly shale some sandstone	
		Meldon Chert Formation	{ mainly chert and limestone	
	Lower	Meldon Slate and Quartzite Formation	{ mainly chert	
			{ mainly tuff	

Transition Series (Devonian/ Carboniferous)	{ Meldon Slate with Lenticles Formation	{ slaty hornfelses and silty quartzite	
---	---	---	---

Igneous Rocks:

Dolerite



Granite



(nomenclature after Edmonds et al, 1968)

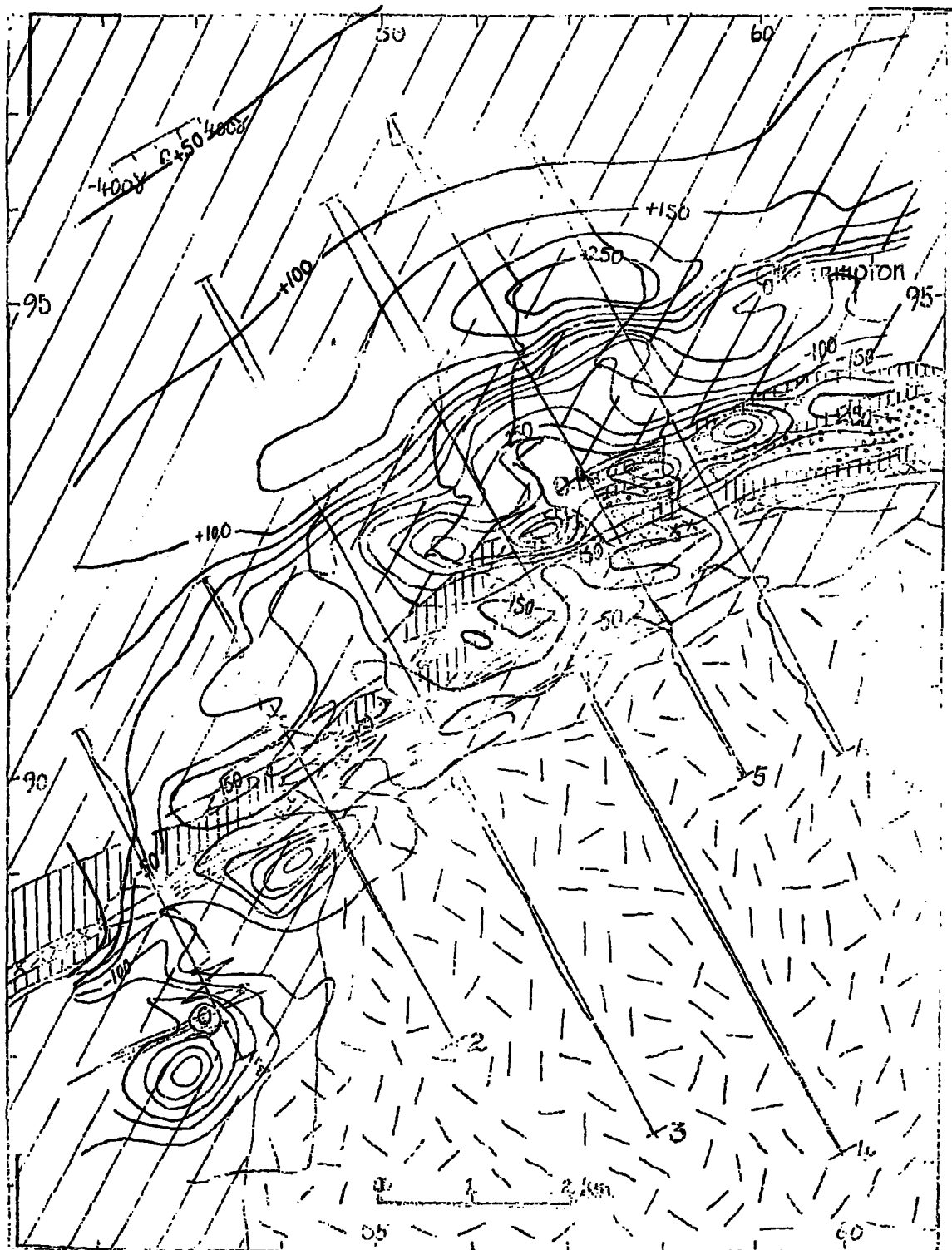


Fig. 4.1 Simplified Geology of north-west Dartmoor showing the magnetic profiles. Geological map after Doberman & Fletcher, 1977.

Aeromagnetic Map -



elongate negative anomaly centred at 565 930 and marked O.A. is the Okehampton Anomaly. It is roughly 6 km. by 1.5 km. in size and it peaks at about 2.5 km. north east of the granite contact. The positive peak, 2 km. to its north, is smaller in amplitude. The peak to peak amplitude is 550γ.

The anomaly lies along the boundary between an area of magnetic high to the north-west and magnetic low to the south-east, and it is clearly caused by a reversely magnetised body as the negative peak occurs to the south of the positive peak and is the larger of the two peaks.

The axes of both anomalies run approximately parallel with the granite contact. The axis of the negative anomaly is almost coincident with the northern boundary of the Meldon inlier and the outer limit of the metamorphic aureole. Consequently the negative anomaly falls over rocks of both Upper and Lower Culm Measure age, some of which have been thermally metamorphosed by the Dartmoor granite. By contrast, the positive peak occurs only over rocks of the Upper Culm Measure Crackington Formation which show no signs of thermal alteration.

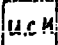
#### 4.4 The Profiles and Geology

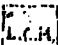
##### 4.4(1) The Okehampton Anomaly

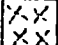
Figs. 4.2 to 4.7 show the ground and aerial profiles with cross sections of near surface geology along lines 1 to 6. Of these, lines 1 and 2 measure small disturbances


The following Figures (Figs. 4.2 - 4.7) show the ground and aerial profiles along Lines 1 - 6 as well as cross-sections of the near-surface geology taken from the Okehampton Geology Map No.324 and Dearman and Butcher (1959). The geographical location of the profiles is shown in Fig. 4.1.

The symbols used are as follows:-

 Upper Culm Measures (Upper Carboniferous)

 Lower Culm Measures (Upper Carboniferous) ... rocks of Transition Series age may be included among these.

 Granite

 outer limit of the metamorphic aureole

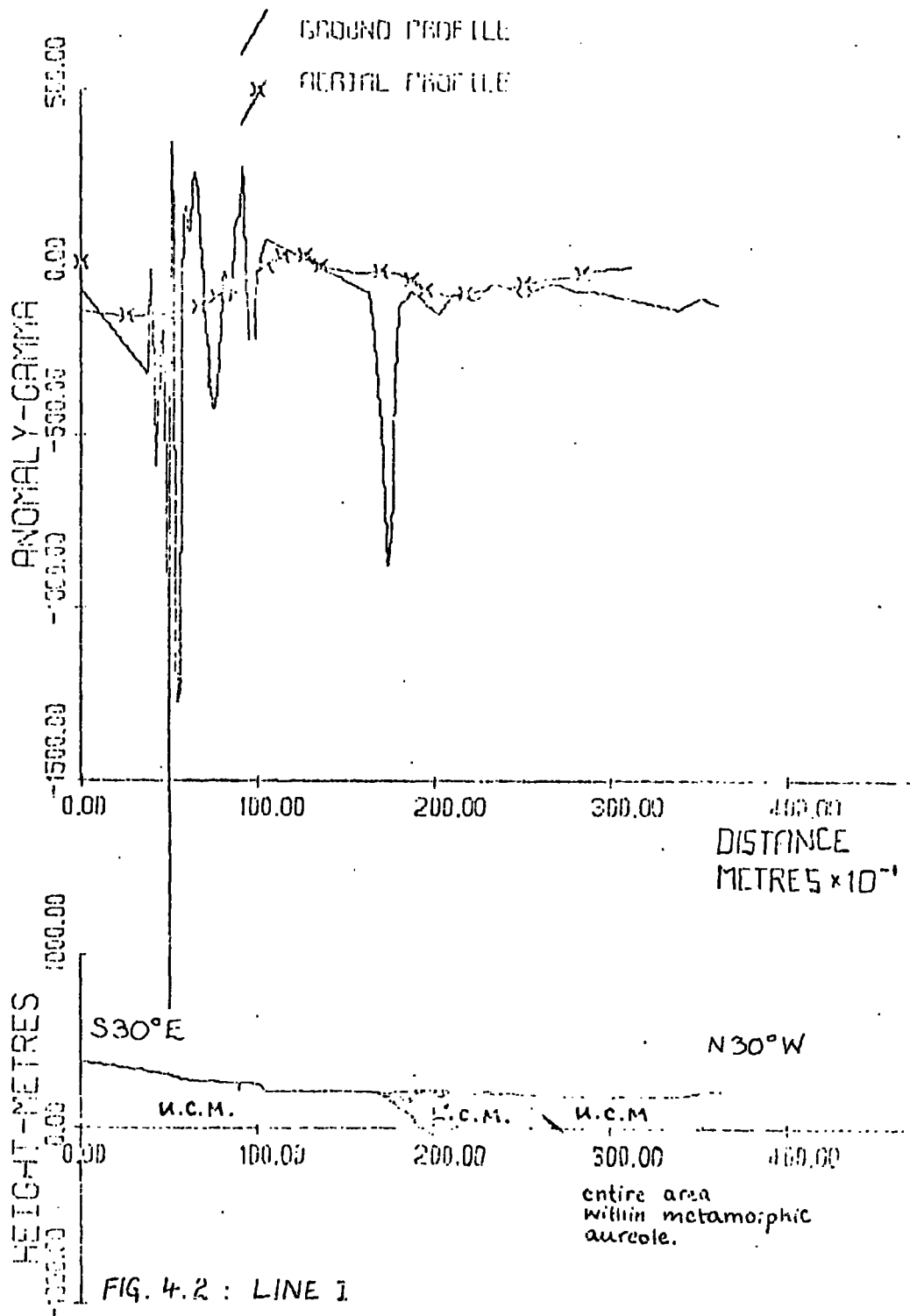


FIG. 4.2 : LINE 1

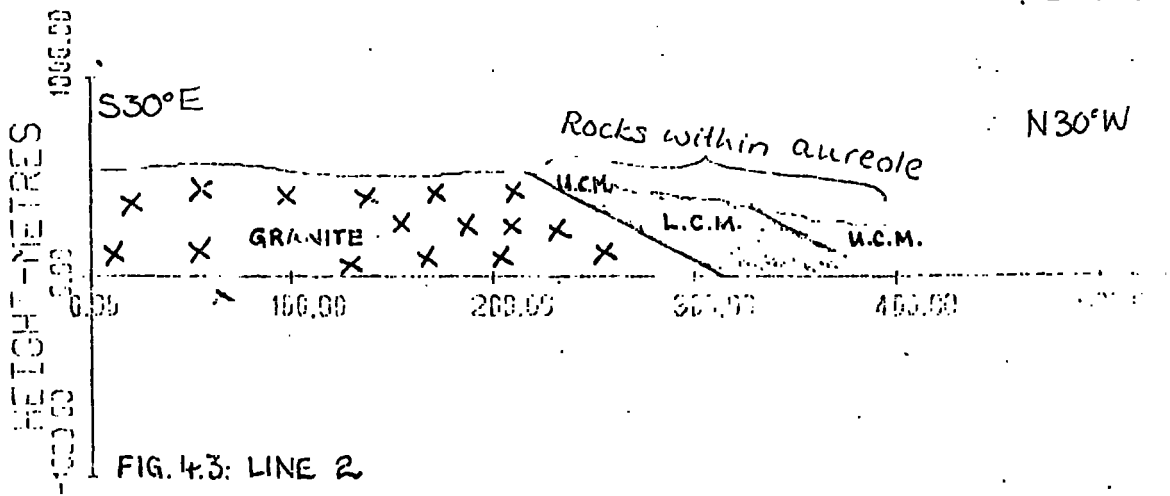
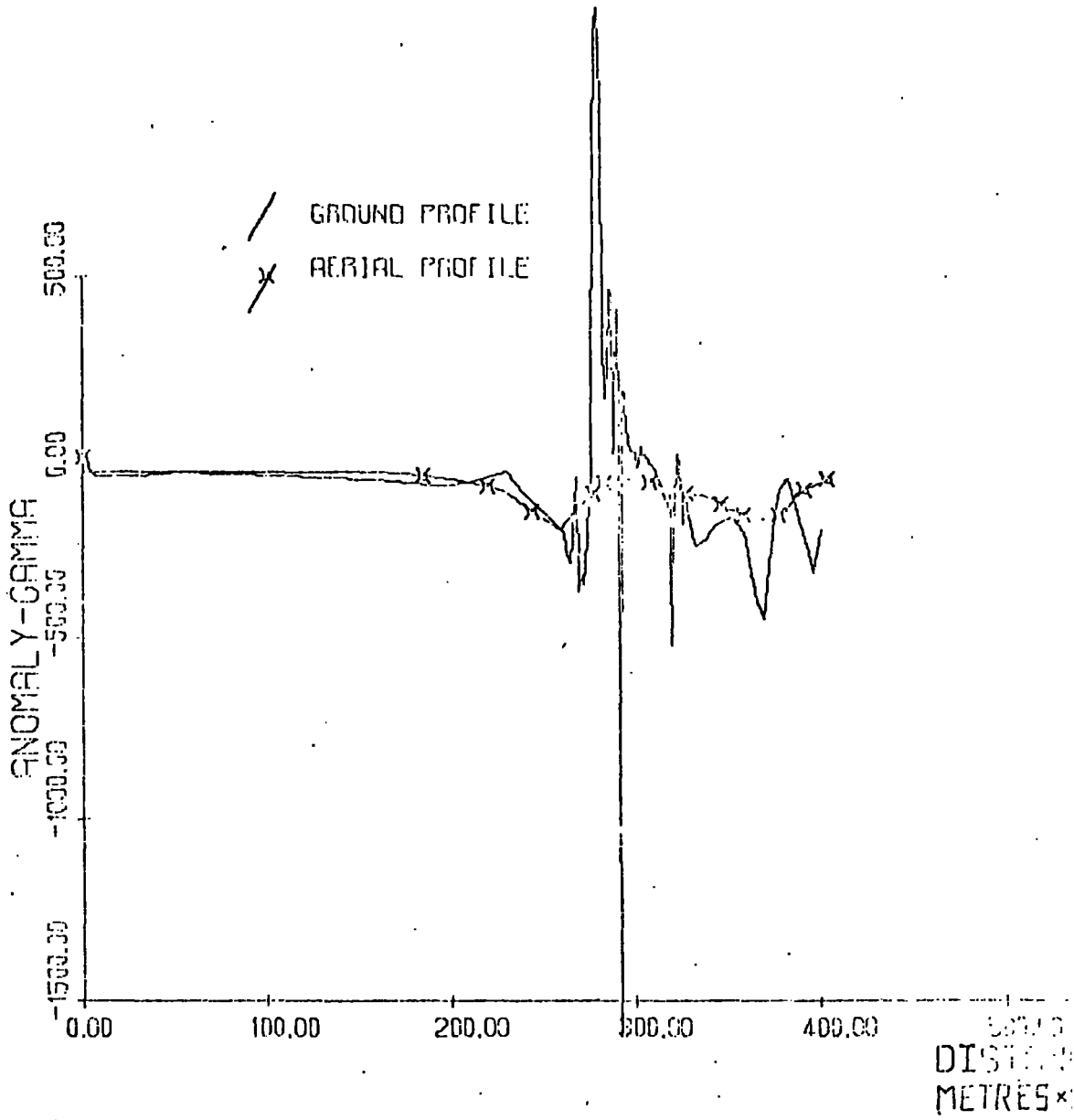


FIG. 4.3: LINE 2

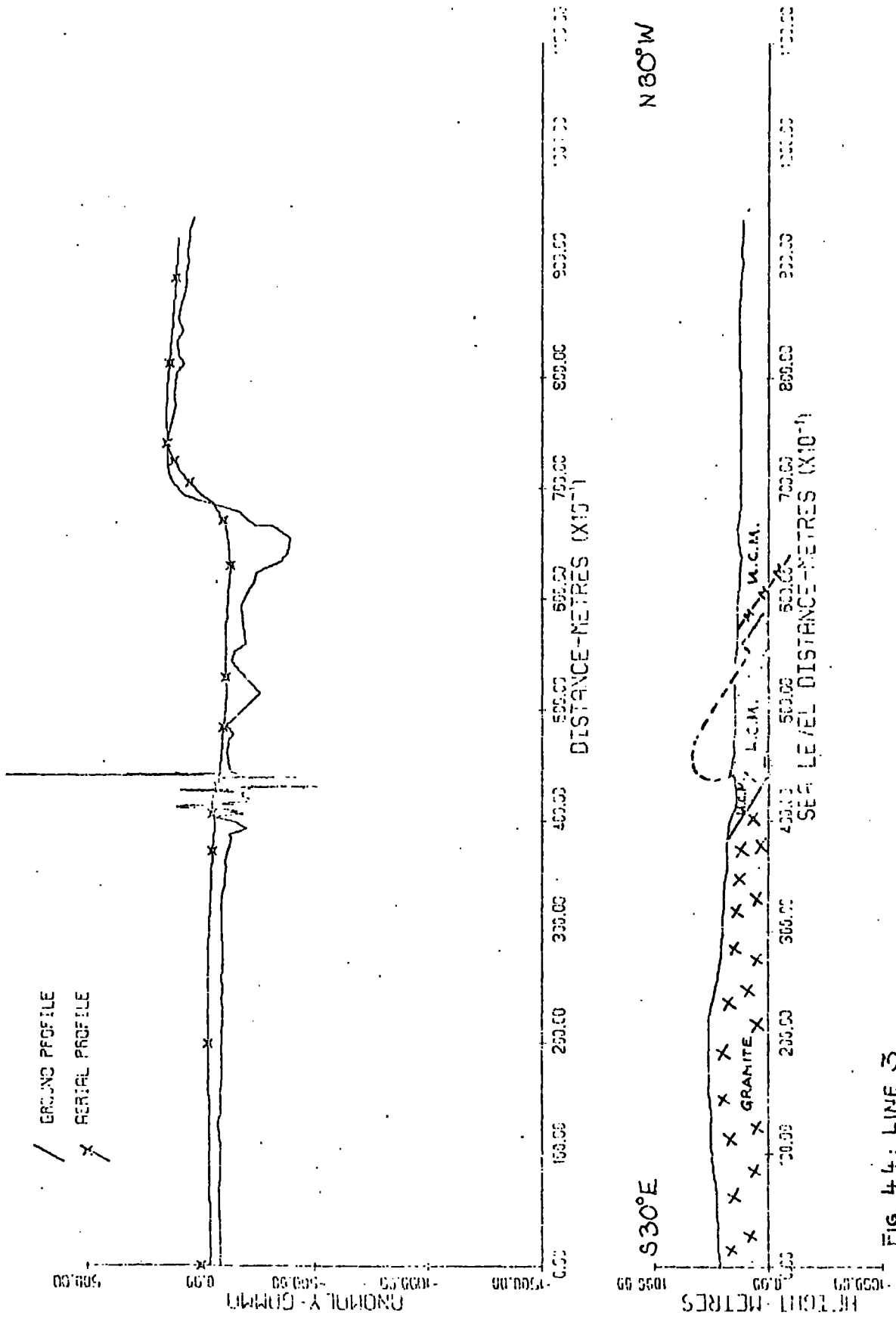


FIG. 4.4: LINE 3

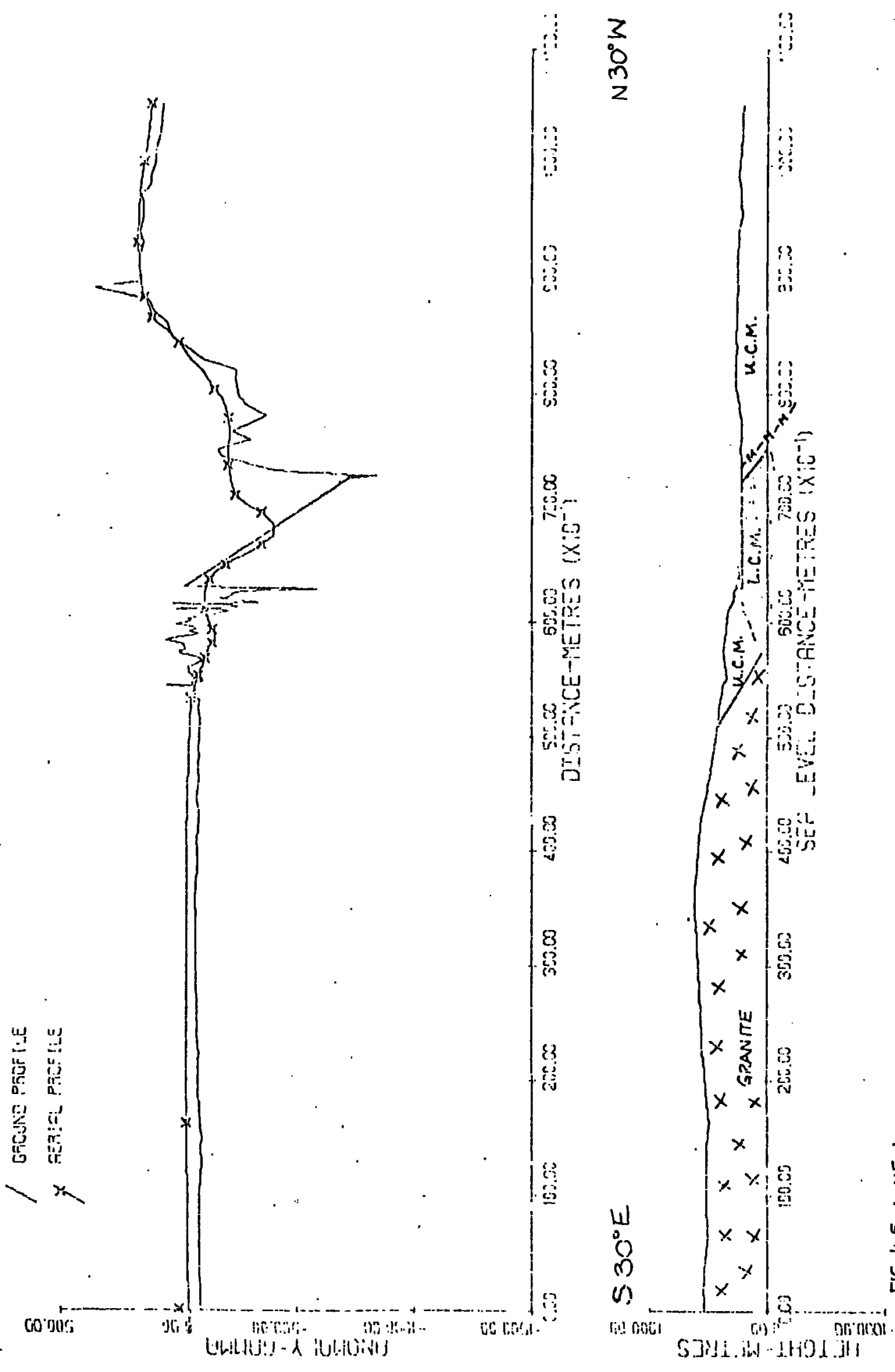


FIG. 4-5: LINE 4

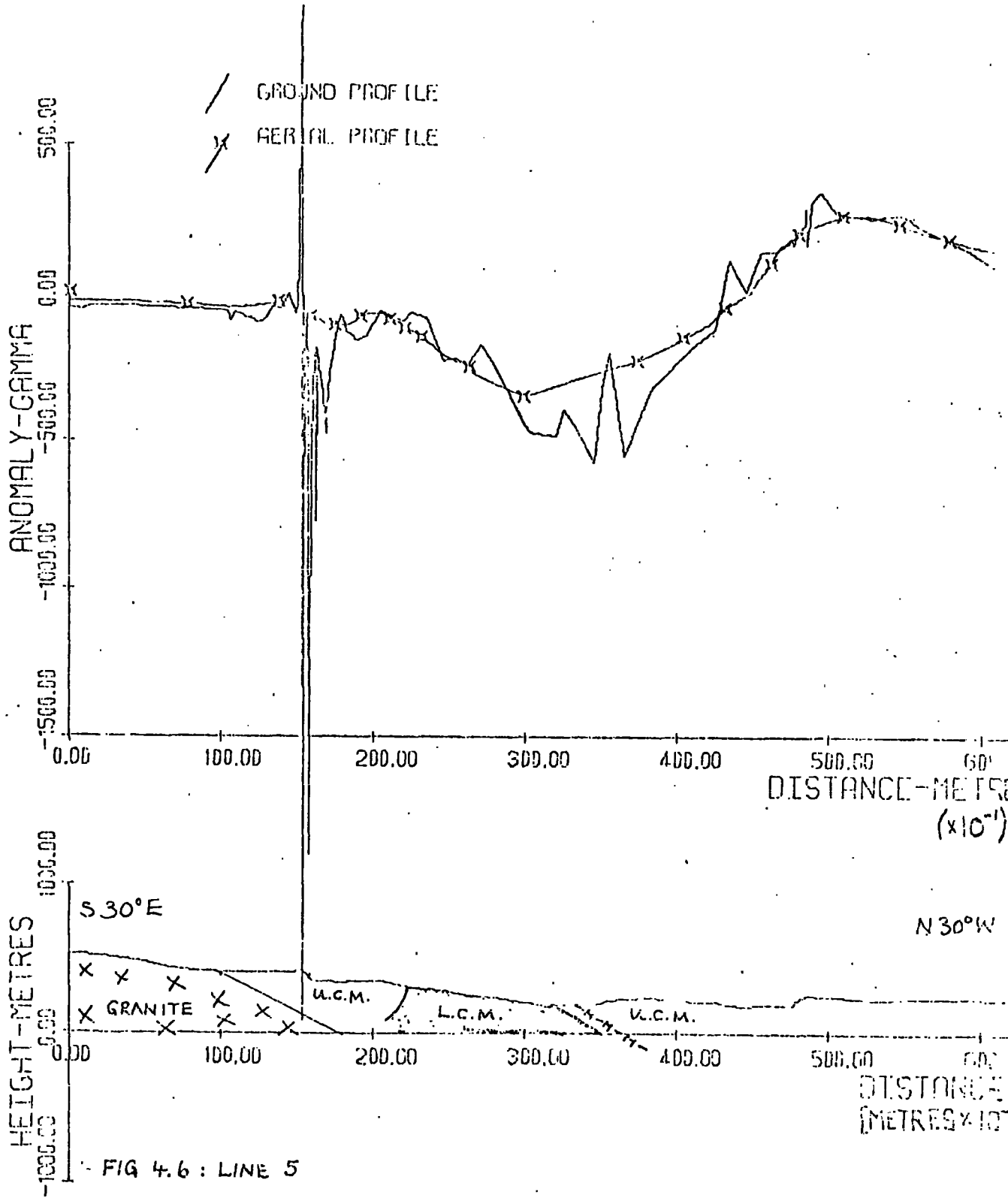


FIG 4.6 : LINE 5





south-west of the Okehampton Anomaly while lines 3,4,5 and 6 transect this major anomaly. With the exception of line 3 all the lines which define the Okehampton Anomaly show that the negative anomaly occurs over rocks of both Lower and Upper Culm Measure age. The major minimum along line 3 occurs approximately 2 km. north of the Meldon inlier, but this profile should be treated separately as it occurs along the Prewley fault (see Fig. 1.2) and so may be anomalous.

By studying lines 4,5 and 6 a number of inferences concerning the body causing the Okehampton Anomaly can be made. The causal body is reversely magnetised. Lines 4 and 6 suggest that it is a composite body as there are a series of steps in the overall anomaly (see Figs. 4.5 and 4.7). Each step marks the approximate position of a particular body. The width of the near surface causal body or bodies can also be estimated as it is comparable to the distance between the negative feature and the positive feature flanking it to the north. So, the body is of the order of 2 km. in width along lines 4,5 and 6 and 1 km. for line 3.

It is apparent that the causal body, or bodies, stretch from the Lower Culm Measure sediments north into the Crackington Formation rocks. However, Dearman and Butcher (1959) have shown that the Lower Culm Measure rocks continue north beneath these later sediments at a shallow depth (see Fig. 1.3). This could suggest that

the causal body is entirely Lower Culm Measure in age, and that it continues beneath the Upper Culm Measure sediments north of the Meldon inlier.

#### 4.4.(ii) The local magnetic disturbances

The large local magnetic disturbances detectable only along the ground traverses all occur over Lower and Upper Culm Measure rocks, and are confined to the metamorphic aureole.

Fig. 4.1 shows a geological map of the area on which the ground profiles have been superimposed. From this it is possible to determine the relationship between the profiles and the outcropping rocks.

Line 1: The cluster of short wavelength anomalies located between 500 m. and 1000m. from the southern end of the line fall over shales and sandstones of the Crackington Formation. The negative peak at 1800 m. occurs over shales and tuffs of the Meldon Slate-and-Quartzite Formation, and rocks of the Meldon Chert Formation.

Line 2: The series of peaks and troughs situated between 2000 m. and 4000 m. from the southern end of line 2 occur over a variety of rock types; tuffs and shales of the Meldon Slate-and-Quartzite Formation, Chert Formation sediments, dolerite and Upper Culm Measure shales of the Crackington Formation.

- Line 3: Line 3 is situated just east of the Prewley fault (see Fig. 1.2). The short wavelength magnetic disturbances occur over Lower Carboniferous shales and cherts as well as shales of the Upper Carboniferous Crackington Formation.
- Line 4: Short wavelength anomalies are found over rocks of the Lower Carboniferous Slate-and-Quartzite and Chert Formations. They are also found over shales of the Crackington Formation where it is exposed between the granite and the inlier. There is a gap in the profile, shown as a dotted line, in which no readings were taken. The aeromagnetic profile suggests that, at this point, this profile should define the southern side of the negative anomaly of which the minimum is situated on the northern side of the gap.
- Line 5: The cluster of large amplitude short wavelength anomalies are found above the Crackington Formation sediments between the inlier and the granite. Small anomalies are also superimposed on the major Okehampton anomaly.
- Line 6: The negative and positive peaks which occur at 1700 m. and 2200 m. from the southern end of this line occur over sediments of the Crackington Formation.

The observations described above suggest that the distribution of the short wavelength anomalies is not lithologically controlled as these disturbances occur over a variety of rock types. These include chert, limestone and tuff from Lower Carboniferous horizons and shale from both the Lower and Upper Culm Measures. There is only one occurrence of a high amplitude disturbance in association with dolerite (line 2) even though dolerite is exposed throughout the inlier. This suggests that the usually marked magnetic properties of this rock may have been reduced here.

#### 4.5 Discussion of the observations

This discussion can be divided into two parts: an analysis of the short wavelength anomalies detectable only on the ground traverses, and an interpretation of the Okehampton Anomaly.

##### 4.5(i) Local Magnetic Disturbances

Figs. 4.2 to 4.7 show that the short wavelength anomalies occur only over rocks which are contained within the metamorphic aureole. These local anomalies are sporadically distributed over a variety of rock types, suggesting that the ferromagnetic mineral, or minerals, which cause them are not contained in specific lithologies but have been emplaced in rocks near to the granite contact. These observations agree with the findings of Cornwell (1967) and Peir and Fenning (1976) who suggested

that the iron sulphide, pyrrhotite, is the major ferromagnetic mineral and that it was metasomatically emplaced during a late stage in the intrusion of the granite. High concentrations of this mineral near to the surface, such as in the samples described in Chapter 3, could produce large local anomalies like those detected along the ground traverses. The sporadic distribution of these magnetic disturbances could then be explained in terms of the hydrothermal emplacement of pyrrhotite, described in Chapters 1 and 3.

#### 4.5.(ii) Okehampton Anomaly

Only a limited amount of information about the body causing the Okehampton Anomaly can be inferred from the ground profiles. Depth estimates (lines 3,4, & 5) suggest that the body is as shallow as 41-128 m. so the surface geology should give some information about its nature. The major negative anomaly runs approximately parallel with the granite contact and straddles the boundary of the metamorphic aureole (see Fig. 4.1). The positive peak lies well beyond this aureole. If the body is of the same nature as the exposed rock it comprises Culm Measure sediments which have only been metamorphosed along their southern edge but which could have been effected by hydrothermal solutions emanating from the granite.

#### 4.6 Graphical Interpretation

Numerous attempts were made to interpret the profiles made along lines 3,4,5 and 6 using the graphical methods

of Bruckshaw and Kunaratnam (1963) and Am (1972). The other two profiles were too complex to permit interpretation using these methods.

These methods provide values for the width and depth to top surface of the causal body and the value of the parameter  $i$ , defined below.  $i$  is known to have a value between  $180-270^{\circ}$  as the negative anomaly lies south of, and is larger than, the positive peak (Bruckshaw and Kunaratnam, 1963). Now,  $i = \phi + \psi - \theta$ , where  $\phi$ ,  $\psi$  and  $\theta$  are angles in the plane of the profile which describe the inclination of the earth's magnetic field ( $\psi$ ), the inclination of the magnetisation of the body ( $\phi$ ), and the dip of the body ( $\theta$ ). Values for  $\phi$  and  $\psi$  are known so it is possible to calculate  $\theta$ . It was hoped that the traverses were lined up perpendicular to the strike of the body as they lie perpendicular to the long axis of the magnetic anomaly, so that the value of  $\theta$  should correspond to the dip of the body.

The values of the declination and inclination of the earth's magnetic field for the epoch 1977.8 were taken from U.S. Admiralty Charts (3rd edition, 1966) and were calculated as Intensity = 0.478 Ce, Declination =  $352^{\circ}$  and Inclination =  $66^{\circ}$ . As the traverses did not run north-south but  $330^{\circ}$  the declination relative to the profile and hence the dip of the field in the plane of the profile had to be calculated using the following formulae:-

$$D' = D - \alpha$$

$$\tan \phi = \tan I / \cos D'$$

where:

D = declination relative to geographic north

I = inclination

$\alpha$  = declination of profile relative to  
geographic north

D' = declination relative to profile

$\phi$  = inclination in plane of profile

These formulae were also used to define the possible directions of magnetisation of the causal body using the measurements of Cornwell (1967) and those described in this thesis (see Chapter 3). The table below lists the results of the calculations.

	Earth's field	Results described in this thesis		Cornwell's results
D	352°	97°	105°	189°
I	66°	15°	-29°	-21°
D'	22°	127°	135°	219°
$\phi$	80°	156°	180°	206°

*remnant* →  
← *resultant*

*remnant*

A number of problems were encountered when parameters taken from the drawn profiles were plotted on the standard curves (Bruckshaw and Kumeratna, 1963, Åk, 1972). Firstly a problem arose because the measurements were taken from the ground profiles. The depth to body has already been

shown to be 41-128 m. and its width is thought to be 1-2 km. This gives a width-depth ratio ( $t/z$ ) of the order of 20. However the standard curves of Åm (1972) and Bruckshaw and Kunaratnam (1963) only go up to a  $t/z$  value of 10 and 15 respectively, so the data could not be plotted. To get around this problem the aerial profiles were studied as the depth to body would be increased by the flying height of 500 ft. (167 m.), and  $t/z$  would fall into the permitted range. But even the aerial profiles could not be successfully interpreted. There is thought to be a twofold reason for this. Both graphical interpretation methods assume that the causal body can be approximated to a dyke like body with infinite sides while the body causing the Okehampton Anomaly is composite and tapers to east and west.

The other problem is the background field. As has already been mentioned the Okehampton Anomaly marks the boundary between a region of high to the north and one of low magnetic field to the south. This means that a sloping regional field exists in the area of the anomaly. It was impossible to gauge its true value as the traverses were insufficiently long to show it clearly. So, as the regional field could not be removed the anomaly could not be studied in isolation.

Despite repeated attempts to plot the measured parameters only one set of results was obtained and even these were unreliable. They are listed below:-



LINE	$i$	$t/z$	$z$	$t$	$\theta_I$	$\theta_{II}$
3	$202^\circ$	5	59 m.	1130 m.	$45^\circ$	$84^\circ$
4	$194^\circ$	3.2	122 m.	925 m.	$53^\circ$	$92^\circ$
5	$189^\circ$	6	42 m.	1254 m.	$58^\circ$	$97^\circ$

where:-

$z$  = depth from surface to top of body

$t$  = width of body

$\theta_I$  and  $\theta_{II}$  = dips of body in plane of profile for two directions of magnetisation:-

(I) values measured here (total)

(II) Cornwell's results (remanent)

Of these the results for lines 4 and 5 proved to be incorrect when they were tested using the computer (see next section). The **dimensions** for line 3, however, gave a reasonable fit.

## 4.7 Computer Modelling

### 4.7(i) Introduction

A number of computer models were made to describe the possible geological structures in the Meldon area which could cause the observed magnetic disturbances. Models were only made to explain the aeromagnetic profiles (taken from the unpublished 1:25,000 map) as the high frequency anomalies observed along the ground traverses were considered too complex to interpret quantitatively. The magnetic properties of the rock samples from Meldon Quarry, described in Chapter 3, were used to indicate the likely direction of magnetisation (the resultant of the induced and remanent components) of the causal body. The geologic structure of the Meldon district is fairly well known (Dearman and Butcher, 1959, Edmonds et al, 1968, Sanderson and Dearman, 1973, Hobson and Sanderson, 1975) so the feasibility of the various models could be assessed.

4.7(ii) Mathematical limitations

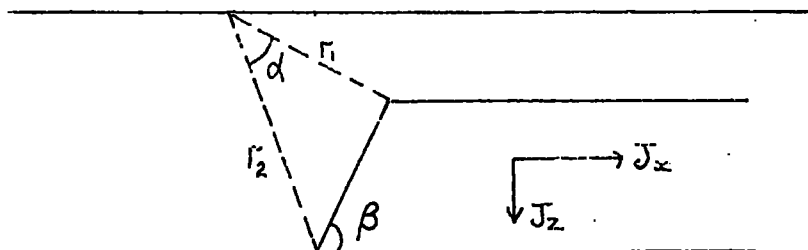
The modelling was done using MAGN, a program compiled by M. H. P. Bott and stored at Durham University, and the output plotted using MAGPLOT (see Appendix B). MAGN computes the anomaly produced by a two dimensional body, or bodies, situated in the plane of the profile.

The value of the vertical and horizontal anomalies at a given point is given by the formulae:-

$$\Delta Z = \frac{\mu_0}{2\pi} \sin\beta \left[ J_x \cdot \left( \ln\left(\frac{r_1}{r_2}\right) \sin\beta + \alpha \cos\beta \right) + J_z \cdot \left( \ln\left(\frac{r_1}{r_2}\right) \cos\beta - \alpha \sin\beta \right) \right]$$

$$\Delta H' = \frac{\mu_0}{2\pi} \sin\beta \left[ J_x \cdot \left( \alpha \sin\beta - \ln\left(\frac{r_2}{r_1}\right) \cos\beta \right) + J_z \cdot \left( \ln\left(\frac{r_2}{r_1}\right) \cdot \sin\beta + \alpha \cos\beta \right) \right]$$

where  $\mu_0$  is the permeability of free space and  $J_x$ ,  $J_z$ ,  $\alpha$ ,  $\beta$ ,  $r_2$  and  $r_1$  are as shown in the diagram below.



Information about the direction of the magnetisation of the body is fed into MAGN in a specific form: as declination relative to the profile ( $D'$ ) and the dip ( $I$ ).

However many combinations of  $D'$  and  $I$  can produce the same value of  $\phi$  where  $\phi$  is defined as  $\phi = \tan^{-1} (\tan I / \cos D')$  or  $\phi = \tan^{-1} (J_z / J_x)$ . So, the models obtained using MAGN only indicate one of the possible directions of magnetisation of the body. It is therefore more realistic to consider the direction of magnetisation in terms of  $\phi$ , and then discuss the possible combinations of  $I$  and  $D'$  which could provide the required value of  $\phi$ .

Another effect of operating in two dimensions is that the value for the intensity of magnetisation used in the model is  $J_{x,z}$ , the resultant of the  $x$  and  $z$  components of the actual intensity ( $J$ ). The true value is calculated using the formula:-

$$J = (J_{x,z}) / (\cos^2 D' \cdot \cos^2 I + \sin^2 I)^{\frac{1}{2}}$$

The first models attempted were those devised using the data obtained by graphical methods. The models for lines 4 and 5 gave a magnetic anomaly which bore no relationship to the observed disturbance but the model for line 3 was successful (see Fig. 4.8). Bodies dipping north at both  $45^\circ$  and  $84^\circ$  produced an adequate fit along line 3, but for reasons that will be described later a dip of  $45^\circ$  was considered more likely.

#### 4.7(iii) Geological Limitations

Because the graphical interpretation gave little guidance for devising the computer models the geology of the area had to be studied in the hope that limitations

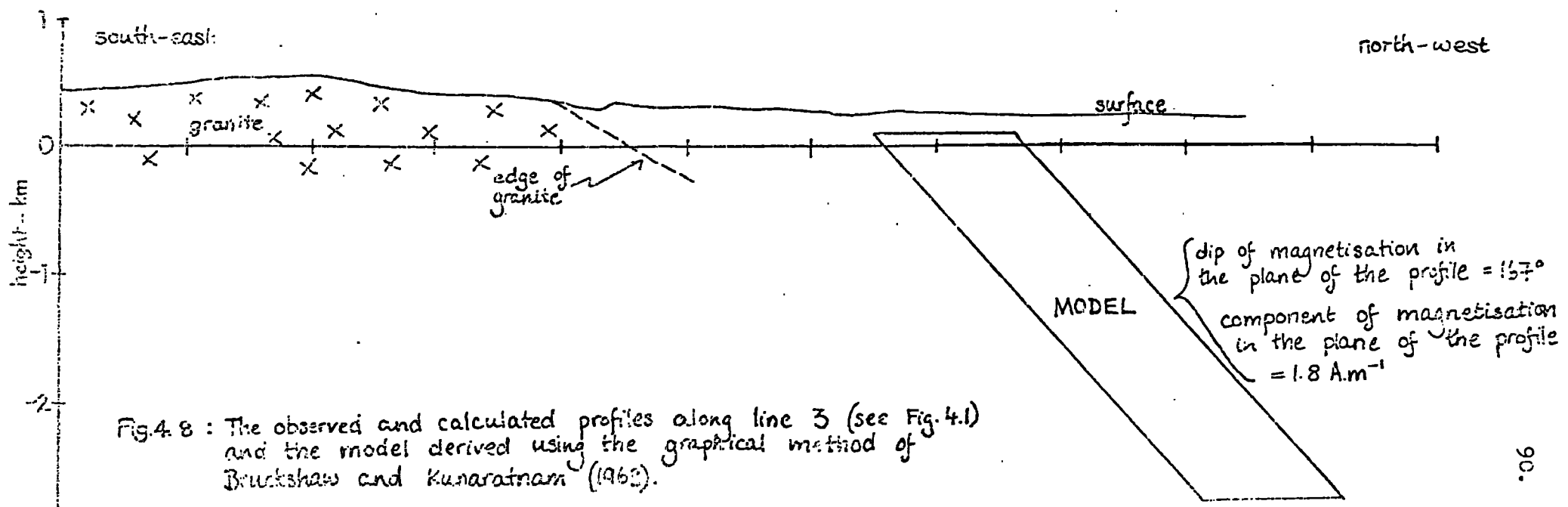
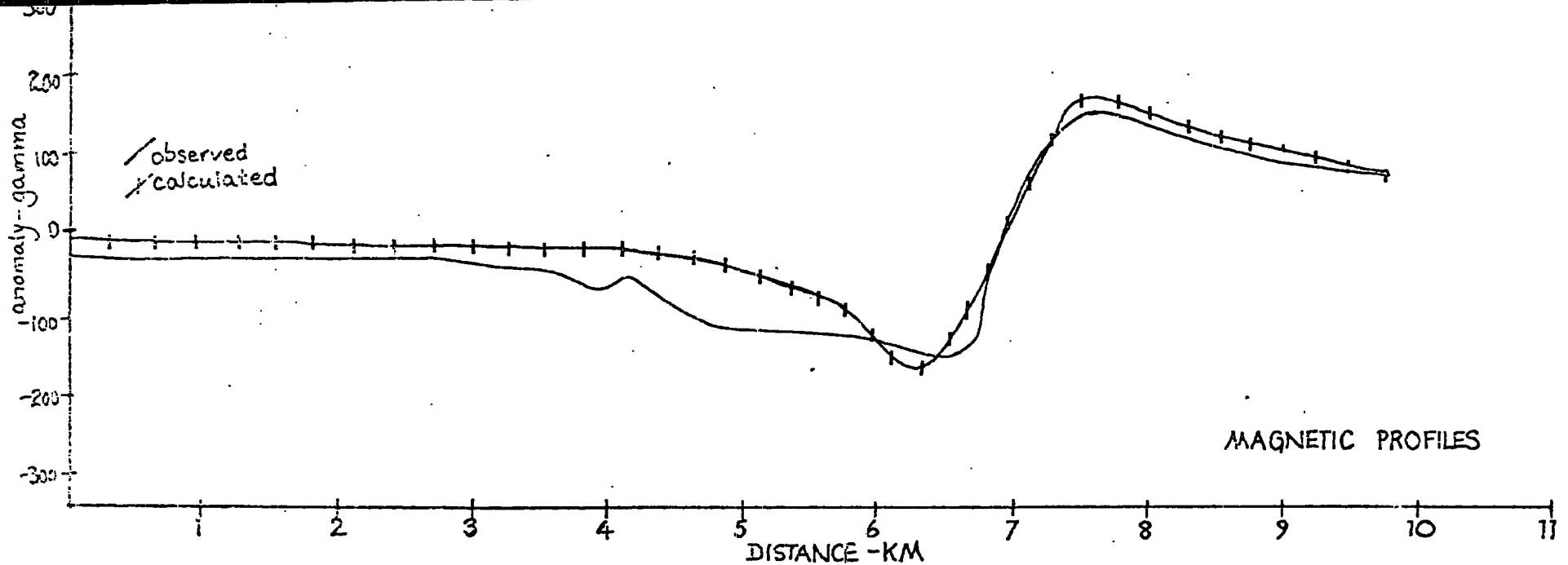


Fig.4.8 : The observed and calculated profiles along line 3 (see Fig.4.1) and the model derived using the graphical method of Bruckshaw and Kunaratnam (1963).

on the size and shape of the causal body might be found.

The depth and width of the causal bodies could be estimated; the depth using graphical methods, and the width by measuring the distance between successive peaks on the aerial profiles. By doing this it was estimated, for example, that there were three bodies crossing line 6 and that they were about 700 m. in width and at a depth of 41-128 m.

The interpretation of lines 1 and 2 was considered separately from lines 3,4,5 and 6 since the latter traversed the major Okehampton Anomaly while lines 1 and 2 covered minor disturbances to its south-west. It was explained earlier in this chapter that pyrrhotite mineralisation within the metamorphic aureole was probably responsible for the short wavelength anomalies located on the ground traverses. It was thought that pyrrhotite mineralisation might also explain the magnetic disturbances detected on the aerial profiles. Since the hydrothermal solutions emanated from the granite during the late stages of its intrusion the causal body, or bodies, are likely to dip at the same angle as the granite contact which is thought to dip north at  $20-30^{\circ}$  (Edmonds et al, 1968).

Pyrrhotite mineralisation, both within and beyond the metamorphic aureole, may also be a contributing factor causing the Okehampton Anomaly but the dip of the strata must be taken into consideration as well. In Chapter 3 it was suggested that pyrrhotite developed

outside the aureole might be concentrated in the Lower Culm Measure rocks as they are a more suitable host for mineralisation than the overlying Crackington Formation sediments. Fig. 1.3 shows cross-sections through the Meldon inlier along lines 3 and 5. These show that although individual beds may dip at angles between  $20^{\circ}$  and  $60^{\circ}$  the Lower Culm Measure rocks, en masse, dip north at  $30^{\circ}$ . So, both the dip of the strata and the development of mineralisation parallel to the granite contact suggests that the causal body, or bodies, should dip north at approximately  $30^{\circ}$  (see p.84).

#### 4.7(iv) The Models

The models were devised with arbitrary values of  $\phi$  and intensity of magnetisation. The magnetisation was of the order of  $1 \text{ A.m.}^{-1}$ , and  $\phi$  was expected to fall in the range  $156-206^{\circ}$  as these were the values achieved experimentally.

The models for lines 1 and 2 consisted of blocks of variously magnetised rock, all dipping  $30^{\circ}\text{N}$ , whose top surfaces were at ground level (see Figs. 4.9 and 4.10).

The model chosen for line 3 is an amended version of that achieved using the dimensions obtained by graphical means. The single body dips north at  $45^{\circ}$  and has a rounded top (see Fig. 4.11).

The profiles along lines 4, 5 and 6 (see Figs. 4.12, 4.13 and 4.14) can be obtained with models which consist of slabs of variously magnetised rock, dipping  $30^{\circ}$  to the

The following figures (Figs. 4.9 to 4.14) show the observed and calculated profiles, and the models along lines 1 to 6 (located on Fig. 4.1). The geological interpretation of these models is also illustrated.

The symbols used are as follows:-

#### GEOLOGY



granite



Upper Carboniferous rocks



Lower Carboniferous and Transition Series rocks



outer limit of metamorphic aureole

#### MAGNETIC PROPERTIES

$j$   $J_{x,z}$ , the magnetisation of the body in the plane of the profile

$\theta$  the inclination of the magnetisation in the plane of the profile



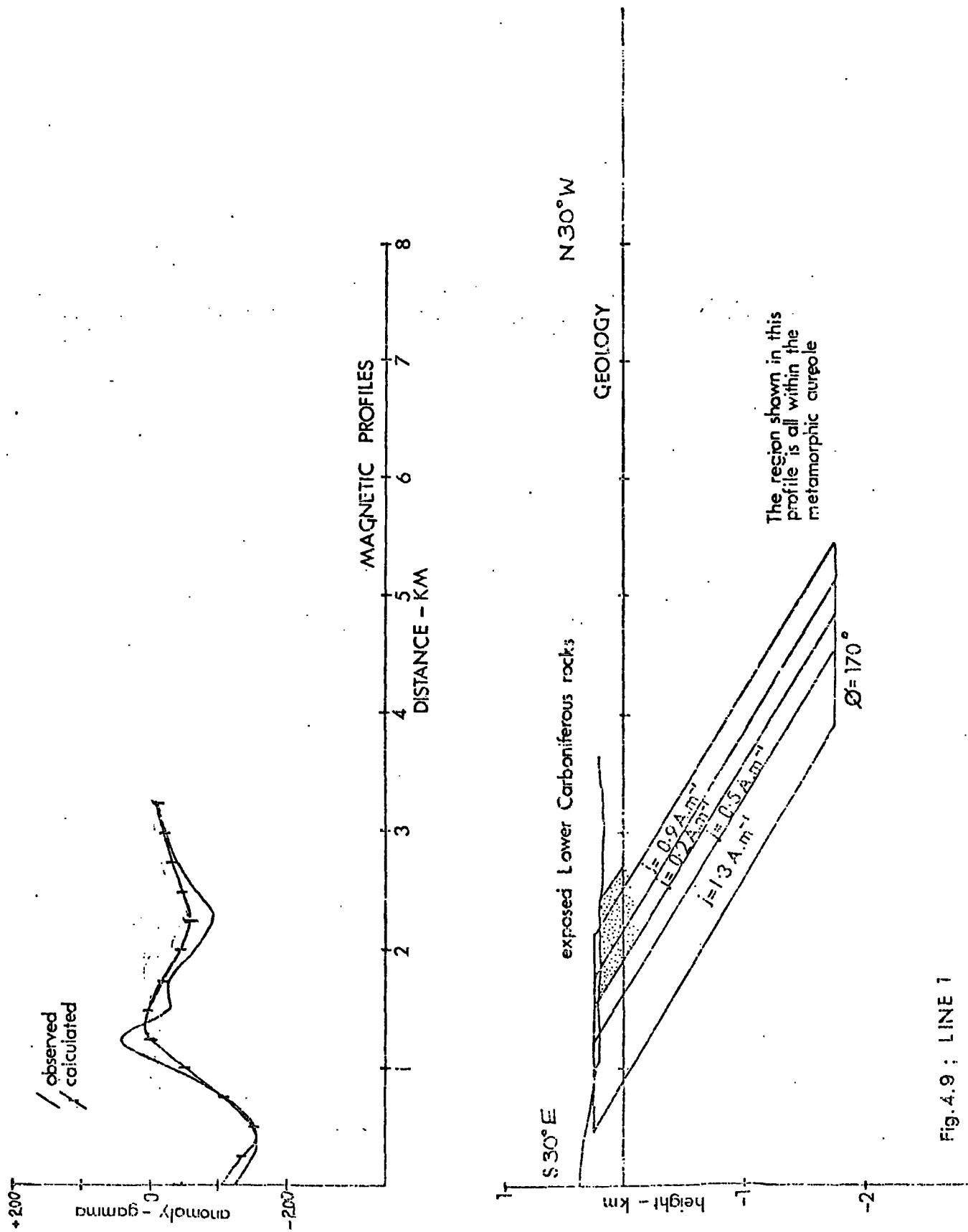


Fig. 4.9 ; LINE 1

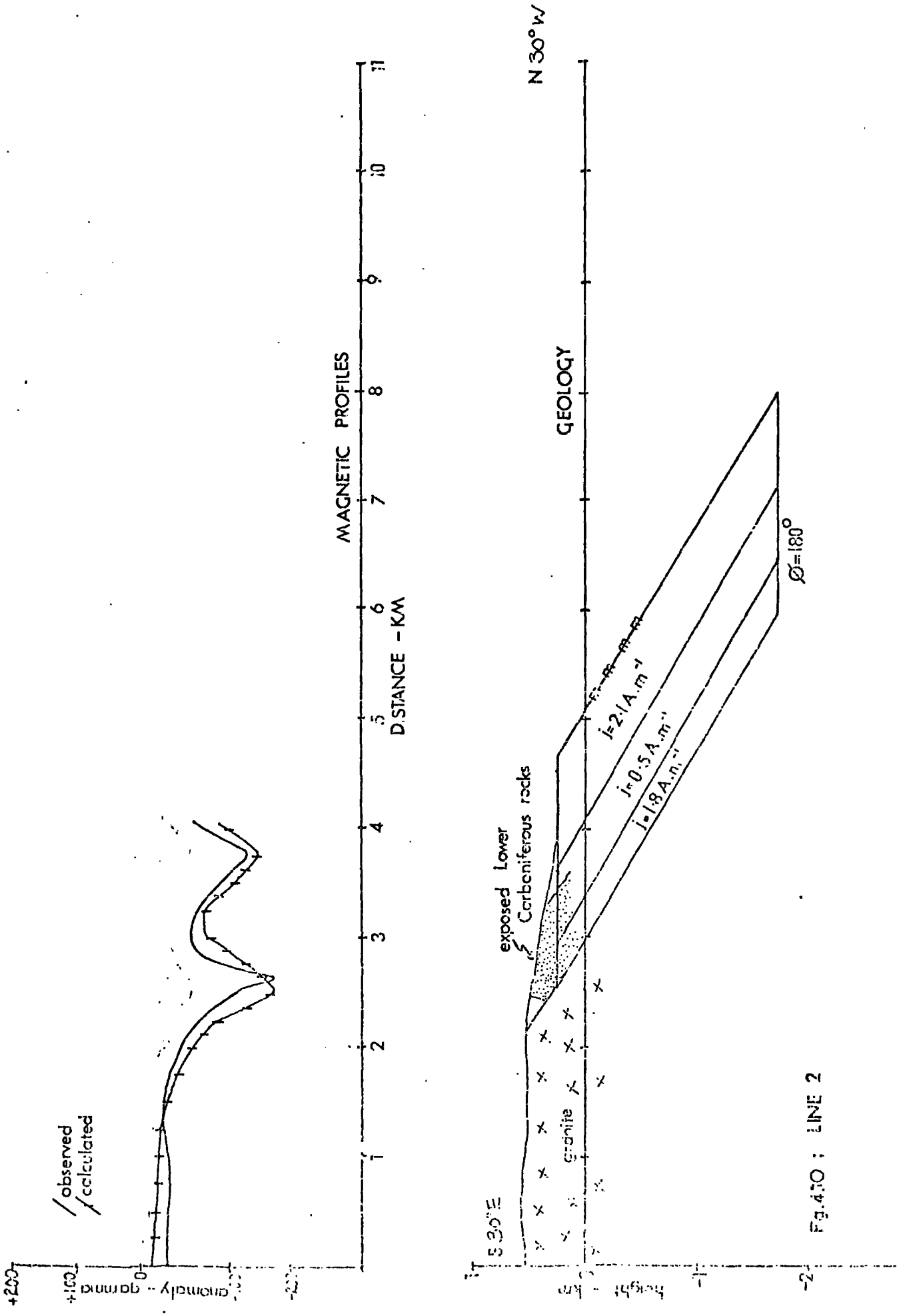


Fig. 4.10 : LINE 2

$f$  calculated

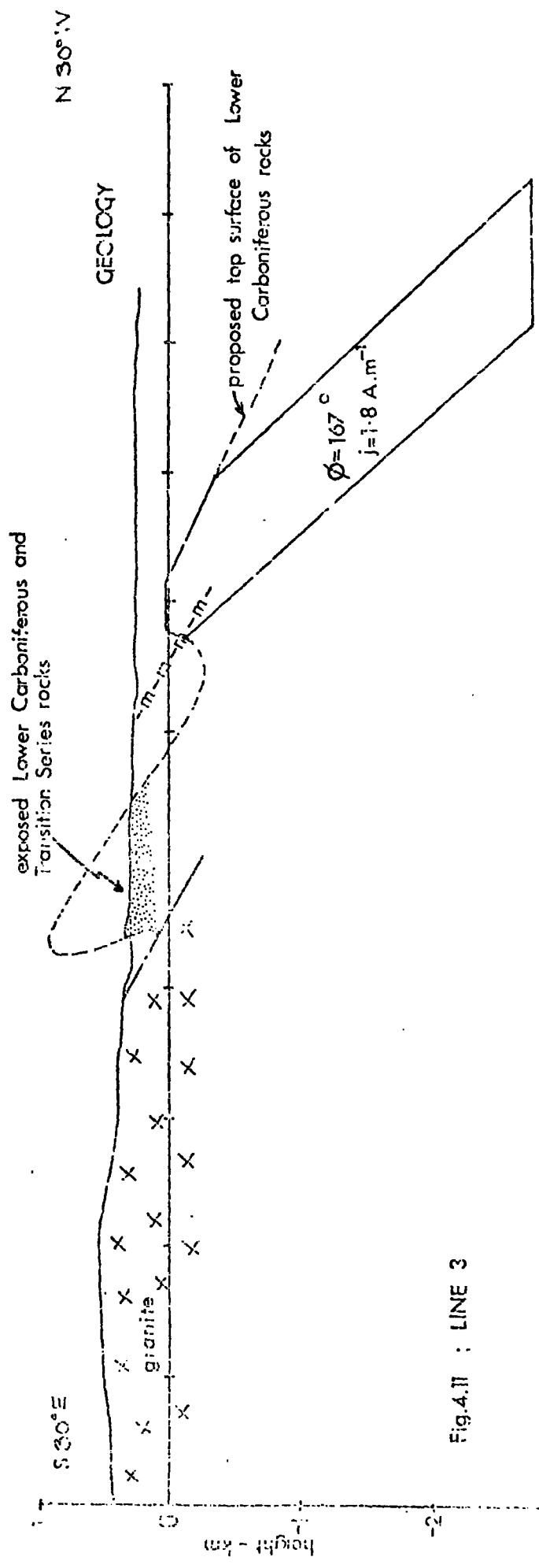
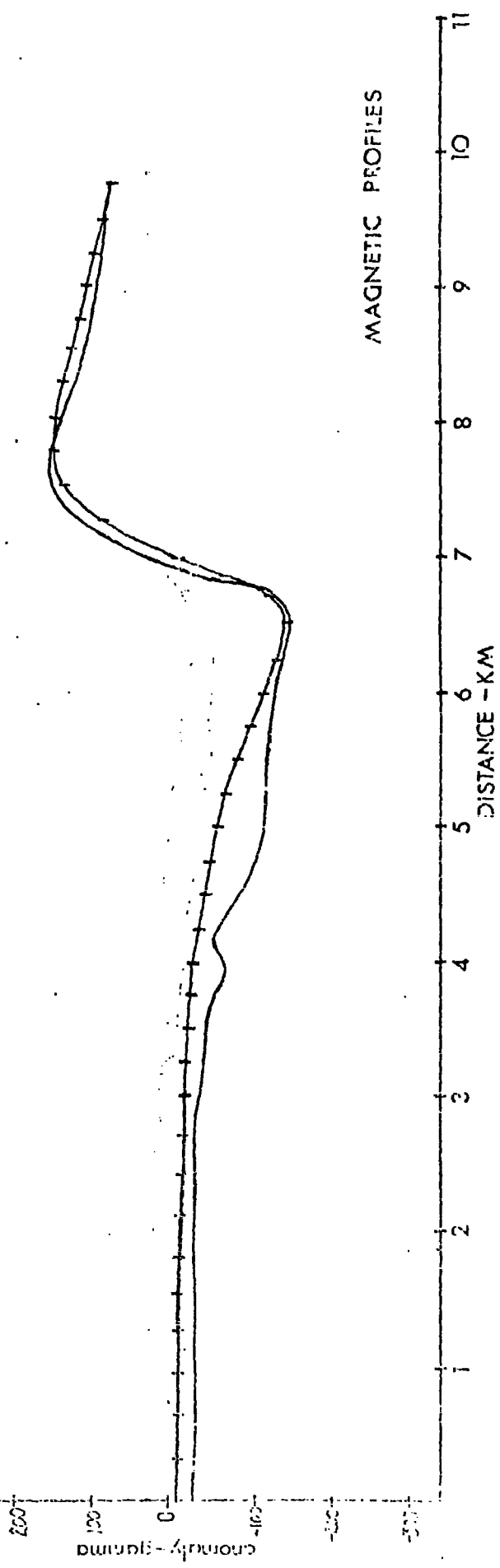


Fig.4.11 : LINE 3

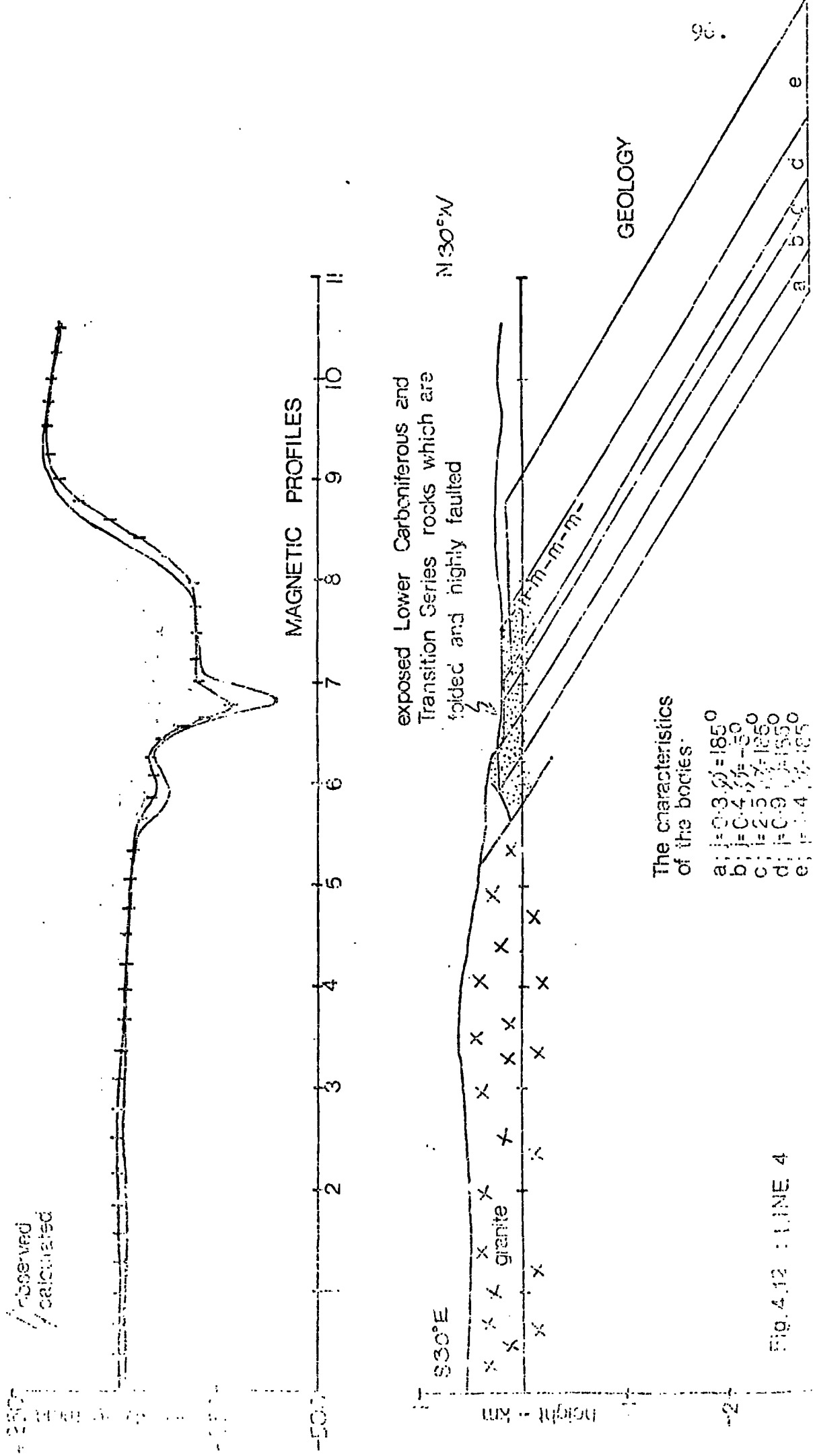


Fig. 4.12 : LINE 4

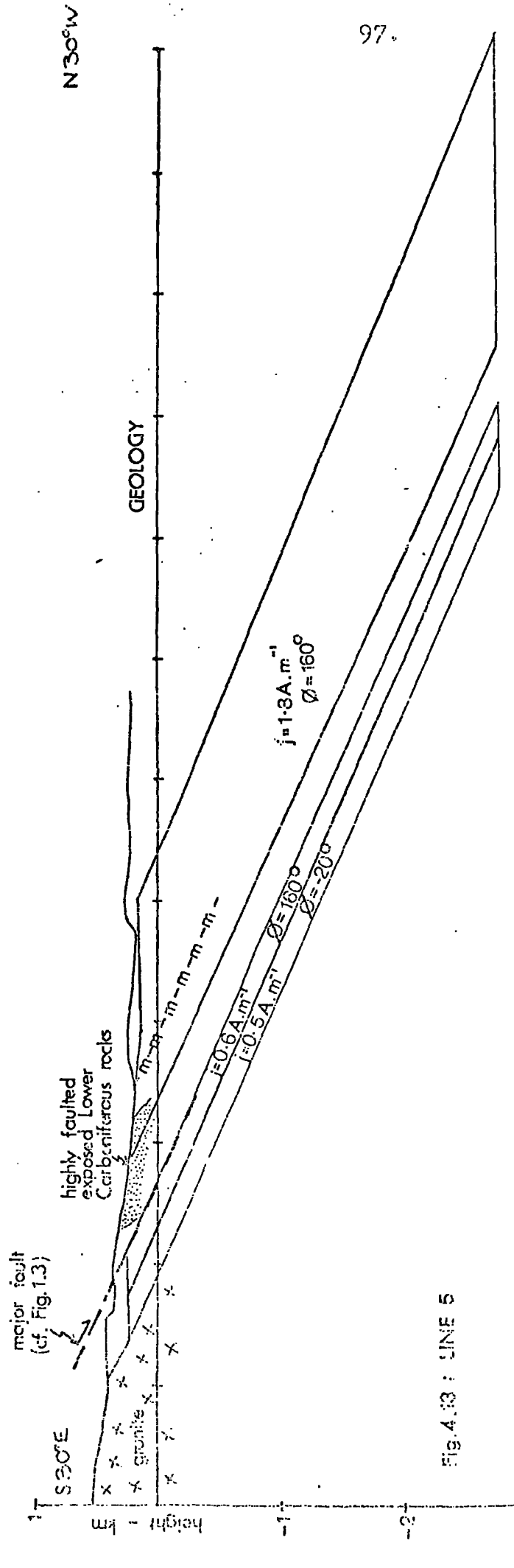
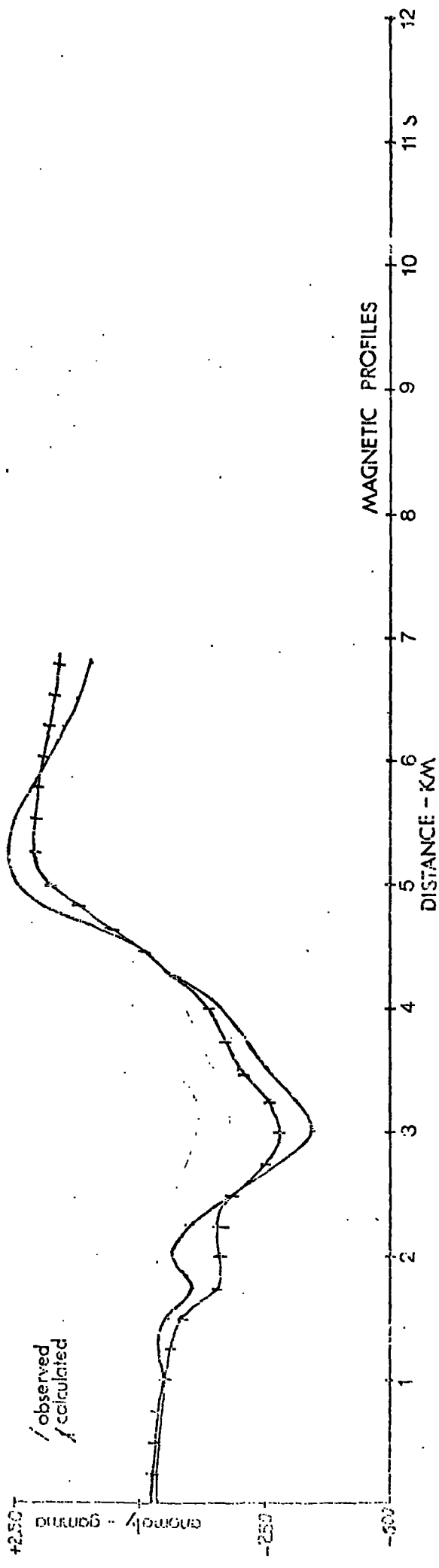


Fig. 4.63 : LINE 5

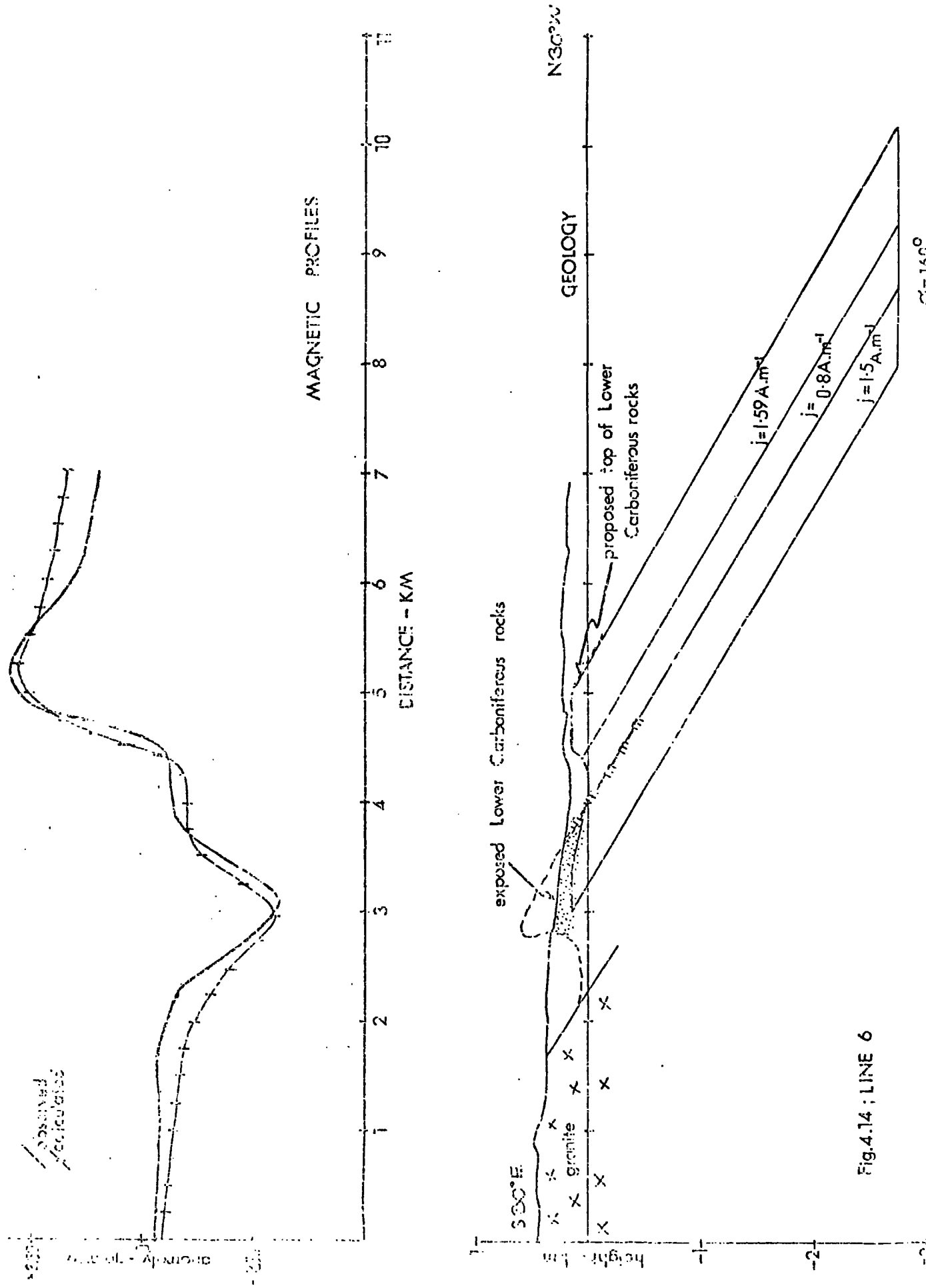


Fig.4.14 ; LINE 6

north, at different depths. A greater variation in magnetic intensity could produce the same effect as varying the depths of the bodies but for reasons that will be explained later the depth variation was preferred.

#### 4.7(v) The directions of magnetisation

The models described above are for arbitrary values of  $\phi$ , the dip of the resultant magnetisation in the plane of the profile. Now, many directions of magnetisation can produce a given value of  $\phi$ , so the question to ask is whether the values of  $\phi$  used in successful models could be obtained by resolving likely directions of magnetisation. It is known that the Dartmoor granite was intruded during the early Permian (Miller and Mohr, 1964) and it is believed that the magnetic properties of the Lower Culm Measure rocks can be attributed to pyrrhotite emplaced at this time. Creer (1966) suggested that a typical value for the early European Permian could be  $D_{EP} = 189^\circ$ ,  $I_{EP} = -9^\circ$ . Measurements made here suggest that the dip of the remanent magnetisation is greater as  $I_{mean} = -29^\circ$ . Cornwell (1967) measured rocks from the same locality and found a mean inclination of  $-21^\circ$ . Cornwell's results gave the same value for the declination,  $189^\circ$ , as Creer but the results described in Chapter 3 suggested that  $D = 105^\circ$ . But, because of the small size of the sample described in this thesis, these results were unreliable and are thought to be erroneous. Consequently a declination of  $189^\circ$  was considered more likely to be

correct. This value corresponds to a declination ( $D'_{EP}$ ) of  $219^\circ$  relative to the profile.

The directions of magnetisation used in the computer models comprise the remanent and induced components. In order to compare the direction of the remanent component with that of the early Permian field it is necessary to calculate the dip ( $I_R^{EP}$ ) of the remanent component in the vertical plane along  $D_{EP} = 189$  ( $D'_{EP} = 219^\circ$ ). Now the mean  $Q$  value for the Meldon samples is 3.57 (see page 50) so  $J_R = 3.57 J_I$  and hence:-

$$J_{RX} = 3.57 \cdot J_I \cdot \cos I_R^{EP} \cdot \cos 219^\circ$$

$$J_{RY} = 3.57 \cdot J_I \cdot \cos I_R^{EP} \cdot \sin 219^\circ$$

$$J_{RZ} = 3.57 \cdot J_I \cdot \sin I_R^{EP}$$

and:-

$$J_{IX} = J_I \cdot \cos I_E \cdot \cos D_E$$

$$J_{IY} = J_I \cdot \cos I_E \cdot \sin D_E$$

$$J_{IZ} = J_I \cdot \sin I_E$$

where  $I_E = 66^\circ$   
 $D_E = 22^\circ$  (see Appendix A)

The dip of the magnetisation of the body in the plane of the profile is defined by  $\theta$ .

$$\theta = \tan^{-1} \left( \frac{J_{IZ} + J_{RZ}}{J_{IX} + J_{RX}} \right)$$



so,

$$\tan\phi = \frac{3.57 \cdot \sin I_R^{EP} + \sin 66^\circ}{3.57 (\cos I_R^{EP} \cdot \cos 219^\circ) + \cos 66^\circ \cdot \cos 22^\circ}$$

From this it was possible to calculate the dip ( $I_R^{EP}$ ) of the remanent component in the direction of the early Permian field for the values of  $\phi$  used in the models.

LINE	$\phi$	$I_R^{EP}$
1	170°	-7°
2	180°	-15°
3	167°	-5°
4	185°	-18°
5	160°	0°
6	160°	0°

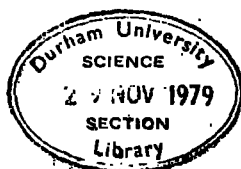
The values for the dip ( $I_R^{EP}$ ) of the remanent component in the direction of the early Permian field shown in the table

above are near horizontal and reversed. They compare well with typical inclinations for the early European Permian suggesting that the remanent magnetisations of rocks in the Meldon district are early Permian.

#### 4.8 Assessment of the models

Graphical interpretations of the body causing the Bkehampton Anomaly were unsatisfactory except to give a rough estimate of its size and shape. The direct methods, using Peter's and Solokov's lengths, assume that the body is near vertical, which was later shown not to be the case. Bruckshaw and Kunaratnam's method is based on the characteristics of an infinitely deep parallel-sided, uniformly magnetised dyke, treated in isolation, and as the causal body tapers to west and east and is situated in an area with a sloping regional field the method failed. However, the method did show that  $i$  lies between  $180^\circ$  and  $270^\circ$ , where  $i = \delta + \psi - \theta$ .  $\psi$  is known as it is the dip of the earth's field in the plane of the profile and  $\theta$ , the dip of the body in the same plane, is assumed to be  $30^\circ$ . From these the dip,  $\delta$ , of the magnetisation of the body falls in the range  $130^\circ - 220^\circ$ . The computer models were devised for arbitrary values of  $\delta$  within this range.

The values of  $\delta$  which gave the best fit were used to calculate the inclination of the remanent magnetisation along the direction of the early Permian field ( $D = 189^\circ$ ). The results fall in the range  $0^\circ \rightarrow -18^\circ$ . This agrees well with the direction of a typical early Permian field as defined by Creer (1966) ( $D = 189^\circ$ ,  $I = -9^\circ$ ) and Cornwall (1967) ( $D = 189^\circ$ ,  $I = -21^\circ$ ).



So far in this chapter it has been assumed that the magnetic properties of the rock causing the Okehampton Anomaly can be attributed to pyrrhotite mineralisation. However, before discussing this and the models in more detail, it is worth considering the other possibilities, if only to show that they are not feasible. These are the Carboniferous dolerites, Lower Carboniferous volcanics and buried Devonian spillites.

It has been suggested (Edmonds et al, 1968) that material giving rise to the Okehampton Anomaly is probably of basic igneous nature, such as dolerite. However, the ground profiles shown on Fig. 4.1 suggest that this assumption may be incorrect. Several dolerite intrusions outcrop among the older rocks in the inlier but they show no associated magnetic disturbance, except along line 2. This indicates that the typically strongly magnetic doleritic rock is behaving abnormally in this area, and has a low magnetisation. In Chapter 1 it was explained that pyrrhotite has been known to develop in dolerite (Edmonds et al, 1968) and this ferromagnetic mineral could reduce the remanent magnetisation of the dolerite by imposing a secondary field with a different direction. Creer (1966) noted that the dolerites found in Devon and Cornwall have a much reduced remanent magnetisation which can be an order of magnitude less than that for dolerites elsewhere. From the observations of Creer (1966) and those made here it seems unlikely

that dolerite causes the Okehampton Anomaly. Also, the large width of the proposed causal body (see Figs. 4.11 to 4.14) makes the possibility of its being a dolerite intrusion unlikely.

An alternative form for the causal body could be volcanic rock such as the pyroclastics exposed at Meldon, or Devonian spillites. The pyroclastics are about 60 m. thick in the Meldon area (see Chapter 1) and they thin away from this centre so it is unlikely that there would be a sufficient thickness of volcanics to cause the Okehampton Anomaly. Devonian spillites are not exposed in the Okehampton area but they are found in association with Lower Carboniferous and Upper Devonian rocks near Tintagel (located on Fig. 1.1) where they reach a thickness of 500 m. (Freshney et al, 1972). However they are not known to cause any magnetic anomalies (Sanderson, personal communication).

The models devised to explain the profiles along lines 1 and 2 describe bands of variously magnetised rock running parallel with the granite contact. Extending these bodies to an infinite depth made little effect on the profiles *so it was decided that the body could be treated as* near surface material. This would fit in with the assumption that the anomalies are caused by pyrrhotite enriched Lower and Upper Culm Measure sediments which have magnetic properties similar to those measured in samples from Meldon Quarry (see Chapter 3); that is, a

near horizontal reversed field. The values for the intensity of magnetisation are larger than those measured here but this could be a result of weathering and consequent loss of ferromagnetic minerals in surface samples from Meldon.

Pyrrhotite is an unstable ferromagnetic iron sulphide which is readily weathered to iron oxide or hydroxide, so it is unlikely to exist in significant quantities in the weathered zone which is thought to go down to about 100 m. (Scrivenor, personal communication). Consequently rock at depth is likely to contain more pyrrhotite and hence have a higher value of magnetisation than the sediments at the surface. The bodies in the models for lines 1 and 2 do approach the surface so the intensity of magnetisation probably represents the mean value for the depleted and pyrrhotite enriched zones.

Of the four lines which cross the Okehampton Anomaly only the model for line 5 suggests that there are bands of both Lower and Upper Culm Measure sediments with significant magnetisation within the metamorphic aureole of the granite. Along line 5 the magnetic rock abuts against the granite while there is a zone of non-magnetic material next to the granite along lines 3, 4, and 6. However it should be noted that the rock next to the granite in model 5 is normally magnetised suggesting that its magnetic direction is largely induced. These observations fit in with those of Beer and Fenning (1976) who noted that pyrrhotite is absent from coarse hornfelses

close to the granite and there is no evidence of much magnetite in these rocks. This would explain the absence of a strong remanent component. It has also been suggested (Beer and Scrivener, personal communication) that any pyrrhotite, introduced by early hydrothermal solutions, is likely to be metamorphosed or redistributed near to the granite contact. The resulting mixture of remanent magnetic directions could produce rock with a high susceptibility but low remanent magnetisation, hence the significant induced component in the body adjacent to the granite along line 5.

It was suggested earlier in this chapter that pyrrhotite mineralisation at the outer edge and beyond the metamorphic aureole is largely confined to the Lower Culm Measure sediments. It is therefore important to assess the models for lines 3,4,5 and 6 in the light of known geology to see if they represent possible structures for Lower Culm Measure sediments.

In Chapter 1 the work of Dearman and Butcher (1959), Edmonds et al (1968), Freshney and Taylor (1971), Sanderson and Dearman (1973), and Hobson and Sanderson (1975) on the structure of the Meldon area was discussed and certain points considered. Firstly, it is feasible that further folds of Lower Culm Measure and Transition Series rocks exist under the Crackington Formation sediments to the north of the Meldon inlier, suggesting that these older foldments could form a dyke-like anticline existing just north of the exposed inlier. In this

area the fold limbs dip north at  $30^{\circ}$  and  $60^{\circ}$  and the axial planes dip at approximately  $45^{\circ}$  in the same direction. The other important structural consideration is the number of faults observed cutting these older rocks. The cross-sections shown in Fig. 1.3 which roughly coincide with parts of lines 3 and 5 show how these faults alter the shape of the inlier and provide a means by which blocks of Lower Culm Measure rock can be moved nearer to, or further from, the surface. These faults, be they normal or reversed, dip north at  $30^{\circ}$  and  $60^{\circ}$ .

So, either faulting or folding could determine the shape of the Lower Culm Measure sediments. This suggests that if the body representing these sediments were the nose of a fold it would dip north at  $45^{\circ}$  while if it were fault bounded it would dip at  $30^{\circ}$  or  $60^{\circ}$ . However the cross-sections on Fig. 1.3 suggest that both faulting and folding play a part in determining the structure so it is important to assess the models in the light of both these considerations.

It was because of these structural considerations that the graphically derived dip of  $45^{\circ}$  for the causal body for line 3 was believed to be correct. This suggested that the body was the nose of a fold so the model was modified accordingly and a better fit was achieved. Fig. 4.11 shows the improved model and the northward extrapolation of the Culm Measure sediments from the Meldor inlier to the proposed fold nose.

The model for line 6 also indicates that folding has occurred. If the bodies are taken to be slabs of Lower Carboniferous or older rock which have been enriched with pyrrhotite then the undulating top surface of the magnetised rock probably represents gentle folding of these older sediments.

The models for lines 4 and 5 both suggest that the highly magnetic rock exists as slabs, dipping  $30^{\circ}\text{N}$ , and which deepen slightly to the north. Inspection of line 4 shows that the majority of bodies, including the normally magnetised slab fall within an area known to contain Lower Culm Measure sediments. It is easy to conceive of the most northerly slab as being a tectonic slab of the same rock type. The dip of the interface between it and the body immediately to its south could then be interpreted as a fault plane dipping north at  $30^{\circ}$ . By contrast the model for line 5 is difficult to explain as the bulk of the magnetised rock exists to the north or south of the inlier while most of the exposed Lower Culm Measure sediments appear to be non-magnetic.

It was mentioned earlier that pyrrhotite is easily weathered and that this radically alters the magnetic properties of the rock containing this mineral. This could mean that the undulations in topography attributed to folding and faulting may be an effect of weathering. However it seems unlikely that the weathered zone would deepen by 150 m. in an equal distance (see line 5: Fig. 4.13), or go down to 250 m., so the suppositions about the structure are likely to be true.



#### 4.9 Conclusions

This chapter effectively covers three aspects of the magnetic disturbances in the Okehampton area. Firstly there is the regional field which changes from high in the north-east to low in the south-west. Straddling the boundary between these two regions there is the major Okehampton Anomaly. Then, superimposed on this anomaly and found to its south over the metamorphic aureole of the Dartmoor granite there are short wavelength anomalies detectable only along the ground traverses.

Even though no evidence to support this hypothesis is set out in this thesis it seems likely that the regional field is caused by the juxtaposition of non-magnetic rocks to the south - the granite and Devonian shales and limestones (see Fig. 1.1) - and the Culm Measure sediments to the north, some of which have been shown to possess a significant magnetisation.

Of the possible causes of the Okehampton Anomaly only pyrrhotite mineralisation seems likely. There is an insufficient thickness of Lower Culm Measure volcanics to cause such a large anomaly and both Devonian spillites, which are likely to exist at depth under the Culm Measures, and dolerite do not possess a significant magnetisation. Therefore the Okehampton Anomaly is believed to be caused by magnetic Culm Measure sediments. More specifically it is thought that the ferromagnetic mineral pyrrhotite developed in the lower Carboniferous

sediments is responsible for the significant magnetic properties of these rocks.

There are three modes of pyrrhotite development in Culm Measure sediments: thermal metamorphic alteration, metasomatism and the penecontemporaneous bedded mineral. It seems likely that the latter two modes of emplacement are responsible for the pyrrhotite in the Lower Culm Measure sediments which cause the Okehampton Anomaly. Of these the hydrothermally emplaced vein mineral seems more likely although there is probably some bedded pyrrhotite as well. It is also likely that, like the bedded mineral, much of the Fe, S and Ni contained in the veins was derived from volcanic sources.

The models have shown that penecontemporaneous bedded pyrrhotite or hydrothermally emplaced vein pyrrhotite may be confined to Lower Culm Measure sediments beyond the metamorphic aureole, and that these sediments continue north under the rocks of the Crackington Formation. The structure of the older sediments is defined by folding and faulting. Along some lines (lines 3 and 6) folding appears to be a more important consideration whereas along lines 4 and 5 the structure appears to be dominated by faults. Fig. 1.3 shows two dissimilar geological cross-sections through the Melton inlier. These confirm that the structure can alter in the very short distance between lines in the manner indicated by the models.

The directions of magnetisation used in the modelling correspond to the early Permian, at which time the pyrrhotite is believed to have been emplaced. The intensity of magnetisation (c.  $1 \text{ A.m.}^{-1}$ ) used in devising the models is greater than that measured in the field (see Chapter 3) but the samples came from near the surface and are therefore likely to be weathered and have a lower magnetisation than the unaltered rocks at depth.

Finally, the mineralisation hypothesis concurs with an observation made by the I.G.S. (Fenning in Edmonds et al, 1968) that the body causing the Okehampton Anomaly has a disseminated nature because there is no associated gravity anomaly.

The third type of pyrrhotite development, and that which is confined to the metamorphic aureole of the granite is the thermally altered detrital sulphides, notably pyrite. Near surface developments of this and the vein mineral are thought to be responsible for the short wavelength anomalies detected on the ground traverses across the metamorphic aureole of the granite. This agrees with the findings of Cornwell (1967), Edmonds et al (1968) and Beer and Fenning (1976).

## CHAPTER 5

### DISCUSSION OF THE RESULTS

#### 5.1 Introduction

This chapter attempts to tie together the results obtained in the previous chapters, and, in particular, to assess the merits of the interpretation described in Chapter 4. Also, because the Okehampton Anomaly is one of many similar anomalies which stretch across Cornubia it is important that it is not treated in isolation but compared with these other magnetic disturbances which may have comparable origins.

#### 5.2 The Models

Chapter 3 describes the study of the rock samples taken from various sites in the area. Measurement of their magnetic properties revealed that the directions of **total** magnetisation are scattered with a mean of  $D = 97^{\circ}$ ,  $I = 15^{\circ}$  and a maximum error of  $30^{\circ}$ . However the small size of the sample (24) makes these results unreliable. The results also revealed that the rock type with the most significant magnetisation was shale and that the shale samples had a mean  $Q$  value of **3.57** (see **page 50**).

Study of the mineralogy showed that the magnetic properties of the samples could be attributed to the ferromagnetic mineral, pyrrhotite. It was present in two forms; disseminated and as a vein mineral. It is thought that the disseminated form is the thermal alteration product of detrital sulphides, notably pyrite, and is restricted to the metamorphic aureole of the granite. The vein mineral is believed to have been hydrothermally emplaced by fluids emanating from the granite which could travel distances as great as 7 km. from the granite contact.

The models obtained in the previous chapter indicate that both the Okehampton Anomaly and the smaller disturbances to its south-west are caused by composite bodies running parallel with the granite contact and dipping north at about  $30^{\circ}$ . The directions of magnetisation used in the models were resolved along a typical early Permian declination of  $189^{\circ}$  (Creer, 1966, Cornwell, 1967) and near horizontal inclinations were obtained, indicating that the bodies had an early Permian direction of magnetisation. The Dartmoor granite was intruded at this time ( $\sim 280$  M.Y., Miller and Mohr, 1964) so it seems likely that the remanent field of the causal body was obtained at the time of the granite intrusion.

The possible causes of the Okehampton Anomaly are believed to be dolerites, Lower Carboniferous volcanics, Devonian spillites or pyrrhotite mineralisation. The ground traverses showed that only one exposed dolerite

had an associated magnetic anomaly, confirming the idea that dolerites have an unusually low magnetisation in this area. The volcanics, although magnetic, are of insufficient thickness to cause the anomaly and the spillites do not possess a sufficiently high magnetisation. Pyrrhotite mineralisation was therefore thought to cause the Okehampton Anomaly and the local disturbances including the short wavelength anomalies. Near surface developments of both vein and disseminated pyrrhotite within the metamorphic aureole are thought to cause the short wavelength anomalies. These types of mineralisation are also thought to cause the small disturbances such as those detected along lines 1 and 2 which would explain why the slabs of magnetised rock run parallel with the granite contact. Vein pyrrhotite can be developed beyond the metamorphic aureole and is thought to be a significant contributor to the Okehampton Anomaly. However evidence north of the Bodmin Moor granite, in a borehole at Wilsey Down, suggests that penecontemporaneous bedded pyrrhotite can exist in Lower Carboniferous sediments interbedded with volcanics from which it was probably derived. Although there is no evidence of bedded pyrrhotite in the Okehampton region it could contribute towards the observed anomaly. However, the early Permian direction of magnetisation suggests that the vein mineral is more likely to be the main cause as it was emplaced at the time of the Dartmoor granite.

Beyond the metamorphic aureole the vein pyrrhotite is thought to have been preferentially emplaced in the Lower Carboniferous sediments so the models shown in Figs. 4.11 to 4.14 indicate the structure of the buried Lower Carboniferous rocks. The causal body is 1-2 km. wide and dips north at  $30^{\circ}$  (or  $45^{\circ}$  in the case of line 3). The surface topography of lines 3 and 6, which traverse the western and eastern ends of the Okehampton Anomaly, indicate that these rocks are folded. Lines 4 and 5, which cross the centre of the anomaly, indicate that the body deepens slightly to the north, possibly as a series of tectonic slices. Fig. 1.3, taken from the work of Dearman and Butcher (1959), indicates that, even over distances as small as that between lines 3 and 5, the structure of the Meldon inlier can alter appreciably. This indicates that the differences in structure suggested by the models are geologically possible. There is one important point to consider at this juncture. Pyrrhotite is easily weathered and this can radically reduce the magnetisation of the rock. It is possible that variations in surface topography of the body could be attributed to the effects of weathering. However the weathered zone is thought (Scrivenor, personal communication) to go down to a depth of 100 m. so structures with a top surface as deep as 250 m. (see line 6, Fig. 4.14) are unlikely to have been produced by weathering. Of course, the variation in depths of the

bodies could be substituted with a greater variation in magnetic intensity from slab to slab, but this approach was not chosen because the intention was to produce models which indicated a possible continuation of Lower Culm Measure rocks from the Meldon inlier north under the Crackington Formation sediments.

The effect of weathering also explains the discrepancy between the values for the magnetisation used in the models and those measured in samples from Meldon quarry (mean =  $0.164 \text{ A.m}^{-1}$ ).

### 5.3 Comparison with anomalies elsewhere in Cornubia

As has been mentioned previously the Okehampton Anomaly is not unique but is one of many similar anomalies which stretch across Cornubia following the southern margin of the extensive magnetic high (see overlay to Fig. 1.1). This occurs over the region where Culm Measure rocks are exposed at the centre of the mid Devon syncline (see Fig. 1.1). The major anomalies are at Okehampton, Crockernwell and Tintagel, but there are others, such as that at Lydford (see Fig. 1.1). They all occur near the southern boundary of the Culm Measure rocks where both Lower and Upper Carboniferous sediments are exposed, and near to exposed or sub-surface granite. No comparable magnetic anomalies are found north of the mid Devon syncline even though Lower and Upper Culm Measure sediments are found there. The older sediments are similar to those found in inliers along the southern



margin of the syncline except that both volcanics and dolerites are absent (Edmonds, 1974).

The models described in the previous section suggest that the magnetic anomalies are caused by pyrrhotite enriched Lower Carboniferous sediments, and that this mineral was deposited by fluids which primarily originated from the granite. If this is so it would explain why no magnetic anomalies are found in association with Lower Culm Measure rocks north of the mid Devon syncline where there are no granites. It was also suggested that the pyroclastics interbedded with Lower Culm Measure sediments may have been a source for the Fe and S required for pyrrhotite mineralisation. So the absence of magnetic disturbances north of the major syncline may be attributed to the lack of volcanics in that area.

Previous workers (Edmonds et al, 1968) have suggested that dolerite intrusions cause the anomalies at Okehampton, Crockernwell and elsewhere, and that "the uniform nature and large areal extent of the anomalies makes the possibility of their arising from mineralisation with the Culm Measure rocks unlikely" (Edmonds et al, 1968). The body defined in the models (see Figs. 4.11 to 4.14) has a magnetic intensity of the same order of magnitude as that for normal dolerite, but dolerites throughout Cornubia have unusually low magnetic intensities (Creer, 1966). Also, the models have shown that the body causing the Okehampton Anomaly

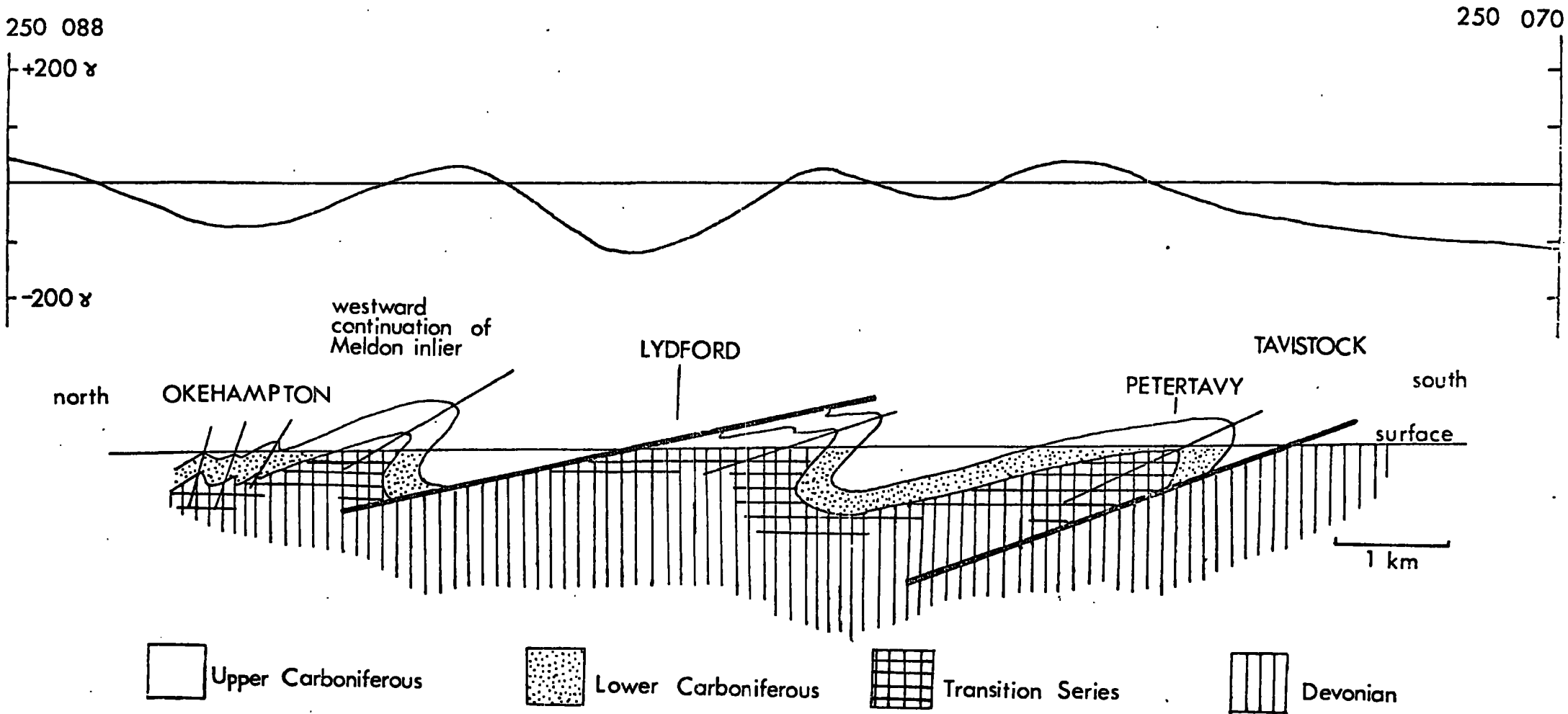


Fig. 5.1. Magnetic Profile and Geological cross-section along a line down the north-west side of the Dartmoor granite. (cross-section after Hohson and Sanderson, 1975, profile from unpublished 1:25,000 aeromagnetic map)

is not uniform but made up of many slabs of variously magnetised rock, and the large areal extent can also be explained in terms of mineralisation as the hydrothermal solutions emanating from the granite can travel distances as great as 7 km. and hence deposit minerals, notably pyrrhotite, over a wide area. The absence of dolerite north of the mid Devon syncline is therefore unlikely to explain the lack of magnetic disturbances.

Study of Fig.1.1 and the accompanying overlay suggests that the major anomalies south of the mid Devon syncline are found near to the inliers of the Lower Culm Measure rocks. This is particularly obvious at Tintagel, Okehampton and Crockernwell but smaller magnetic disturbances occur over other inliers such as those down the western side of the Dartmoor granite. It is worth looking at this area in more detail as it is located just south of the main area of study.

Hobson and Sanderson (1975) studied the structure of the Carboniferous sediments situated west of this granite. A cross-section running north-south through Lydford is illustrated in Fig. 5.1 as is the magnetic profile along the same line, taken from the unpublished I.G.S. 1:25,000 aeromagnetic map. This profile shows that negative disturbances, similar to the Okehampton Anomaly, are found just north of the Lydford and Petertavy inliers. In Chapter 1 it was explained that these inliers are the anticlinal noses of folded Lower

Culm Measure and Transition Series rocks. The folds change from being overturned in the Okehampton region to recumbent further south, and they dip north at shallow angles. It is therefore possible that the hypothesis put forward to explain the Okehampton Anomaly may hold true in this area; that reversely magnetised pyrrhotite enriched Lower Culm Measure rocks, continuing north at depth from the exposed inlier, cause the observed magnetic disturbances. If this is the case the question to ask is why the amplitude of the observed anomaly is greater in some areas than others.

It has already been pointed out (see Chapter 1) that the volcanics interbedded with the Lower Carboniferous sediments thin away from the Meldon centre (Dearman and Butcher, 1959), and it is believed that volcanics may be a significant source for pyrrhotite. In Chapter 3 the petrology of the rock samples from Meldon Quarry was described. It was noted that the vein pyrrhotite often contained exsolved crystals of the nickel iron sulphide, pentlandite. This suggests that hydrothermal solutions which deposited the pyrrhotite contained a high concentration of nickel. Such concentrations could not be obtained from the carbonate, argillaceous and arenaceous sediments found in the area, so it seems that the source was probably the volcanic rocks. So, where the pyroclastics are thickest the magnetic disturbances will be the strongest. This supposition concurs with observations made in the north Dartmoor region.

Unlike the Meldon inlier the inlier of Lower Culm Measure rocks situated east of the Sticklepath fault (see Fig. 1.1) contains no pyroclastic rocks except at its eastern end. The Okehampton and Crockernwell Anomalies are situated over the Meldon inlier and the eastern end of this inlier respectively (see overlay to Fig. 1.1). No magnetic anomaly is observed over the area where no volcanics are exposed. Fig. 1.2 shows that volcanics are found with Lower Carboniferous sediments north-west of the Dartmoor granite and Fig. 5.1 shows that magnetic anomalies are associated with these sediments.

### Conclusions

Evidence outlined in this thesis suggests that the Okehampton Anomaly is caused by pyrrhotite enriched Lower Culm Measure rocks which dip north at approximately  $30^{\circ}$ , under overlying Upper Carboniferous sediments of the Crackington Formation. This ferromagnetic mineral was mainly developed as a result of metasomatic activity during the late stages of the granite intrusion. As the models confirm, the remanent field therefore has an early Permian direction. Small amounts of bedded pyrrhotite may also be present but its early Carboniferous direction of magnetisation is unlikely to have much effect on the overall anomaly. It has been suggested, however, that the volcanics associated with this bedded pyrrhotite

were an important source for Fe and S, thus explaining the correlation between major anomalies and areas, like the Meldon inlier, where Lower Carboniferous pyroclastics are exposed.

The table below summarises the results.

<u>Major anomalies</u>	<u>Minor anomalies</u>
Vein pyrrhotite preferentially deposited in Lower Carboniferous sediments (Early Permian direction of magnetisation).	Vein and disseminated pyrrhotite within the metamorphic aureole (early Permian direction of magnetisation).
Some bedded pyrrhotite (Lower Carboniferous direction of magnetisation).	
Very small contributions from dolerite (Lower and Upper Carboniferous directions of magnetisation) and volcanics (Lower Carboniferous direction of magnetisation).	

REFERENCES

- Am, K., 1972. "The arbitrarily magnetised dyke: interpretation by characteristics", *Geop exploration* 10, 63-69
- Beer, K. E. and Fenning, P. J., 1976. "Geophysical anomalies and mineralisation at Sourton Tors, Okehampton, Devon", N.E.R.C. Report No. 76/1 H.M.S.O.
- Bott, M. H. P., Day, A. A. and Masson-Smith, D., 1958. "The geological interpretation of gravity and magnetic surveys in Devon and Cornwall", *Phil. Trans. Roy. Soc. Lond.*, 251, 161-191
- Brammall, A. and Harwood, H. G., 1923. "The Dartmoor granite: its mineralogy, structure and petrology", *Miner. Mag.* 20, 39-53
- Bruckshaw, K. M. and Kunaratnam, K., 1963. "The interpretation of magnetic anomalies due to dykes", *Geophys. Pros.* 11, 509-522
- Chamalaun, F. M. and Creer, K. M., 1964. "Thermal demagnetism studies on the O.R.S. of the Anglo-Welsh Curvette", *J. Geophys. Res.* 69, 1604-1616
- Collinson, D. W., Molyneux, L. and Stone, D. B., 1963. "A total and an isotropic magnetic meter", *J. Sci. Instrum.* 40, 310-312
- Cornwell, J. D., 1967. "The magnetisation of Lower Carboniferous rocks from the N-W border of the Dartmoor granite, Devonshire", *Geophys. J.R. Astr. Soc.* 12, 381-403
- Creer, K. M., 1966. "Palaeomagnetic studies on basic dykes and sills from S. W. England", *Geophys. J.R. Astr. Soc.* 11, 415-422
- Dearman, W. R., 1968. "Tectonics and granite emplacement on the N-W margin of Dartmoor, Devonshire", *Trans. R. Geol. Soc. Corn.* 20, 45-64

- Dearman, W. R., 1969. "On the association of upright and recumbent folds on the southern margin of the Carboniferous synclinorium of Devonshire and N. Cornwall", Proc. Ussher Soc. 2, 115-121
- Dearman, W. R. and Butcher, N. E., 1959. "The geology of the Devonian and Carboniferous Rocks of the north-west border of the Dartmoor granite, Devonshire", Proc. Geol. Assoc. 70, 51-92.
- Dearman, W. R. and El Sharkawi, M. A. H., 1965. "The Shape of the mineral deposits in the Lower Culm Measures of north-west Dartmoor", Trans. Roy. Geol. Soc. Corn. 19, 286-296
- De la Beche, 1839. "Report on the geology of Cornwall, Devon and West Somerset", Mem. Geol. Surv.
- Edmonds, E. A., 1974. "Classification of the Carboniferous rocks of S.W. England", I.G.S. Report No. 74/13
- Edmonds, E. A., et al, 1968. "Geology of the country around Okehampton", N.E.R.C. Publication, H.M.S.O.
- Edmonds, E. A., et al, 1975. "British Regional Geology: South-West England", 4th Edition, N.E.R.C. Publication. H.M.S.O.
- Dobrin, M. B., 1976. "Introduction to Geophysical Prospecting", 3rd Edition, McGraw-Hill Book Co.
- Freshney, E. C., 1969. "Preliminary report on the Wilsey Down borehole, North Cornwall", Proc. Ussher Soc. 2, 107-108
- Freshney, E. C. and Taylor, R. T., 1971. "The structure of Mid-Devon and north Cornwall", Proc. Ussher Soc. 2, 241-248
- Freshney, E. C., et al, 1972. "Geology of the coast between Tintagel and Bude", Pub. H.M.S.O.
- Green, F. W., 1977. "The magnetic anomalies of north-west Dartmoor", B.Sc. dissertation, Durham
- Harbord, N. H., 1962. "Mineralogy of Yoredale Series Rocks in Upper Teesdale with special reference to clay minerals", Ph.D. Thesis, Durham
- Hobson, D. M. and Sanderson, D. J., 1975. "Major early folds at the southern margin of the Culm synclinorium". Jl. Geol. Soc. Lond. 131, 337-352



- IAGA Division 1 Study Group, 1976. "International Geomagnetic Reference Field, 1975", Geophys. J. R. Astr. Soc. 44, 733-734
- McKeown et al, 1973. "Geology of the country around Boscastle and Holsworthy", Pub. H.M.S.O.
- Miller, J. A. and Mohr, P. A., 1964. "Potassium-argon measurements on the granite and some associated rocks from south-west England", Geol. J. 4, 105-126
- Molyneux, L., 1971. "A complete result magnetometer for measuring the remanent magnetisation of rocks", Geophys. J. R. Astr. Soc. 24, 429-433
- Ordnance Survey Maps: 1" Okehampton Sheet No. 191 (1st series; 1:50,000), 6" (1:10,560) SX59, SE, SW, NE, NW and SX58, NE, NW, Geology Map No. 324: Okehampton
- Osman, C. W., 1924. "The geology of the northern border of Dartmoor between Whiddon Down and Butterdon Down", Quart. J. Geol. Soc. 80, 315-337
- Sanderson, D. J. and Dearman, W. R., 1973. "Structural zones of the variscan fold belt in S.W. England, the location and development", Jl. Geol. Soc. Lond. 129, 527-536
- Sedgwick, A. and Murchison, R. I., 1840. "On the physical structure of Devonshire, and on subdivisions and geological relations of its older stratified deposits, Trans. Geol. Soc. 5, 633-705
- Selwood, E. B. and McCourt, S., 1973. "The Bridford Thrust", Proc. Ussher Soc. 2, 529-535
- Stone, M. and Austin, W. G. C., 1961. "The metasomatic origin of the potash feldspar megacrysts in the granites of south-west England", J. Geol. 69, 464-472
- Tarling, D. H., 1971. "Principles and Applications of Palaeomagnetism", Pub. Chapman and Hall
- U.S. Naval Oceanographic Office, Chart 1700 (Magnetic Inclination), Chart 1703 (Total Intensity of the Earth's Magnetic Field), Chart 1706 (Magnetic Variation), Pub. U.S. Naval Oceanographic Office (3rd Edition) 1966

- Ussher, W. A. E., 1888. "The granite of Dartmoor",  
Parts 1 and 2, Trans. Devon. Assoc. 20, 141-157
- Ussher, W. A. E., 1892. "The British Culm Measures",  
Proc. Somerset Arch. N.H. Soc. 38, 111-219
- Ussher, W. A. E., 1900. "The Devonian, Carboniferous  
and New Red rocks of west Somerset, Devon and  
Cornwall", Proc. Somerset Arch. N.H. Soc. 46,  
1-64
- Ussher, W. A. E., 1901, "The Culm Measure types of Great  
Britain", Trans. Inst. Mining Eng. 20, 360-391
- Winkler, H. G. F., 1967. "Petrogenesis of Metamorphic  
Rocks", 2nd edition, Pub. Springer-Verlag N.Y.  
Inc.

APPENDIX A

Derivations

(i) To calculate the mean value of the magnetic field from a set of dissimilar fields

Each field is divided into its components

$$\underline{J}_x = J \cos I \cos D$$

$$\underline{J}_y = J \cos I \sin D$$

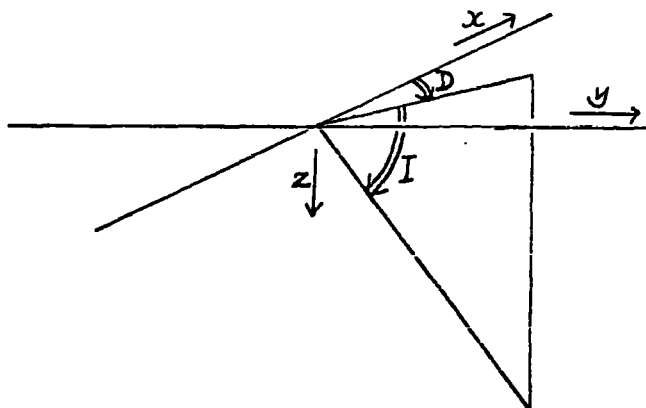
$$\underline{J}_z = J \sin I$$

such that  $J$  = intensity of magnetisation

$I$  = inclination )

) as shown below

$D$  = declination )



The mean value for  $\underline{J}_x$ ,  $\underline{J}_y$  and  $\underline{J}_z$  is calculated. The characteristics of the mean field can then be computed:-

$$\tan(D_{\text{mean}}) = \frac{\underline{J}_y \text{ mean}}{\underline{J}_x \text{ mean}}$$

$$\tan(I_{\text{mean}}) = \frac{\underline{J}_z \text{ mean} \times \sin(D_{\text{mean}})}{\underline{J}_y \text{ mean}}$$

$$\underline{J}_{\text{mean}} = \frac{\underline{J}_z \text{ mean}}{\sin(I_{\text{mean}})}$$

By using this method the summation of the fields is correctly weighted.

Table Ai lists the components of the remanent, induced and resultant fields. The remanent field components were calculated using experimental data (Table 3.2), the induced fields were computed using the information listed below and the resultant the sum of the above.

The Earth's Magnetic field at Okehampton 1977-8

Intensity      0.478 Oe

Declination    8°W i.e. +352°

Inclination    66°

(Ref: U.S. Naval Oceanographic Office charts)

(ii) Fisherian Statistics

As magnetisation is a vector it can be expressed in cartesian co-ordinates by its direction cosines:

$$\begin{array}{l} x = \cos D \sin I \\ y = \sin D \cos I \\ z = \sin I \end{array} \quad \left. \vphantom{\begin{array}{l} x \\ y \\ z \end{array}} \right\} \quad \begin{array}{l} \text{where} \\ I = \text{Inclination} \\ D = \text{Declination} \end{array}$$

(see Table Aii)

The length of the mean magnetic direction can then be calculated:-

$$R = \sqrt{(\sum x)^2 + (\sum y)^2 + (\sum z)^2}$$

From this the precision parameter, K. can be estimated.

$$K \approx k = \frac{N-1}{N-R} \quad \text{where } N = \text{no. of samples}$$

The cone of confidence  $\alpha_{95}$  and the circular standard deviation,  $\theta_{63}$ , can be computed.

$$\alpha_{95} = \cos^{-1} 1 - \frac{N-R}{R} \left\{ \left( P^{\frac{-1}{N-1}} - 1 \right) \right\}$$

where  $\alpha_{95}$  is the angle of the cone in which there is a 95% probability that the true direction lies.  
i.e.  $P = 0.05$

$$\theta_{63} = \frac{81}{K}$$

A circle of radius  $\theta_{63}$  degrees about the mean will encompass 63% of the data points.

The larger  $K$  and the smaller  $\alpha_{95}$  and  $\theta_{63}$  the less random will be the results.

The circular standard error (c.s.e) is also a measure of the degree of scatter. Like  $\theta_{63}$  to which it is related by the formula shown below, the larger its value the more scattered the results.

$$\text{c.s.e.} = \theta_{63} \cdot N^{-\frac{1}{2}}$$

Ref. Tarling, 1971

Table Ai: Showing the x,v,z components of the remanent (R), induced (I) and resultant (R+I) magnetisation of rocks from Meldon Quarry (all values in e.m.u. unless otherwise stated)

Sample Name	Remanent ( $\times 10^{-6}$ )			Resultant ( $\times 10^{-6}$ )			Induced ( $\times 10^{-6}$ )		
	$J_x^R$	$J_y^R$	$J_z^R$	$J_x^{R+I}$	$J_y^{R+I}$	$J_z^{R+I}$	$J_x^I$	$J_y^I$	$J_z^I$
M601.3	0.062	0.113	- 0.02	5.63	0.02	12.01	5.57	- 0.93	12.03
M601.2.2	0.18	- 0.16	0.15	7.38	1.41	16.4	7.20	- 1.25	16.25
M602.2	9.84	- 0.086	0.15	12.35	- 0.53	5.82	2.51	- 0.44	5.67
M603.3.2	- 1.95	0.348	- 2.90	0.41	- 0.062	2.42	2.36	- 0.41	5.32
M603.2.2	- 2.35	0.064	- 2.3	- 0.02	- 0.35	2.94	2.33	- 0.41	5.27
M603.1.1	- 3.89	0.955	- 4.21	- 1.54	0.545	1.09	2.35	- 0.41	5.30
M800.1.1	-205.12	948.90	-858.9	- 97.83	930.26	-616.62	107.29	-18.64	242.28
M800.2.2	-310.27	705.05	-632.8	-230.13	691.13	-451.82	80.14	-13.92	180.98
M800.2.1	-504.87	830.48	-982.10	-404.76	813.09	-756.03	100.11	-17.39	226.07
M102.1	0.054	0.078	0.03	1.53	- 0.18	3.38	1.48	- 0.26	3.35
M103.2.2	65.27	227.49	- 53.12	71.38	226.43	- 38.31	6.11	- 1.06	13.81
M103.1.2	- 0.124	- 0.077	0.08	1.64	- 0.387	4.06	1.76	- 0.31	3.98
M103.2.1	- 1.295	43.62	- 12.06	1.30	43.17	- 6.22	2.59	- 0.45	5.84
M104.1.1	- 47.49	12.28	- 96.5	- 30.81	11.99	- 58.82	16.68	- 0.29	37.63
M104.1.2	-324.9	30.97	-817.95	-298.79	26.43	-758.98	26.11	- 4.54	58.97
M101.1.1	65.51	570.43	565.24	118.41	561.24	684.7	52.9	- 9.19	119.46
M101.3	185.86	501.83	693.37	249.44	490.84	836.95	63.58	-10.99	143.58
M901.2	- 0.007	0.056	0.02	0.64	- 0.06	1.49	0.65	- 0.12	1.47
M901.1	- 0.003	0.053	0.15	0.70	- 0.08	1.76	0.71	- 0.13	1.61
M904.1	- 0.95	- 4.52	- 0.69	5.63	- 5.66	14.16	6.58	- 1.14	14.85
M904.2	22.27	- 14.66	2.41	28.94	- 15.88	17.67	6.76	- 1.22	15.26
M905.2.2	0.54	0.033	0.06	6.83	- 1.32	14.25	6.29	- 1.35	14.19
M905.3.2	0.089	0.069	0.07	7.35	- 1.19	16.47	7.26	- 1.26	16.40
M905.3.1	- 0.006	0.0003	0.03	7.01	- 1.22	15.89	7.02	- 1.22	15.86
Mean	- 44.0	160.4	- 91.7	- 19.3	156.8	- 43.2	21.5	- 3.64	48.56

Whence the declination (D), Inclination (I) and mean magnetisation (J) can be calculated:

$$D^R = 105^\circ$$

$$I^R = -29^\circ$$

$$J^R = 190 \times 10^{-6} \text{ e.m.u.}$$

$$= 190 \times 10^{-3} \text{ A.m.}^{-1}$$

$$D^{R+I} = 97^\circ$$

$$I^{R+I} = 15^\circ$$

$$J^{R+I} = 164 \times 10^{-6} \text{ e.m.u.}$$

$$= 164 \times 10^{-3} \text{ A.m.}^{-1}$$

$$D^I = 350^\circ$$

$$I^I = 66^\circ$$

$$J^I = 53 \times 10^{-6} \text{ e.m.u.}$$

$$= 53 \times 10^{-3} \text{ A.m.}^{-1}$$

Table Aii: Showing direction cosines ( $x, y, z$ ) of the remanent and resultant magnetisations

Name	Remanent			Resultant		
	$x$	$y$	$z$	$x$	$y$	$z$
M601.3	0.4741	0.8623	0.1779	0.4305	0.0015	0.9026
M601.2.2	0.6455	-0.5592	0.5203	0.4090	0.0782	0.9092
M602.2	0.9999	-0.0087	0.0148	0.9038	-0.0388	0.4262
M603.3.2	0.5547	0.0993	-0.8261	0.9836	-0.1488	0.1018
M603.2.2	-0.7105	0.0192	-0.7034	-0.0383	0.0022	0.9993
M603.1.1	-0.6697	0.1645	-0.7242	-0.7843	0.0278	0.5548
M800.1.1	-0.1583	0.7320	-0.6626	-0.0874	0.8303	-0.5505
M800.2.2	-0.3112	0.7072	-0.6347	-0.2685	0.8062	-0.5273
M800.2.1	-0.3654	0.6010	-0.7108	-0.3424	0.6830	-0.6393
M102.1	0.5451	0.7818	0.3040	0.4119	-0.0485	0.9099
M103.2.2	0.2753	0.9593	-0.224	0.3035	0.9384	-0.1652
M103.1.2	-0.7095	-0.4777	0.5180	0.3731	-0.0381	0.9236
M103.2.1	-0.0286	0.9634	-0.2663	0.2310	0.9630	0.1337
M104.1.1	-0.4388	0.1131	-0.8914	-0.4563	0.1776	-0.8719
M104.1.2	-0.3689	0.0352	-0.9283	-0.3657	0.0324	-0.9302
M101.1.1	0.0813	0.7080	0.7015	0.1325	0.6283	0.7667
M101.2	0.2113	0.5775	0.7885	0.2485	0.4889	0.8362
M901.1	-0.7515	0.6097	0.2521	-0.3941	0.0370	0.9183
M901.1	-0.0206	0.3373	0.9412	-0.3693	0.0422	0.9274
M904.1	0.2031	-0.9679	-0.1478	-0.3465	0.3484	0.8710
M904.2	0.8316	-0.5475	0.0898	-0.7735	0.3073	0.4709
M905.2.2	0.9927	0.0616	0.1037	-0.4305	0.0851	0.8986
M905.3.2	0.6725	0.5197	0.5269	-0.4065	0.0658	0.9113
M905.3.1	-0.1785	0.0098	0.9839	-0.4029	0.0269	0.9125



APPENDIX B

Listings of Computer Programs



\* \* \* \*  
 \* GREENLY \*  
 \* \* \* \*

PROGRAMME TO CALCULATE DZ AND DH (DIURNAL VARIATION) FROM BASE  
 STATION DATA, HENCE TO CALCULATE DZ, DH & LF FOR THE FIELD DATA,  
 SUBTRACTING DF FROM THE FIELD DATA CORRECTS FOR DIURNAL EFFECTS

\*\* F.W.GREEN 1978 \*\*

FIELD DATA READ IN ON UNIT 3  
 ML=NO. OF DATA POINTS  
 AX=DISTANCE FROM ORIGIN OF EACH TRAVERSE  
 AA=MAGNETIC ANOMALY  
 TI=TIME (MINUTES)

BASE STATION DATA READ IN ON UNITS 4 & 5  
 UNIT 4:  
 MH=NO. OF POINTS DESCRIBING THE HORIZONTAL COMPONENT  
 HX=X CO-ORDINATE (RELATED TO TIME)  
 HY=Y CO-ORDINATE (RELATED TO DH)

UNIT 5:  
 MZ=NO. OF POINTS DESCRIBING THE VERTICAL COMPONENT  
 ZX=X CO-ORDINATE (RELATED TO TIME)  
 ZY=Y CO-ORDINATE (RELATED TO DZ)

OUTPUT ON UNIT 6

```

DIMENSION X(300),A(300),T(300),HX(200),HY(200),ZX(200),ZY(200)
DIMENSION HSUM(200),ZSUM(200),DH(200),DZ(200),AX(300),AA(300)
DIMENSION CHX(200),CZX(200),ZT(200),HT(200),TT(300),CCA(300)
DIMENSION CA(300),DDF(300),DDZ(300),DDH(300),DDDF(200),DDDF(200)
DIMENSION CONSTH(200),CONSTZ(200),HTDIF(200),ZTDIF(200),CT(300)
DIMENSION AN(300),DCA(300)
READ(3,33) ML
READ(4,33) MH
READ(5,33) MZ
33 FORMAT(13)
READ(4,45) HX(1),HY(1)
45 FORMAT(12X,14.0,2X,F4.0)
HSUM(1)=HY(1)
DO 10 I=2,MH
READ(4,45,END=10) HX(I),HY(I)
HSUM(I)=HSUM(I-1)+HY(I)
10 CONTINUE
HMEAN=HSUM(MH)/MH
DO 11 I=1,MH
DH(I)=(HY(I)-HMEAN)*0.424
CHX(I)=HX(I)*0.2
11 CONTINUE
READ(5,45) ZX(1),ZY(1)
ZSUM(1)=ZY(1)
DO 12 I=2,MZ
READ(5,45,END=12) ZX(I),ZY(I)
ZSUM(I)=ZSUM(I-1)+ZY(I)
12 CONTINUE
ZMEAN=ZSUM(MZ)/MZ
DO 13 I=1,MZ
DZ(I)=(ZY(I)-ZMEAN)*0.43
CZX(I)=ZX(I)*0.2
13 CONTINUE
DO 90 I=1,ML
READ(3,34,END=90) AX(I),TT(I),AA(I)
34 FORMAT(1X,F6.2,12X,F7.2,4X,F6.2)
90 CONTINUE
IF (TT(ML) .GE. TT(1)) GO TO 91
DO 90 J=1,ML
I=ML-J+1
TI(I)=TT(J)
A(I)=AA(J)
98 CONTINUE
GO TO 93
91 DO 97 J=1,ML
I=J
TI(I)=TT(J)
A(I)=AA(J)
97 CONTINUE
93 ZF=(CZX(1)-TI(1))
TH=(CHX(1)-TI(1))
ZI(1)=TI(1)
HT(1)=TI(1)
DO 14 I=2,ML
IF (TZF) 17,19,19

```

```

19 ZT(1)=CZX(1)-T(1)
14 CONTINUE
   DO 15 I=2,ML
   IF (THF) 10,10,10
16 HT(1)=CHX(1)+THF
18 HT(1)=CHX(1)-THF
15 CONTINUE
   DZF(1)=JH(1)*0.4018+DZ(1)*0.9157
   CA(1)=A(1)-DZF(1)
   K=2
100 DO 23 I=2,ML
   IF (T(1) .EQ. T(I-1)) GO TO 1
54 IF (T(1) .GT. T(K)) GO TO 53
   GO TO 59
53 K=K+1
   IF (K .GT. ML) GO TO 55
   GO TO 54
55 L2DIF(K)=DZ(K)-DZ(K-1)
   ZTDIF(K)=ZT(K)-ZT(K-1)
   IF (ZTDIF(K) .EQ. 0.0) GO TO 77
   CONSTZ(K)=L2DIF(K)/ZTDIF(K)
   GO TO 79
77 CONSTZ(K)=0.0
79 DZ(1)=(T(1)-ZT(K))*CONSTZ(K)+DZ(K-1)
   GO TO 23
   1 DZ(1)=DZ(1-1)
   GO TO 23
55 IF (1 .LE. ML) GO TO 1
23 CONTINUE
40 J=2
60 DO 24 I=2,ML
   IF (T(1) .EQ. T(I-1)) GO TO 2
31 IF (HT(J) .LT. T(1)) GO TO 30
   GO TO 32
30 J=J+1
   IF (J .GT. MH) GO TO 50
   GO TO 31
32 DHDIF(J)=DH(J)-DH(J-1)
   HTDIF(J)=HT(J)-HT(J-1)
   IF (HTDIF(J) .EQ. 0.0) GO TO 78
   CONSTH(J)=DHDIF(J)/HTDIF(J)
   GO TO 30
78 CONSTH(J)=0.0
50 DH(1)=(T(1)-HT(J))*CONSTH(J)+DH(J-1)
   GO TO 24
   2 DH(1)=DH(1-1)
   GO TO 24
50 IF (1 .LE. ML) GO TO 2
24 CONTINUE
49 DO 51 I=2,ML
   DDF(I)=JSH(I)*0.4018+DDZ(I)*0.9157
   CA(I)=A(I)-DDF(I)
51 CONTINUE
   IF (TT(ML) .GE. TT(1)) GO TO 99
   LL=ML-1+1
   J=ML-1+1
   CCA(J)=CA(1)
   CT(J)=T(1)
   AN(J)=A(1)
54 CONTINUE
   GO TO 61
59 DO 86 I=1,ML
   J=1
   CCA(J)=CA(1)
   CT(J)=T(1)
   AN(J)=A(1)
66 CONTINUE
31 DO 36 I=1,ML
   DCA(1)=AN(1)-CCA(1)
   WRITE(6,71) XX(I),CT(1),CCA(1),AN(1),DCA(1)
71 FORMAT(1X,13.2,1X,F5.0,2X,F6.2,2X,F6.2,2X,F7.2)
88 CONTINUE
   MF=ML
   CALL PSYMB(2.0,8.0,-0.2,3,0.0,-1)
   CALL PSYMB(2.25,0.0,-0.2,'UNCORRECTED',0.0,9)
   CALL PSYMB(2.25,0.3,-0.2,'UNCORRECTED',0.0,11)
   CALL PSYMB(1.9,6.2,-0.25,97,0.0,-1)
   CALL PSYMB(1.9,7.0,-0.25,97,0.0,-1)
   CALL PAXIS(1.0,1.0,'DISTANCE-METRES',-15,22.0,0.0,0.0,500.0,1.0)
   CALL PAXIS(1.0,1.0,'ANGULAR-GAMMA',13,8.0,90.0,-1000.0,250.0,1.0)
   CALL PLTPTS(0.0,500.0,-1000.0,250.0,1.0,1.0)
   CALL PLTVAL(XX(1),CA(1),MR,1,0,0,1.0)
   CALL PLTVAL(XX(1),CCA(1),MR,1,3,0,1.0)
   CALL PAXIS(1.0,2.0,'ZERO RESIDUAL',-13,22.0,0.0,0.0,500.0,1.0)
   CALL PAXIS(25.0,1.0,'GAMMA',-3,2.0,90.0,-100.0,100.0,1.0)
   CALL PLTPTS(0.0,500.0,-100.0,100.0,1.0,1.0)
   CALL PLTVAL(XX(1),CCA(1),MR,1,0,0,1.0)
   CALL PLTEND
   STOP
   END

```



APPENDIX C

Data describing the ground  
and aerial profiles

Data describing the ground traverse along line 1

Date	Time minutes	Distance from origin-metres	Height metres	Reading gamma.	Anomaly gamma
25 10 77	908	0.0	380.0	47701	-79.61
25 10 77	896	379.00	330.0	47456	-325.91
25 10 77	894	380.00	329.0	47485	-296.72
25 10 77	894	381.00	328.0	47520	-261.74
25 10 77	893	382.00	328.0	47549	-232.65
25 10 77	892	383.00	327.0	47573	-208.56
25 10 77	889	384.00	326.0	47614	-167.26
25 10 77	890	385.00	325.0	47665	-116.39
25 10 77	890	386.00	325.0	47690	-91.40
25 10 77	888	387.00	324.0	47722	-59.20
25 10 77	887	388.00	323.0	47755	-42.12
25 10 77	886	391.00	322.0	47761	-20.07
25 10 77	1050	394.00	321.0	47742	-39.13
17 10 77	1047	404.00	320.0	47591	-217.68
17 10 77	1046	406.00	320.0	47545	-263.69
17 10 77	1047	410.00	319.0	47467	-321.70
17 10 77	1046	412.00	319.0	47410	-396.71
17 10 77	1046	416.00	319.0	47259	-549.72
17 10 77	1046	420.00	318.0	47213	-595.74
17 10 77	1045	423.00	318.0	47243	-565.75
17 10 77	1045	426.00	318.0	47373	-435.76
17 10 77	1044	429.00	317.0	47404	-324.78
17 10 77	1044	432.00	317.0	47527	-261.79
17 10 77	1043	435.00	317.0	47559	-249.60
17 10 77	1043	438.00	316.0	47524	-284.61
17 10 77	1042	441.00	316.0	47490	-313.63
17 10 77	1042	444.00	316.0	47435	-378.64
17 10 77	1041	447.00	316.0	47436	-370.65
17 10 77	1040	450.00	315.0	47486	-312.66
17 10 77	1040	453.00	315.0	47560	-248.67
17 10 77	1039	456.00	315.0	47604	-204.68
17 10 77	1039	459.00	314.0	47615	-193.69
17 10 77	1039	462.00	314.0	47590	-216.91
17 10 77	1038	465.00	314.0	47526	-262.92
17 10 77	1038	467.00	313.0	47505	-303.93
17 10 77	1037	469.00	313.0	47470	-338.94
17 10 77	1037	471.00	313.0	47421	-367.95
17 10 77	1036	473.00	312.0	47369	-439.96
17 10 77	1036	475.00	312.0	47314	-494.96
17 10 77	1035	477.00	312.0	47262	-546.97
17 10 77	1035	479.00	312.0	47202	-606.97
17 10 77	1034	481.00	311.0	47127	-661.98
17 10 77	1034	482.00	311.0	47067	-741.99
17 10 77	1034	483.00	311.0	47016	-752.99
17 10 77	1033	484.00	310.0	46970	-839.00
17 10 77	1033	485.00	310.0	46922	-867.00
17 10 77	1032	486.00	310.0	46885	-926.01
17 10 77	1032	487.00	309.0	46820	-969.01
17 10 77	1031	488.00	309.0	46764	-1045.01
17 10 77	1031	489.00	309.0	46699	-1116.02
17 10 77	1030	491.00	308.0	46639	-1270.03
17 10 77	1030	492.00	308.0	46590	-1219.03
17 10 77	1030	493.00	308.0	46531	-1278.03
17 10 77	1029	493.50	308.0	46510	-1299.03
17 10 77	1029	494.00	307.0	46443	-1361.04
17 10 77	1028	494.50	307.0	46387	-1422.04
17 10 77	1028	495.00	307.0	46306	-1501.04
17 10 77	1027	495.50	306.0	46233	-1571.04
17 10 77	1027	496.00	306.0	46162	-1646.24

Line 1 contd.

Date	Time minutes	Distance from origin-metres	Height metres	Reading gamma	Anomaly gamma
17 10 77	1027	496.50	306.0	46060	-1749.64
17 10 77	1026	497.00	305.0	45960	-1643.05
17 10 77	1026	497.50	305.0	45864	-1545.65
17 10 77	1025	498.00	305.0	45671	-2150.65
17 10 77	1025	498.50	304.0	45699	-2110.65
17 10 77	1024	499.00	304.0	45665	-2144.66
17 10 77	1024	499.50	304.0	45677	-2152.07
17 10 77	1023	500.00	304.0	45675	-2136.66
17 10 77	1022	500.50	303.0	45764	-2045.66
17 10 77	1021	501.00	303.0	45922	-1857.66
17 10 77	1021	501.50	303.0	46069	-1740.67
17 10 77	1021	502.00	302.0	46232	-1577.66
17 10 77	1020	502.50	302.0	46452	-1357.67
17 10 77	1020	503.00	302.0	46661	-1146.67
17 10 77	1020	503.50	301.0	46866	-941.66
17 10 77	1019	504.00	301.0	47057	-752.66
17 10 77	1018	504.50	301.0	47219	-590.66
17 10 77	1017	505.00	300.0	47416	-391.66
17 10 77	1016	505.50	300.0	47559	-250.66
17 10 77	1017	506.00	300.0	47635	-176.66
17 10 77	1016	507.00	299.0	47819	9.91
17 10 77	1016	508.00	299.0	47942	132.91
17 10 77	1015	510.00	299.0	48066	256.90
17 10 77	1015	511.00	298.0	48157	347.90
17 10 77	1015	512.00	298.0	48140	350.89
17 10 77	1014	513.00	298.0	48119	309.89
17 10 77	1014	514.00	297.0	48084	274.89
17 10 77	1014	515.00	297.0	48042	232.86
17 10 77	1013	516.00	297.0	47997	167.86
17 10 77	1013	517.00	296.0	47942	152.87
17 10 77	1012	518.00	296.0	47891	61.87
17 10 77	1011	519.00	296.0	47837	28.26
17 10 77	1011	520.00	296.0	47761	-27.73
17 10 77	1010	521.00	295.0	47716	-92.65
17 10 77	1010	522.00	295.0	47644	-164.66
17 10 77	1010	523.00	295.0	47541	-267.66
17 10 77	1009	524.00	294.0	47439	-369.99
17 10 77	1009	525.00	294.0	47321	-487.99
17 10 77	1008	526.00	294.0	47207	-602.66
17 10 77	1008	527.00	293.0	47069	-740.66
17 10 77	1008	528.00	293.0	46961	-846.66
17 10 77	1007	529.00	293.0	46866	-941.54
17 10 77	1007	530.00	292.0	46797	-1010.54
17 10 77	1007	531.00	292.0	46745	-1062.35
17 10 77	1006	533.00	292.0	46682	-1124.54
17 10 77	1006	535.00	292.0	46635	-1175.55
17 10 77	1005	537.00	292.0	46602	-1264.24
17 10 77	1005	539.00	291.0	46562	-1224.25
17 10 77	1004	541.00	291.0	46567	-1258.93
17 10 77	1004	543.00	291.0	46551	-1254.94
17 10 77	1003	545.00	290.0	46536	-1271.54
17 10 77	1003	546.00	290.0	46532	-1275.34
17 10 77	1002	547.00	290.0	46532	-1275.57
17 10 77	1002	548.00	289.0	46542	-1265.57
17 10 77	1002	549.00	289.0	46549	-1258.56
17 10 77	1001	550.00	289.0	46572	-1255.61
17 10 77	1000	551.00	288.0	46596	-1212.64
17 10 77	1000	551.50	288.0	46616	-1190.65
17 10 77	999	552.00	288.0	46646	-1162.75
17 10 77	998	552.50	286.0	46676	-1153.16





Line 1 contd .

Date	Time minutes	Distance from origin-metres	Height metres	Reading gamma	Anomaly gamma		
17	10	77	947	709.00	269.0	47577	-221.27
17	10	77	947	710.00	268.0	47569	-229.27
17	10	77	946	711.00	268.0	47557	-240.00
17	10	77	943	710.00	268.0	47501	-250.73
17	10	77	944	717.50	268.0	47535	-264.55
17	10	77	945	719.00	268.0	47529	-275.57
17	10	77	942	720.00	267.0	47432	-304.20
17	10	77	941	725.00	267.0	47401	-314.13
17	10	77	939	730.00	267.0	47457	-359.71
17	10	77	938	740.00	266.0	47384	-412.60
17	10	77	937	750.00	266.0	47370	-420.89
17	10	77	936	760.00	266.0	47379	-426.15
17	10	77	935	765.00	265.0	47369	-404.23
17	10	77	934	770.00	265.0	47425	-374.52
17	10	77	934	775.00	265.0	47456	-358.54
17	10	77	933	780.00	274.0	47450	-297.95
17	10	77	933	785.00	264.0	47543	-257.97
17	10	77	932	790.00	264.0	47564	-269.67
17	10	77	930	795.00	264.0	47625	-168.05
17	10	77	932	799.50	263.0	47672	-121.71
17	10	77	930	804.00	263.0	47727	-61.61
17	10	77	929	810.00	263.0	47755	-24.50
17	10	77	929	821.00	263.0	47742	-47.34
17	10	77	928	825.00	263.0	47727	-61.65
17	10	77	928	830.00	262.0	47809	-99.65
17	10	77	927	840.00	262.0	47877	-112.71
17	10	77	925	849.00	262.0	47867	-102.66
17	10	77	925	855.00	262.0	47723	-65.22
17	10	77	925	860.00	262.0	47754	-54.24
17	10	77	923	865.00	262.0	47763	-24.94
17	10	77	919	870.00	261.0	47822	34.50
17	10	77	919	875.00	261.0	47885	95.28
17	10	77	918	880.00	261.0	47909	121.15
17	10	77	917	890.00	261.0	47925	136.24
17	10	77	917	900.00	260.0	47915	132.20
17	10	77	915	905.00	207.0	47917	129.99
17	10	77	916	900.00	260.0	47921	108.54
17	10	77	915	905.00	260.0	47958	171.10
17	10	77	915	910.00	260.0	48012	225.00
17	10	77	915	915.00	260.0	48065	278.00
17	10	77	914	920.00	260.0	48021	252.44
17	10	77	914	925.00	260.0	47930	141.42
17	10	77	913	930.00	259.0	47769	70.47
17	10	77	912	935.00	259.0	47767	-61.14
17	10	77	912	939.00	259.0	47683	-100.10
17	10	77	911	942.00	259.0	47641	-140.56
17	10	77	910	944.00	258.0	47604	-182.45
17	10	77	910	946.00	258.0	47574	-212.46
17	10	77	907	951.00	257.0	47565	-225.97
17	10	77	909	955.50	257.0	47610	-176.50
17	10	77	906	956.00	257.0	47663	-103.26
17	10	77	906	961.00	255.0	47734	-57.70
17	10	77	905	966.00	258.0	47726	-52.62
17	10	77	905	971.00	258.0	47699	-61.65
17	10	77	905	976.00	258.0	47646	-150.24
17	10	77	903	981.00	255.0	47596	-162.20
17	10	77	902	984.00	255.0	47575	-202.21
17	10	77	902	987.00	255.0	47551	-220.22
17	10	77	907	990.00	254.0	47557	-217.93
17	10	77	901	992.50	254.0	47591	-165.10

line 1 contd.

Date	Time minutes	Distance from origin-metres	Height metres	Reading gamma	Anomaly gamma
17 10 77	900	995.00	234.0	47677	-56.13
17 10 77	900	1010.00	233.0	47762	0.81
17 10 77	899	1050.00	215.0	47848	89.22
20 10 77	812	1050.00	207.0	47837	-82.92
20 10 77	819	1050.00	207.0	47682	-100.14
20 10 77	818	1070.00	207.0	47547	-281.55
20 10 77	817	1085.00	206.0	47481	-367.76
20 10 77	816	1700.00	205.0	47357	-472.64
20 10 77	815	1720.00	205.0	47120	-709.44
20 10 77	823	1740.00	204.0	46953	-379.52
20 10 77	826	1765.00	204.0	47043	-789.81
20 10 77	831	1770.00	207.0	47175	-659.71
20 10 77	830	1775.00	208.0	47300	-535.49
20 10 77	830	1785.00	208.0	47493	-342.78
20 10 77	829	1795.00	206.0	47601	-255.72
20 10 77	832	1805.00	210.0	47700	-155.13
20 10 77	833	1815.00	212.0	47722	-112.80
20 10 77	837	1840.00	213.0	47722	-109.33
20 10 77	839	1870.00	215.0	47755	-78.82
20 10 77	841	1920.00	217.0	47735	-59.37
20 10 77	844	1965.00	219.0	47709	-124.25
20 10 77	848	2030.00	217.0	47683	-150.47
20 10 77	849	2110.00	214.0	47749	-90.16
20 10 77	852	2240.00	211.0	47730	-110.67
20 10 77	857	2330.00	206.0	47735	-56.62
20 10 77	859	2400.00	200.0	47777	-66.22
20 10 77	864	2515.00	192.0	47746	-78.52
20 10 77	870	2620.00	188.0	47765	-65.97
20 10 77	872	2705.00	184.0	47767	-60.61
20 10 77	877	2800.00	177.0	47771	-80.16
20 10 77	887	2870.00	172.0	47770	-78.45
20 10 77	896	2950.00	172.0	47759	-67.07
20 10 77	701	3060.00	176.0	47751	-59.54
20 10 77	768	3390.00	184.0	47759	-133.46
20 10 77	775	3510.00	206.0	47775	-101.42
20 10 77	789	3630.00	215.0	47756	-125.67

Data describing the ground traverse along line 2

Date	Time minutes	Distance from origin-metres	Height metres	Reading gamma.	Anomaly gamma.	
15	10	77	0.0	536.0	47757	-7.71
15	10	77	70.00	538.0	47716	-48.77
15	10	77	150.00	542.0	47716	-50.09
15	10	77	250.00	547.0	47717	-48.25
15	10	77	340.00	556.0	47717	-46.77
15	10	77	400.00	563.0	47718	-43.25
15	10	77	480.00	566.0	47720	-43.50
15	10	77	510.00	570.0	47721	-41.02
15	10	77	600.00	572.0	47724	-42.15
15	10	77	700.00	569.0	47725	-46.92
15	10	77	800.00	561.0	47725	-44.69
15	10	77	900.00	547.0	47724	-45.57
15	10	77	1000.00	532.0	47727	-50.15
15	10	77	1100.00	518.0	47727	-49.72
15	10	77	1300.00	512.0	47727	-55.13
15	10	77	1400.00	512.0	47728	-57.11
15	10	77	1490.00	512.0	47725	-59.02
15	10	77	1600.00	513.0	47725	-60.00
15	10	77	1690.00	515.0	47720	-67.20
15	10	77	1750.00	520.0	47715	-72.24
15	10	77	1900.00	526.0	47715	-76.90
15	10	77	2000.00	529.0	47711	-75.55
15	10	77	2100.00	525.0	47729	-66.52
15	10	77	2200.00	523.0	47746	-53.50
15	10	77	2300.00	509.0	47771	-46.82
15	10	77	2400.00	489.0	47788	-101.21
15	10	77	2610.00	467.0	47559	-200.56
15	10	77	2824.00	450.0	47574	-254.50
15	10	77	2852.00	444.0	47565	-293.93
15	10	77	2880.00	430.0	47743	-353.42
15	10	77	2887.00	430.0	47458	-358.45
15	10	77	2889.80	427.0	47426	-373.14
15	10	77	2890.20	426.0	47425	-372.14
15	10	77	2895.00	426.0	47435	-368.57
15	10	77	2907.00	426.0	47472	-351.40
15	10	77	2914.00	426.0	47465	-337.14
15	10	77	2921.00	426.0	47447	-354.00
15	10	77	2935.00	427.0	47505	-296.53
15	10	77	2942.00	427.0	47539	-213.40
15	10	77	2949.00	427.0	47685	-114.17
15	10	77	2956.00	427.0	47707	-56.47
15	10	77	2957.40	428.0	47742	-50.15
15	10	77	2960.20	428.0	47842	40.16
15	10	77	2962.00	428.0	47950	140.16
15	10	77	2963.40	428.0	48076	273.82
15	10	77	2964.80	428.0	48211	408.81
15	10	77	2966.20	428.0	48519	515.23
15	10	77	2967.60	428.0	48464	603.70
15	10	77	2969.00	429.0	48487	656.76
15	10	77	2970.40	429.0	48556	755.59
15	10	77	2971.80	429.0	48615	818.36
15	10	77	2973.20	429.0	48656	880.56
15	10	77	2974.60	429.0	48784	962.50
15	10	77	2976.00	430.0	48815	1011.56
15	10	77	2977.40	430.0	48875	1071.57
15	10	77	2978.80	430.0	48913	1111.57
15	10	77	2980.20	430.0	48946	1144.17
15	10	77	2981.60	430.0	48986	1176.17
15	10	77	2983.00	430.0	48997	1194.77



Line 2 contd.

Date	Time minutes	Distance from origin-metres	Height metres	Reading gamma	Anomaly gamma		
15	10	77	981	2381.00	415.0	47836	25.74
15	10	77	982	2382.40	414.0	47817	4.55
15	10	77	983	2383.80	414.0	47817	4.54
15	10	77	984	2385.20	414.0	47847	54.57
15	10	77	985	2386.60	413.0	47800	67.55
15	10	77	986	2388.00	412.0	47834	171.04
15	10	77	987	2389.40	412.0	48021	206.63
15	10	77	988	2390.80	412.0	48080	256.72
15	10	77	989	2392.20	411.0	48132	318.71
15	10	77	990	2393.60	411.0	48171	357.35
15	10	77	991	2395.00	410.0	48233	389.07
15	10	77	992	2396.40	410.0	48219	405.86
15	10	77	993	2397.80	410.0	48224	407.89
15	10	77	994	2399.20	409.0	48174	377.89
15	10	77	995	2400.60	409.0	48166	351.89
15	10	77	996	2402.00	409.0	48166	291.89
15	10	77	997	2403.40	409.0	48166	291.89
15	10	77	998	2404.80	408.0	48000	193.82
15	10	77	999	2406.20	408.0	47864	49.82
15	10	77	1000	2407.60	408.0	47889	-125.86
15	10	77	1001	2409.00	408.0	47532	-282.87
15	10	77	1002	2410.40	408.0	47328	-483.85
15	10	77	1003	2411.80	407.0	47125	-688.88
15	10	77	1004	2413.20	407.0	46842	-876.48
15	10	77	1005	2414.60	406.0	46655	-1284.32
15	10	77	1006	2416.00	405.0	46570	-1427.32
15	10	77	1007	2417.40	405.0	46267	-1550.16
15	10	77	1008	2418.80	405.0	46221	-1555.50
15	10	77	1009	2420.20	405.0	46489	-1327.82
15	10	77	1010	2421.60	404.0	46511	-955.83
15	10	77	1011	2423.00	404.0	47205	-811.85
15	10	77	1012	2424.40	404.0	47002	-254.86
15	10	77	1013	2425.80	403.0	47123	-55.49
15	10	77	1014	2427.20	403.0	47000	51.86
15	10	77	1015	2428.60	403.0	47741	124.86
15	10	77	1016	2430.00	402.0	47502	165.84
15	10	77	1017	2431.40	402.0	47574	177.84
15	10	77	1018	2432.80	402.0	47550	182.87
15	10	77	1019	2434.20	401.0	47555	179.86
15	10	77	1020	2435.60	401.0	47505	171.41
15	10	77	1021	2437.00	401.0	47576	161.84
15	10	77	1022	2438.40	400.0	47584	149.84
15	10	77	1023	2439.80	400.0	47556	142.86
15	10	77	1024	2441.20	400.0	47547	132.85
15	10	77	1025	2442.60	400.0	47556	121.82
15	10	77	1026	2444.00	399.0	47525	115.99
15	10	77	1027	2445.40	399.0	47515	103.45
15	10	77	1028	2446.80	399.0	47505	97.44
15	10	77	1029	2448.20	398.0	47505	84.76
15	10	77	1030	2449.60	398.0	47500	69.76
15	10	77	1031	2451.00	398.0	47377	55.15
15	10	77	1032	2452.40	397.0	47305	47.55
15	10	77	1033	2453.80	397.0	47335	37.55
15	10	77	1034	2455.20	397.0	47844	26.50
15	10	77	1035	2456.60	396.0	47349	22.48
15	10	77	1036	2458.00	396.0	47357	19.45
15	10	77	1037	2459.40	396.0	47831	14.10
15	10	77	1038	2460.80	396.0	47707	-30.82
15	10	77	1039	2462.20	395.0	47749	-27.19
15	10	77	1040	2463.60	395.0	47547	29.76
15	10	77	1041	2465.00	395.0	47827	5.81

Line 2 cont d.

Date	Time minutes	Distance from origin-metres	Height metres	Reading gamma	Anomaly gamma.		
15	10	77	1019	3039.20	394.0	47821	3.58
15	10	77	1020	3046.20	394.0	47826	6.40
15	10	77	1020	3053.20	394.0	47825	7.36
15	10	77	1021	3060.20	393.0	47817	-1.64
15	10	77	1022	3067.20	393.0	47815	-5.16
15	10	77	1022	3074.20	393.0	47804	-16.19
15	10	77	1023	3081.20	392.0	47795	-21.05
15	10	77	1024	3088.20	392.0	47797	-21.25
21	10	77	731	3100.00	392.0	47781	-35.96
21	10	77	732	3104.00	391.0	47762	-34.99
21	10	77	733	3109.00	390.0	47764	-33.01
21	10	77	734	3114.00	389.0	47752	-45.04
21	10	77	735	3119.00	389.0	47747	-50.07
21	10	77	736	3124.00	388.0	47745	-54.16
21	10	77	737	3134.00	387.0	47735	-62.15
21	10	77	738	3144.00	386.0	47716	-79.21
21	10	77	739	3154.00	386.0	47899	-96.27
21	10	77	740	3164.00	385.0	47887	-110.32
21	10	77	741	3164.00	384.0	47857	-140.44
21	10	77	744	3189.00	383.0	47857	-100.47
21	10	77	744	3190.00	383.0	47857	-140.47
21	10	77	745	3191.00	382.0	47809	-138.47
21	10	77	745	3192.00	381.0	47553	-244.46
21	10	77	746	3193.00	380.0	47512	-285.49
21	10	77	746	3194.00	380.0	47426	-377.49
21	10	77	743	3195.00	379.0	47450	-367.56
21	10	77	747	3196.00	378.0	47349	-448.51
21	10	77	748	3197.00	377.0	47366	-489.51
21	10	77	748	3198.00	376.0	47285	-512.51
21	10	77	749	3199.00	376.0	47275	-522.52
21	10	77	749	3200.00	375.0	47219	-516.52
21	10	77	751	3201.00	374.0	47304	-493.53
21	10	77	751	3202.00	373.0	47356	-459.54
21	10	77	757	3203.00	372.0	47362	-415.54
21	10	77	757	3204.00	372.0	47413	-382.55
21	10	77	758	3205.00	371.0	47455	-362.56
21	10	77	759	3207.50	370.0	47565	-232.57
21	10	77	760	3210.00	369.0	47625	-172.56
21	10	77	760	3212.50	369.0	47685	-134.56
21	10	77	761	3215.00	367.0	47654	-143.56
21	10	77	761	3217.50	366.0	47631	-166.56
21	10	77	762	3220.00	366.0	47646	-149.56
21	10	77	762	3225.00	365.0	47695	-102.56
21	10	77	763	3226.00	364.0	47754	-43.57
21	10	77	763	3229.00	363.0	47794	-3.59
21	10	77	764	3232.00	363.0	47806	10.59
21	10	77	764	3236.00	362.0	47759	-13.72
21	10	77	765	3240.00	361.0	47762	-35.75
21	10	77	765	3244.00	360.0	47752	-45.78
21	10	77	766	3249.00	360.0	47727	-70.80
21	10	77	768	3254.00	359.0	47713	-84.83
21	10	77	767	3259.00	358.0	47691	-106.86
21	10	77	766	3256.50	357.0	47615	-164.85
21	10	77	766	3264.00	356.0	47688	-117.85
21	10	77	770	3271.50	355.0	47694	-103.85
21	10	77	772	3279.00	355.0	47670	-127.87
21	10	77	773	3289.00	354.0	47655	-165.85
21	10	77	775	3299.00	353.0	47612	-166.85
21	10	77	775	3309.00	348.0	47581	-217.14
21	10	77	777	3330.00	338.0	47555	-245.26

Line 2 contd.

Date	Time minutes	Distance from origin -metres	Height metres	Reading gamma	Anomaly gamma
21 10 77	780	3390.00	330.0	47570	-222.00
21 10 77	782	3445.00	320.0	47615	-183.91
21 10 77	785	3535.00	307.0	47635	-164.42
21 10 77	787	3595.00	284.0	47597	-202.75
21 10 77	790	3685.00	260.0	47399	-401.15
21 10 77	790	3700.00	284.0	47350	-450.34
21 10 77	793	3740.00	276.0	47540	-254.57
21 10 77	800	3760.00	267.0	47630	-182.00
21 10 77	798	3790.00	265.0	47709	-91.05
21 10 77	802	3850.00	261.0	47742	-59.00
22 10 77	882	3970.00	258.0	47400	-318.35
22 10 77	885	4010.00	253.0	47005	-200.55



Data describing the ground traverse along line 3

Date	Time minutes	Distance from origin-metres	Height metres	Reading gamma	Anomaly gamma
16 10 77	903	0.00	431.00	47734	-03.91
16 10 77	973	170.00	440.00	47734	-03.92
16 10 77	904	640.00	461.00	47737	-01.52
16 10 77	909	800.00	453.00	47739	-03.50
16 10 77	955	1000.00	515.00	47730	-02.01
16 10 77	950	1200.00	515.00	47745	-70.04
16 10 77	947	1355.00	507.00	47735	-00.15
16 10 77	944	1450.00	523.00	47733	-00.20
16 10 77	941	1550.00	520.00	47733	-00.37
16 10 77	934	1650.00	529.00	47730	-09.47
16 10 77	932	1720.00	530.00	47731	-00.57
16 10 77	910	2000.00	530.00	47732	-00.05
16 10 77	915	2095.00	530.00	47729	-92.20
16 10 77	910	2190.00	530.00	47720	-93.72
16 10 77	907	2205.00	523.00	47729	-95.24
16 10 77	903	2330.00	492.00	47730	-92.47
16 10 77	902	2400.00	469.00	47727	-95.50
16 10 77	090	2570.00	452.00	47731	-90.30
16 10 77	007	2670.00	436.00	47730	-93.50
16 10 77	004	2775.00	424.00	47730	-90.59
16 10 77	001	2875.00	410.00	47731	-93.55
16 10 77	077	2975.00	412.00	47729	-92.11
16 10 77	069	3015.00	403.00	47727	-90.75
16 10 77	005	3400.00	392.00	47720	-102.53
16 10 77	002	3485.00	384.00	47720	-103.07
16 10 77	050	3547.50	375.00	47715	-110.02
16 10 77	052	3622.50	373.00	47710	-100.72
16 10 77	048	3697.50	372.00	47702	-110.14
16 10 77	041	3832.50	369.00	47682	-133.91
16 10 77	040	3862.50	360.00	47692	-123.03
16 10 77	039	3870.50	355.00	47691	-170.03
16 10 77	007	3920.50	353.00	47620	-157.90
16 10 77	035	3935.50	350.00	47645	-172.73
16 10 77	034	3950.50	353.00	47652	-165.72
16 10 77	033	3965.50	340.00	47659	-150.71
16 10 77	032	3980.50	341.00	47679	-150.09
16 10 77	031	3995.50	337.00	47715	-102.92
16 10 77	030	4010.50	333.00	47747	-70.90
16 10 77	030	4025.50	320.00	47735	-83.00
16 10 77	024	4035.50	324.00	47655	-103.90
16 10 77	022	4045.50	320.00	47632	-107.19
16 10 77	016	4055.50	316.00	47709	-113.79
16 10 77	017	4065.50	311.00	47650	-102.23
16 10 77	017	4075.50	307.00	47685	-103.27
16 10 77	010	4085.50	302.00	47700	-110.20
16 10 77	015	4095.50	298.00	47690	21.72
16 10 77	703	4101.50	294.00	47694	90.70
16 10 77	702	4107.50	292.00	47691	00.45
16 10 77	701	4113.50	292.00	47690	112.57
16 10 77	701	4110.50	290.00	47695	51.57
16 10 77	700	4115.50	290.00	47695	30.09
16 10 77	779	4122.50	289.00	47697	4.03
16 10 77	700	4125.50	288.00	47737	-05.97
16 10 77	770	4120.50	288.00	47702	-99.99
16 10 77	777	4134.50	288.00	47655	-142.51
16 10 77	770	4140.50	287.00	47721	-90.04
16 10 77	770	4140.50	287.00	47694	-157.05
16 10 77	775	4152.50	287.00	47600	-154.50
16 10 77	774	4164.50	287.00	47600	-204.49

Line 3 contd.

Date	Time minutes	Distance from origin-metres	Height metres	Reading gamma	Anomaly gamma		
16	10	77	775	4176.50	287.0	47592	-212.05
16	10	77	772	4188.50	287.0	47601	-205.02
16	10	77	771	4200.50	288.0	47625	-179.96
16	10	77	770	4200.50	288.0	47621	-179.94
16	10	77	770	4212.50	288.0	47617	-183.95
16	10	77	769	4220.50	288.0	47622	-175.03
16	10	77	768	4224.10	288.0	47621	-176.00
16	10	77	768	4227.70	288.0	47614	-183.09
16	10	77	768	4231.30	288.0	47600	-189.10
16	10	77	767	4232.50	288.0	47611	-185.00
16	10	77	767	4233.70	288.0	47610	-186.00
16	10	77	766	4234.90	288.0	47614	-181.00
16	10	77	766	4236.10	288.0	47617	-185.00
16	10	77	765	4237.30	288.0	47615	-189.15
16	10	77	765	4238.50	288.0	47605	-194.15
16	10	77	764	4239.70	288.0	47594	-203.03
16	10	77	764	4240.90	288.0	47594	-203.03
16	10	77	764	4242.10	288.0	47637	-180.04
16	10	77	763	4243.30	289.0	47635	-110.31
16	10	77	763	4244.50	289.0	47725	-70.31
16	10	77	762	4245.70	289.0	47735	-59.07
16	10	77	762	4246.90	289.0	47709	-85.00
16	10	77	762	4248.10	289.0	47605	-111.00
16	10	77	761	4249.30	289.0	47646	-147.00
16	10	77	761	4250.50	289.0	47656	-127.00
16	10	77	760	4251.70	289.0	47714	-78.90
16	10	77	750	4252.90	289.0	47775	0.20
16	10	77	759	4254.10	289.0	47841	40.22
16	10	77	759	4255.30	289.0	47833	90.51
16	10	77	758	4256.50	289.0	47867	94.98
16	10	77	758	4257.70	290.0	47790	5.90
16	10	77	757	4261.90	290.0	47712	-79.55
16	10	77	757	4263.10	290.0	47674	-117.00
16	10	77	756	4264.30	290.0	47695	-96.00
16	10	77	756	4265.50	290.0	47699	-92.00
16	10	77	755	4266.70	290.0	47672	-110.00
16	10	77	755	4267.90	290.0	47670	-112.00
16	10	77	755	4269.10	290.0	47680	-102.00
16	10	77	754	4270.30	290.0	47681	-110.94
16	10	77	754	4271.50	290.0	47619	-172.94
16	10	77	753	4272.70	290.0	47599	-199.04
16	10	77	753	4273.90	290.0	47576	-114.04
16	10	77	752	4275.10	290.0	47561	-211.15
16	10	77	752	4276.30	291.0	47579	-213.15
16	10	77	752	4277.50	291.0	47599	-193.15
16	10	77	751	4278.70	291.0	47610	-172.00
16	10	77	751	4279.90	291.0	47600	-162.00
16	10	77	751	4281.10	291.0	47582	-208.00
16	10	77	750	4282.30	291.0	47520	-202.50
16	10	77	750	4283.50	291.0	47445	-345.54
16	10	77	749	4284.70	291.0	47500	-407.00
16	10	77	719	4285.90	291.0	47600	-181.00
16	10	77	719	4286.00	291.0	47400	-575.00
16	10	77	716	4287.00	291.0	47340	-435.00
16	10	77	717	4288.00	291.0	47300	-479.17
16	10	77	716	4289.00	292.0	47350	-251.04
16	10	77	715	4290.00	292.0	47330	-142.00
16	10	77	712	4291.00	292.0	47357	-424.00
16	10	77	710	4292.00	292.0	47270	-305.00
16	10	77	709	4293.00	292.0	47275	-500.27

Line 3 contd.

Date	Time minutes	Distance from origin-metres	Height metres	Reading gamma	Anomaly gamma		
16	10	77	708	4294.00	292.0	47284	-497.14
16	10	77	707	4295.00	292.0	47301	-480.02
16	10	77	706	4296.00	292.0	47361	-399.69
16	10	77	704	4297.00	292.0	47459	-321.63
16	10	77	703	4298.00	292.0	47509	-391.51
16	10	77	702	4299.00	293.0	47295	-485.38
16	10	77	702	4300.00	293.0	47219	-501.58
16	10	77	701	4301.00	293.0	47311	-489.59
16	10	77	700	4302.00	293.0	47347	-436.47
16	10	77	700	4303.00	294.0	47407	-573.46
16	10	77	699	4305.00	294.0	47520	-200.37
16	10	77	698	4307.00	294.0	47590	-190.61
16	10	77	698	4309.00	294.0	47618	-162.61
16	10	77	698	4311.00	295.0	47651	-129.62
16	10	77	697	4313.00	295.0	47611	-169.46
16	10	77	696	4315.00	295.0	47622	-158.56
16	10	77	696	4317.00	295.0	47569	-191.30
16	10	77	695	4319.00	296.0	47632	-148.14
16	10	77	694	4321.00	296.0	47660	-113.97
16	10	77	694	4323.00	296.0	47671	-108.96
16	10	77	693	4325.50	296.0	47736	-41.82
16	10	77	692	4327.00	296.0	47731	-46.66
16	10	77	692	4332.00	296.0	47632	-147.67
16	10	77	691	4337.00	297.0	47637	-142.51
16	10	77	691	4342.00	297.0	47594	-165.53
16	10	77	690	4347.00	297.0	47573	-206.37
16	10	77	689	4352.00	298.0	47602	-177.22
16	10	77	688	4357.00	298.0	47626	-153.06
16	10	77	687	4362.00	295.0	47636	-140.91
16	10	77	686	4364.00	295.0	47680	-96.41
16	10	77	685	4366.00	296.0	47680	-98.29
16	10	77	684	4366.00	296.0	47667	-95.71
16	10	77	684	4370.00	296.0	47674	-106.72
16	10	77	683	4372.00	296.0	47660	-122.90
16	10	77	682	4373.00	296.0	47646	-137.08
16	10	77	678	4374.00	296.0	47462	-319.63
16	10	77	677	4375.00	297.0	47635	-146.55
16	10	77	677	4376.00	297.0	47625	-156.55
16	10	77	676	4377.00	297.0	47596	-186.65
16	10	77	676	4378.00	297.0	47553	-229.65
16	10	77	675	4379.00	298.0	47494	-269.10
16	10	77	675	4380.00	298.0	47431	-352.10
16	10	77	674	4381.00	298.0	47377	-406.73
16	10	77	674	4382.00	299.0	47366	-417.74
16	10	77	673	4383.00	299.0	47416	-367.13
16	10	77	673	4384.00	299.0	47534	-251.13
16	10	77	672	4385.00	299.0	47696	-67.16
16	10	77	672	4386.00	300.0	47846	62.64
16	10	77	671	4387.00	300.0	47962	195.51
16	10	77	671	4388.00	300.0	48054	267.51
16	10	77	670	4388.50	300.0	48144	357.03
16	10	77	669	4389.00	300.0	48241	434.55
16	10	77	669	4389.50	301.0	48322	535.54
16	10	77	668	4390.00	301.0	48533	751.16
16	10	77	667	4391.00	301.0	48641	853.99
16	10	77	667	4391.50	302.0	48632	844.99
16	10	77	666	4392.00	302.0	48536	800.45
16	10	77	665	4392.50	302.0	48506	726.25
16	10	77	664	4393.00	303.0	48411	625.64
16	10	77	664	4393.50	303.0	48392	604.04

Date	Time minutes	Distance From origin-metres	Height metres	Reading gamma	Anomaly gamma		
16	10	77	564	4394.00	304.0	48260	472.03
16	10	77	664	4394.50	304.0	48170	382.03
16	10	77	663	4395.00	304.0	48140	359.83
16	10	77	663	4395.50	304.0	48077	238.83
16	10	77	659	4396.00	304.0	47730	-59.00
16	10	77	659	4397.00	305.0	47720	-63.00
16	10	77	658	4398.00	305.0	47751	-58.21
16	10	77	657	4399.00	305.0	47812	22.58
16	10	77	657	4400.00	306.0	47851	61.58
16	10	77	656	4401.00	306.0	47900	190.37
16	10	77	655	4402.00	307.0	47926	136.70
16	10	77	654	4403.00	307.0	47940	150.98
16	10	77	654	4404.00	312.0	47927	137.96
16	10	77	653	4405.00	315.0	47913	123.86
16	10	77	653	4406.00	335.0	47894	104.88
16	10	77	652	4407.00	321.0	47865	74.92
16	10	77	651	4408.00	315.0	47833	42.44
16	10	77	650	4409.00	335.0	47800	9.47
16	10	77	650	4410.00	349.0	47782	-28.54
16	10	77	649	4411.00	352.0	47722	-68.80
16	10	77	648	4412.00	349.0	47685	-107.31
16	10	77	641	4413.00	346.0	47664	-129.12
16	10	77	632	4414.00	346.0	47637	-159.77
16	10	77	626	4430.00	338.0	47671	-128.03
16	10	77	524	4520.00	324.0	47679	-120.68
16	10	77	621	4605.00	312.0	47685	-116.05
16	10	77	619	4700.00	306.0	47661	-120.92
16	10	77	617	4768.00	304.0	47680	-142.72
16	10	77	515	4840.00	303.0	47681	-117.31
18	10	77	663	5135.00	302.0	47548	-200.96
18	10	77	666	5348.00	300.0	47648	-184.30
18	10	77	666	5420.00	298.0	47675	-136.84
18	10	77	872	5500.00	292.0	47666	-145.06
18	10	77	874	5570.00	285.0	47616	-193.44
19	10	77	590	5920.00	276.0	47648	-174.02
19	10	77	593	6015.00	270.0	47630	-193.80
19	10	77	597	6130.00	264.0	47555	-232.03
19	10	77	598	6220.00	258.0	47585	-242.01
19	10	77	602	6275.00	255.0	47532	-295.77
19	10	77	600	6315.00	249.0	47487	-344.05
19	10	77	605	6380.00	241.0	47449	-373.52
19	10	77	606	6425.00	238.0	47440	-380.09
19	10	77	606	6540.00	270.0	47436	-390.64
19	10	77	614	6650.00	276.0	47509	-310.06
19	10	77	618	6655.00	269.0	47594	-234.21
19	10	77	617	6710.00	265.0	47630	-199.76
19	10	77	621	6775.00	261.0	47653	-169.42
19	10	77	622	6815.00	255.0	47712	-112.42
19	10	77	626	6865.00	252.0	47801	-11.07
19	10	77	630	6920.00	247.0	47890	75.67
19	10	77	634	7030.00	249.0	47942	125.29
19	10	77	637	7120.00	248.0	47965	145.89
19	10	77	539	7215.00	248.0	47988	149.43
19	10	77	642	7320.00	248.0	47987	149.76
19	10	77	644	7430.00	249.0	47989	148.16
19	10	77	656	7715.00	249.0	47926	115.52
19	10	77	659	7820.00	255.0	47931	113.11
19	10	77	660	8010.00	254.0	47923	111.79
19	10	77	663	8110.00	258.0	47892	75.85
19	10	77	671	8170.00	258.0	47908	101.49
19	10	77	674	8315.00	263.0	47986	105.77
19	10	77	675	8400.00	265.0	47831	62.57
19	10	77	680	8515.00	262.0	47899	98.79
19	10	77	682	8600.00	258.0	47951	67.58
19	10	77	684	8720.00	255.0	47882	76.24
19	10	77	687	8820.00	246.0	47879	66.78
19	10	77	690	8920.00	238.0	47876	64.45
19	10	77	692	9020.00	232.0	47870	55.95
19	10	77	695	9120.00	236.0	47872	58.85
19	10	77	697	9230.00	235.0	47868	56.47
19	10	77	700	9320.00	227.0	47865	49.24
19	10	77	704	9420.00	226.0	47852	31.77



## Line 4 contd.

Date	Time minutes	Distance from origin-metres	Height metres	Reading gamma	Anomaly gamma		
11	10	77	839	5347.00	392.0	47775	-41.00
11	10	77	839	5352.00	391.0	47762	-34.00
11	10	77	840	5357.00	390.0	47767	-29.71
11	10	77	840	5362.00	389.0	47753	-23.74
11	10	77	840	5367.00	388.0	47753	-23.77
11	10	77	841	5372.00	387.0	47750	-20.80
11	10	77	841	5377.00	386.0	47750	-30.82
11	10	77	842	5382.00	385.0	47774	-42.03
11	10	77	842	5387.00	384.0	47765	-51.00
11	10	77	843	5392.00	384.0	47750	-56.51
11	10	77	843	5402.00	383.0	47750	-60.90
11	10	77	844	5412.00	382.0	47753	-64.02
11	10	77	844	5420.00	381.0	47752	-65.10
14	10	77	856	5440.00	380.0	47822	50.33
14	10	77	857	5445.00	379.0	47750	-50.53
14	10	77	857	5450.00	378.0	47754	-60.02
14	10	77	858	5455.00	377.0	47741	-61.38
14	10	77	859	5460.00	375.0	47744	-50.78
14	10	77	860	5465.00	373.0	47745	-40.13
14	10	77	861	5470.00	371.0	47720	-62.70
14	10	77	862	5475.00	369.0	47704	-60.00
14	10	77	863	5480.00	368.0	47695	-103.00
14	10	77	864	5485.00	362.0	47695	-104.00
14	10	77	865	5490.00	359.0	47733	-102.41
14	10	77	866	5495.00	355.0	47705	-93.75
14	10	77	867	5500.00	352.0	47714	-80.20
14	10	77	868	5505.00	348.0	47723	-75.04
14	10	77	869	5510.00	344.0	47720	-75.50
14	10	77	870	5515.00	341.0	47752	-70.56
14	10	77	871	5520.00	343.0	47740	-52.55
14	10	77	873	5530.00	344.0	47746	-54.04
14	10	77	874	5540.00	346.0	47750	-54.55
14	10	77	876	5550.00	347.0	47750	-39.52
14	10	77	877	5560.00	349.0	47757	-39.54
14	10	77	878	5570.00	350.0	47750	-30.40
14	10	77	880	5580.00	352.0	47753	-44.32
14	10	77	880	5590.00	353.0	47762	-35.30
14	10	77	881	5600.00	353.0	47763	-35.75
14	10	77	882	5610.00	350.0	47748	-34.50
14	10	77	889	5620.00	356.0	47740	-62.23
14	10	77	890	5630.00	360.0	47729	-72.70
14	10	77	891	5640.00	361.0	47715	-61.05
14	10	77	892	5650.00	363.0	47710	-65.42
14	10	77	893	5660.00	364.0	47707	-54.33
14	10	77	894	5670.00	366.0	47707	-62.54
14	10	77	895	5680.00	367.0	47715	-60.75
14	10	77	896	5690.00	369.0	47737	-63.57
14	10	77	897	5700.00	370.0	47747	-55.04
14	10	77	898	5710.00	372.0	47760	-42.00
14	10	77	901	5720.00	373.0	47802	-0.43
14	10	77	903	5730.00	375.0	47750	-10.00
14	10	77	904	5740.00	376.0	47804	1.02
14	10	77	904	5750.00	375.0	47775	-27.44
14	10	77	905	5750.20	374.0	47771	-32.21
14	10	77	906	5760.40	372.0	47775	-25.10
14	10	77	907	5765.20	370.0	47765	-21.60
14	10	77	907	5759.40	368.0	47767	-17.00
14	10	77	908	5815.90	366.0	47810	12.05
14	10	77	910	5832.40	364.0	47825	52.57
14	10	77	911	5840.50	363.0	47834	25.45

## Line 4 contd.

Date	Time minutes	Distance from origin-metres	Height metres	Reading gamma	Anomaly gamma		
14	10	77	912	5665.40	361.0	47767	-41.36
14	10	77	913	5673.60	359.0	47753	-55.22
14	10	77	914	5681.60	357.0	47743	-65.37
14	10	77	915	5690.00	355.0	47729	-79.61
14	10	77	915	5900.50	353.0	47767	-41.71
14	10	77	916	5923.00	352.0	47746	-62.99
14	10	77	917	5939.50	350.0	47746	-69.29
14	10	77	918	5950.00	348.0	47771	-38.73
14	10	77	919	5972.50	346.0	47817	8.22
14	10	77	920	5989.00	344.0	47773	-30.41
14	10	77	921	6005.50	342.0	47761	-49.63
14	10	77	922	6022.00	340.0	47779	-31.65
14	10	77	924	6038.50	339.0	47695	-117.67
14	10	77	923	6055.00	337.0	47681	-130.79
14	10	77	925	6038.00	335.0	47598	-214.72
14	10	77	925	6090.20	333.0	47653	-159.76
14	10	77	927	6100.30	331.0	47720	-94.66
14	10	77	926	6104.40	329.0	47827	12.60
14	10	77	928	6108.50	328.0	47783	-30.51
14	10	77	929	6112.60	326.0	47655	-158.70
14	10	77	928	6116.70	324.0	47616	-137.56
14	10	77	929	6120.80	322.0	47591	-222.74
14	10	77	932	6123.30	320.0	47566	-229.06
14	10	77	930	6125.00	318.0	47578	-236.35
14	10	77	930	6129.10	316.0	47566	-248.36
14	10	77	933	6137.30	315.0	47614	-201.49
14	10	77	935	6141.40	313.0	47718	-97.69
14	10	77	934	6145.50	311.0	47838	23.70
14	10	77	935	6149.50	309.0	47770	-45.73
14	10	77	936	6153.70	307.0	47656	-161.18
14	10	77	937	6157.80	306.0	47526	-295.66
14	10	77	937	6161.90	304.0	47466	-335.68
14	10	77	936	6166.00	303.0	47506	-313.40
14	10	77	938	6170.10	301.0	47531	-290.43
14	10	77	939	6174.20	300.0	47536	-263.14
14	10	77	939	6178.30	298.0	47553	-266.16
14	10	77	940	6182.40	296.0	47592	-227.42
14	10	77	949	6186.20	295.0	47628	-138.57
14	10	77	950	6196.40	293.0	47647	-169.99
14	10	77	950	6204.60	292.0	47618	-199.63
14	10	77	951	6221.10	291.0	47599	-218.08
14	10	77	952	6237.60	289.0	47590	-227.15
14	10	77	953	6254.10	287.0	47574	-241.16
14	10	77	954	6262.30	288.0	47555	-263.26
14	10	77	954	6270.50	286.0	47435	-361.33
14	10	77	955	6278.70	284.0	47247	-567.91
14	10	77	956	6282.80	282.0	47233	-582.66
14	10	77	956	6286.90	280.0	47354	-421.66
14	10	77	957	6291.00	278.0	47596	-220.42
14	10	77	958	6295.10	276.0	47676	-139.17
14	10	77	958	6299.20	275.0	47791	-26.19
30	10	77	773	7260.00	216.0	47064	-724.19
30	10	77	777	7265.00	217.0	47031	-753.33
30	10	77	771	7270.00	219.0	47004	-779.69
30	10	77	771	7275.00	220.0	46961	-862.91
30	10	77	770	7279.00	220.0	46940	-842.96
30	10	77	769	7284.00	219.0	47039	-743.04
30	10	77	768	7289.00	217.0	47093	-663.16
30	10	77	767	7294.00	216.0	47123	-557.17
30	10	77	766	7298.50	215.0	47146	-633.21

Line 4 contd.

Date	Time minutes	Distance from origin-metres	Height metres	Reading gamma	Anomaly gamma		
30	10	77	766	7299.00	216.0	47168	-611.23
30	10	77	765	7301.50	216.0	47216	-562.28
30	10	77	765	7304.00	216.0	47241	-537.30
30	10	77	764	7309.00	218.0	47297	-460.35
30	10	77	764	7319.00	219.0	47360	-417.41
30	10	77	763	7339.00	220.0	47411	-365.56
30	10	77	762	7359.00	222.0	47449	-326.71
30	10	77	762	7379.00	223.0	47479	-296.82
30	10	77	760	7399.00	224.0	47506	-266.60
30	10	77	790	7426.00	224.0	47569	-221.24
30	10	77	793	7456.00	225.0	47610	-161.22
30	10	77	797	7505.00	226.0	47630	-162.67
30	10	77	800	7595.00	223.0	47489	-305.42
30	10	77	802	7660.00	221.0	47567	-226.14
30	10	77	809	7710.00	218.0	47514	-280.53
30	10	77	816	7780.00	223.0	47441	-356.59
30	10	77	820	7805.00	230.0	47425	-371.24
30	10	77	822	7895.00	243.0	47506	-291.63
30	10	77	828	7970.00	253.0	47546	-256.71
30	10	77	830	8056.00	267.0	47559	-243.59
30	10	77	832	8150.00	272.0	47560	-240.55
30	10	77	835	8205.00	270.0	47553	-245.16
30	10	77	838	8290.00	269.0	47699	-162.66
30	10	77	842	8400.00	264.0	47774	-34.21
30	10	77	845	8490.00	267.0	47633	25.14
30	10	77	847	8610.00	264.0	47851	43.63
30	10	77	850	8710.00	260.0	47911	101.54
30	10	77	853	8807.00	256.0	47929	116.95
30	10	77	855	8907.00	254.0	48105	350.70
30	10	77	861	8970.00	253.0	47983	147.96
30	10	77	863	9075.00	249.0	47977	161.37
30	10	77	865	9205.00	247.0	47979	161.74
30	10	77	872	9325.00	240.0	47965	144.22
30	10	77	874	9425.00	236.0	47962	160.49
30	10	77	877	9555.00	215.0	47974	143.36
30	10	77	884	9665.00	218.0	47965	143.46
30	10	77	891	9785.00	221.0	47985	156.99
30	10	77	897	9785.00	223.0	47961	124.73
30	10	77	906	9830.00	227.0	47946	116.33
30	10	77	911	9895.00	236.0	47949	117.57
30	10	77	914	10012.00	233.0	47935	94.86
30	10	77	923	10125.00	223.0	47915	95.64
30	10	77	930	10260.00	215.0	47917	73.66
30	10	77	932	10465.00	206.0	47914	68.40
30	10	77	934	10525.00	201.0	47914	64.65



Data describing the ground traverse along Line 5

Date	Time minutes	Distance from origin-metres	Height metres	Reading gamma	Anomaly gamma
10 10 77	795	0.0	532.0	47739	-47.59
10 10 77	795	95.00	529.0	47741	-61.70
10 10 77	796	155.00	523.0	47743	-43.42
10 10 77	800	210.00	516.0	47740	-46.66
10 10 77	801	295.00	507.0	47745	-45.66
10 10 77	803	360.00	496.0	47741	-45.71
10 10 77	804	430.00	486.0	47742	-45.15
10 10 77	807	490.00	476.0	47739	-46.57
10 10 77	807	610.00	453.0	47739	-49.12
10 10 77	808	670.00	443.0	47753	-51.96
10 10 77	809	750.00	435.0	47735	-55.39
10 10 77	816	840.00	424.0	47736	-55.10
10 10 77	821	930.00	419.0	47734	-59.62
10 10 77	826	1010.00	415.0	47734	-60.51
10 10 77	830	1055.50	415.0	47731	-65.92
10 10 77	834	1061.00	414.0	47696	-59.25
10 10 77	839	1080.50	413.0	47733	-62.62
10 10 77	856	1112.00	413.0	47725	-71.05
10 10 77	860	1137.50	412.0	47724	-73.93
10 10 77	863	1163.00	412.0	47717	-62.77
10 10 77	867	1186.50	411.0	47717	-63.51
10 10 77	900	1250.00	412.0	47708	-102.95
10 10 77	905	1290.00	412.0	47722	-90.86
10 10 77	905	1310.00	412.0	47736	-76.94
10 10 77	905	1320.00	413.0	47755	-57.96
10 10 77	906	1340.00	413.0	47767	-46.22
10 10 77	907	1390.00	414.0	47761	-52.96
10 10 77	910	1440.00	414.0	47807	-5.60
10 10 77	915	1490.00	415.0	47740	-75.61
10 10 77	915	1500.00	415.0	47780	-35.49
10 10 77	916	1501.00	416.0	47791	-24.26
10 10 77	917	1502.00	416.0	47800	-14.35
10 10 77	920	1503.00	416.0	47810	-6.28
10 10 77	921	1504.00	417.0	47820	3.60
10 10 77	922	1505.00	417.0	47839	22.67
10 10 77	923	1506.00	418.0	47856	39.94
10 10 77	923	1507.00	418.0	47879	62.93
10 10 77	924	1508.00	419.0	47898	82.01
10 10 77	925	1509.00	419.0	47951	135.09
10 10 77	925	1510.00	420.0	48044	226.06
10 10 77	926	1511.00	420.0	48160	344.16
10 10 77	926	1522.00	420.0	48296	480.12
10 10 77	926	1523.00	421.0	48412	596.11
10 10 77	927	1524.00	421.0	48571	755.16
10 10 77	927	1525.00	422.0	48686	870.16
10 10 77	926	1526.00	422.0	48761	965.26
10 10 77	928	1527.00	423.0	48786	972.25
10 10 77	928	1528.00	423.0	48751	955.25
10 10 77	929	1529.00	423.0	48451	655.32
10 10 77	929	1530.00	424.0	48624	206.32
10 10 77	929	1531.00	424.0	47465	-350.66
10 10 77	930	1532.00	425.0	47046	-769.96
10 10 77	930	1533.00	425.0	46725	-1050.96
10 10 77	930	1534.00	426.0	46526	-1269.91
10 10 77	932	1535.00	427.0	46521	-1293.67
10 10 77	932	1536.00	427.0	46442	-1372.67
10 10 77	932	1537.00	428.0	46270	-1544.66
10 10 77	933	1538.00	428.0	45969	-1936.16
10 10 77	933	1539.00	429.0	45750	-2007.11

Line 5 contd.

Date	Time minutes	Distance from origin-metres	Height metres	Reading gamma	Anomaly gamma		
10	10	77	933	1540.00	430.0	45567	-2250.11
10	10	77	939	1540.50	430.0	45385	-2461.67
10	10	77	940	1541.00	430.0	45798	-2018.92
10	10	77	941	1541.50	429.0	46038	-1777.10
10	10	77	941	1542.00	427.0	46601	-1214.10
10	10	77	941	1542.50	426.0	47533	-282.10
10	10	77	942	1543.00	424.0	47665	-130.20
10	10	77	943	1543.50	423.0	47767	-48.45
10	10	77	944	1544.00	421.0	47806	-10.29
10	10	77	944	1544.50	420.0	47795	-20.29
10	10	77	944	1545.00	418.0	47785	-31.29
10	10	77	945	1545.50	416.0	47620	-156.42
10	10	77	945	1546.00	415.0	47500	-316.43
10	10	77	945	1547.00	413.0	47385	-431.43
10	10	77	947	1548.00	412.0	47299	-519.11
10	10	77	948	1553.00	410.0	47260	-557.52
10	10	77	949	1556.00	408.0	47541	-272.77
10	10	77	949	1555.00	405.0	47754	-59.79
10	10	77	950	1568.00	402.0	47458	-318.72
10	10	77	952	1571.00	399.0	47277	-538.45
10	10	77	952	1573.00	397.0	46368	-947.44
10	10	77	954	1574.00	395.0	46939	-677.74
10	10	77	954	1576.00	393.0	46233	-1585.75
10	10	77	955	1577.00	391.0	46020	-1794.74
10	10	77	955	1578.00	389.0	45927	-1867.74
10	10	77	956	1579.00	387.0	45914	-1900.57
10	10	77	956	1580.00	385.0	46000	-1814.58
10	10	77	957	1581.00	383.0	46096	-1716.41
10	10	77	957	1582.00	381.0	46278	-1556.41
10	10	77	958	1583.00	379.0	46514	-1257.82
10	10	77	958	1584.00	377.0	46676	-1155.82
10	10	77	959	1585.00	375.0	46791	-1021.34
10	10	77	960	1586.00	373.0	46913	-901.83
10	10	77	960	1587.00	372.0	47012	-802.83
10	10	77	960	1588.00	369.0	47065	-749.84
10	10	77	961	1589.00	398.0	47126	-688.17
10	10	77	961	1590.00	396.0	47202	-612.18
10	10	77	961	1591.00	364.0	47245	-569.18
10	10	77	962	1592.00	361.0	47286	-527.01
10	10	77	962	1594.00	360.0	47341	-472.02
10	10	77	963	1601.00	358.0	47390	-423.06
10	10	77	963	1603.00	356.0	47467	-326.06
10	10	77	964	1611.00	355.0	47565	-228.13
10	10	77	965	1616.00	355.0	47627	-186.18
10	10	77	965	1621.00	354.0	47636	-775.20
10	10	77	965	1626.00	353.0	47626	-193.22
10	10	77	966	1636.00	353.0	47571	-242.28
10	10	77	967	1640.00	352.0	47520	-253.35
10	10	77	968	1650.00	352.0	47514	-299.75
10	10	77	968	1660.00	351.0	47459	-353.67
10	10	77	968	1670.00	350.0	47594	-416.71
10	10	77	968	1680.00	350.0	47355	-477.75
10	10	77	967	1691.00	349.0	47415	-397.95
10	10	77	967	1696.00	348.0	47480	-332.98
10	10	77	967	1700.00	348.0	47531	-276.02
10	10	77	969	1716.00	347.0	47574	-239.93
10	10	77	969	1720.00	347.0	47589	-224.83
10	10	77	969	1730.00	346.0	47643	-171.56
10	10	77	969	1740.00	345.0	47660	-155.72
10	10	77	969	1750.00	345.0	47695	-120.76

Line 5 contd.

Date	Time minutes	Distance from origin-metres	Height metres	Reading gamma	Anomaly gamma		
10	10	77	993	1770.00	344.0	47739	-75.32
10	10	77	994	1790.00	344.0	47732	-83.19
10	10	77	995	1810.00	343.0	47685	-130.67
10	10	77	995	1830.00	352.0	47601	-134.70
10	10	77	996	1850.00	351.0	47673	-144.67
10	10	77	996	1870.00	351.0	47659	-158.75
10	10	77	997	1900.00	350.0	47659	-158.59
10	10	77	998	1940.00	349.0	47667	-150.91
10	10	77	999	1990.00	349.0	47715	-103.27
10	10	77	1000	2040.00	340.0	47759	-39.62
10	10	77	1006	2150.00	335.0	47735	-84.14
10	10	77	1009	2200.00	323.0	47724	-95.40
10	10	77	1012	2250.00	315.0	47757	-62.67
10	10	77	1014	2350.00	300.0	47735	-85.19
10	10	77	1015	2400.00	289.0	47590	-230.79
10	10	77	1017	2550.00	269.0	47599	-222.24
10	10	77	1020	2630.00	252.0	47583	-238.65
10	10	77	1022	2710.00	249.0	47647	-175.67
10	10	77	1025	2800.00	240.0	47579	-245.57
21	10	77	915	2990.00	207.0	47370	-444.40
21	10	77	917	3030.00	207.0	47343	-468.82
21	10	77	919	3075.00	190.0	47336	-474.57
21	10	77	922	3150.00	184.0	47332	-481.18
21	10	77	927	3200.00	186.0	47327	-488.60
21	10	77	932	3250.00	187.0	47429	-395.25
21	10	77	938	3310.00	189.0	47372	-442.41
21	10	77	944	3350.00	190.0	47242	-572.76
21	10	77	948	3500.00	201.0	47409	-225.89
21	10	77	947	3550.00	210.0	47615	-260.83
21	10	77	952	3650.00	226.0	47260	-555.26
29	10	77	704	3830.00	238.0	47475	-323.72
29	10	77	717	4120.00	207.0	47622	-176.65
29	10	77	719	4250.00	207.0	47672	-126.60
29	10	77	722	4340.00	190.0	47911	112.21
29	10	77	725	4450.00	184.0	47800	0.37
29	10	77	727	4500.00	180.0	47941	139.72
29	10	77	735	4650.00	187.0	47943	141.77
29	10	77	762	4750.00	189.0	47989	183.72
29	10	77	763	4764.00	190.0	47965	162.00
29	10	77	757	4778.00	201.0	47997	190.90
29	10	77	761	4792.00	210.0	48011	208.94
29	10	77	761	4806.00	226.0	48012	207.91
29	10	77	762	4820.00	238.0	48025	219.40
29	10	77	763	4834.00	240.0	48030	228.69
29	10	77	767	4837.00	240.0	48037	234.49
29	10	77	768	4840.00	243.0	48040	237.06
29	10	77	768	4841.50	253.0	48040	243.06
29	10	77	769	4845.00	254.0	48071	269.34
29	10	77	769	4844.50	254.0	48068	266.33
29	10	77	770	4845.00	254.0	48069	268.06
29	10	77	770	4846.50	255.0	47965	162.06
29	10	77	773	4864.50	256.0	48023	213.06
29	10	77	766	4865.00	256.0	48040	226.27
29	10	77	779	4880.00	256.0	48119	307.21
29	10	77	782	4940.00	255.0	48153	340.63
29	10	77	784	5040.00	249.0	48085	271.17
29	10	77	787	5290.00	233.0	48056	250.65
29	10	77	789	5370.00	235.0	48071	255.40
29	10	77	791	5475.00	238.0	48071	263.24
29	10	77	794	5570.00	238.0	48041	229.45
29	10	77	807	5690.00	236.0	47988	152.45
29	10	77	804	6100.00	229.0	47915	79.78
29	10	77	802	6250.00	229.0	47885	53.34
29	10	77	857	6400.00	222.0	47876	48.63
29	10	77	820	6585.00	220.0	47676	-122.35
29	10	77	850	6710.00	216.0	47727	-94.53

Data describing the traverse along Line 6

Date	Time minutes	Distance from origin-metres	Height metres	Reading gamma	Anomaly gamma		
8	10	77	971	0.0	446.0	47736	-83.34
8	10	77	970	100.00	449.0	47737	-81.32
8	10	77	967	200.00	453.0	47734	-84.23
8	10	77	966	290.00	455.0	47732	-86.52
8	10	77	965	380.00	456.0	47730	-82.57
8	10	77	963	480.00	456.0	47732	-87.29
8	10	77	960	580.00	456.0	47711	-108.06
8	10	77	959	690.00	456.0	47735	-84.32
8	10	77	945	820.00	461.0	47729	-91.29
8	10	77	942	890.00	468.0	47726	-95.36
8	10	77	935	960.00	453.0	47722	-98.36
8	10	77	932	1050.00	438.0	47723	-97.51
8	10	77	930	1110.00	424.0	47725	-96.09
8	10	77	928	1190.00	405.0	47716	-103.39
8	10	77	926	1270.00	400.0	47720	-101.69
8	10	77	924	1350.00	390.0	47715	-106.95
8	10	77	920	1420.00	383.0	47729	-92.33
8	10	77	916	1540.00	378.0	47709	-112.89
8	10	77	915	1740.00	375.0	47791	-31.36
8	10	77	906	1880.00	368.0	47994	172.56
8	10	77	900	2000.00	361.0	47705	-117.43
8	10	77	899	2090.00	376.0	47680	-142.29
8	10	77	896	2200.00	384.0	47611	-211.47
8	10	77	888	2305.00	384.0	47262	-533.63
8	10	77	889	2315.00	381.0	47453	-363.89
8	10	77	890	2325.00	366.0	47578	-239.94
8	10	77	891	2335.00	363.0	47636	-160.99
8	10	77	884	2370.00	360.0	47703	-116.11
8	10	77	880	2460.00	356.0	47723	-91.96
8	10	77	879	2560.00	353.0	47679	-136.72
8	10	77	873	2700.00	346.0	47654	-160.55
8	10	77	864	2800.00	350.0	47632	-179.59
8	10	77	854	2855.00	315.0	47546	-260.51
8	10	77	834	3060.00	303.0	47475	-324.35
8	10	77	830	3100.00	298.0	47547	-256.41
8	10	77	814	3200.00	287.0	47656	-144.36
8	10	77	810	3300.00	279.0	47503	-257.37
8	10	77	806	3400.00	264.0	47551	-249.02
8	10	77	805	3500.00	246.0	47576	-223.02
8	10	77	799	3600.00	219.0	47704	-97.01
8	10	77	772	3650.00	204.0	47656	-144.16
8	10	77	760	3780.00	192.0	47746	-55.74
8	10	77	751	3800.00	180.0	47782	-16.67
19	10	77	352	4100.00	172.0	47776	-37.46
19	10	77	656	4220.00	172.0	47736	-60.06
19	10	77	659	4290.00	172.0	47681	-144.93
19	10	77	662	4330.00	189.0	47642	-165.94
19	10	77	664	4420.00	206.0	47612	-215.76
19	10	77	666	4470.00	216.0	47601	-229.72
19	10	77	669	4486.00	223.0	47545	-285.15
19	10	77	370	4492.00	226.0	47512	-317.64
19	10	77	667	4510.00	227.0	47495	-336.37
19	10	77	671	4526.00	225.0	47413	-416.16
19	10	77	672	4552.00	220.0	47392	-455.65
19	10	77	660	4560.00	216.0	47397	-426.13
19	10	77	666	4600.00	216.0	47415	-464.51
19	10	77	669	4635.00	217.0	47467	-350.22
19	10	77	668	4670.00	209.0	47529	-267.65
19	10	77	667	4705.00	207.0	47561	-255.06

Line 6 contd.

Date	Time minutes	Distance from origin-metres	Height metres	Reading gamma	Anomaly gamma		
19	10	77	895	4715.00	206.0	47625	-194.34
19	10	77	907	4720.00	204.0	47657	-164.70
19	10	77	900	4730.00	203.0	47716	-105.92
19	10	77	905	4735.00	202.0	47744	-78.05
19	10	77	903	4745.00	200.0	47784	-58.33
19	10	77	902	4765.00	200.0	47829	6.50
19	10	77	999	4765.00	198.0	47800	37.07
19	10	77	909	4790.00	196.0	47870	48.35
19	10	77	910	4800.00	190.0	47850	75.50
19	10	77	912	4810.00	195.0	47927	104.40
19	10	77	912	4820.00	194.0	47949	120.47
19	10	77	913	4830.00	193.0	47971	149.12
19	10	77	914	4840.00	223.0	47987	165.77
19	10	77	919	4870.00	225.0	48019	203.50
19	10	77	922	4890.00	223.0	48034	219.03
19	10	77	923	4910.00	231.0	48103	287.95
19	10	77	924	4930.00	233.0	48121	305.85
19	10	77	925	4950.00	236.0	48132	316.75
19	10	77	927	4970.00	236.0	48151	335.14
19	10	77	927	4980.00	235.0	48153	337.05
19	10	77	937	5010.00	234.0	48175	357.00
19	10	77	930	5040.00	233.0	48183	364.78
19	10	77	939	5080.00	232.0	48104	345.52
19	10	77	943	5120.00	230.0	48169	350.32
19	10	77	945	5150.00	230.0	48194	375.04
19	10	77	951	5160.00	229.0	48195	376.02
19	10	77	952	5190.00	227.0	48193	373.55
19	10	77	953	5220.00	226.0	48190	370.00
19	10	77	955	5250.00	224.0	48177	357.01
19	10	77	955	5280.00	223.0	48171	351.74
19	10	77	957	5310.00	221.0	48163	343.06
19	10	77	958	5340.00	220.0	48151	331.59
19	10	77	959	5382.00	220.0	48141	321.51
19	10	77	962	5420.00	223.0	48120	300.42
19	10	77	967	5480.00	226.0	48075	255.29
19	10	77	972	5510.00	230.0	48082	262.22
19	10	77	974	5535.00	234.0	48066	260.10
19	10	77	975	5575.00	238.0	48060	240.07
19	10	77	976	5600.00	240.0	48053	233.01
19	10	77	977	5550.00	239.0	48042	221.90
19	10	77	990	5940.00	230.0	47950	126.55
19	10	77	1001	6060.00	217.0	47958	136.53
19	10	77	1004	6150.00	206.0	47927	105.21
19	10	77	1005	6240.00	195.0	47910	87.89
19	10	77	1007	6315.00	192.0	47901	78.65
19	10	77	1011	6400.00	200.0	47897	74.52
19	10	77	1024	6440.00	203.0	47911	80.16
19	10	77	1026	6540.00	203.0	47899	75.85
19	10	77	1030	6605.00	200.0	47883	59.39
19	10	77	1034	6700.00	193.0	47893	69.20
19	10	77	1037	6790.00	184.0	47871	46.55
19	10	77	1040	6900.00	172.0	47860	61.50

LINE 1: Data describing the aerial traverse

	Distance from origin-metres	Anomaly gamma
1	0.0	-140
2	102.4	-150
3	256.0	-155
4	448.0	-150
5	563.2	-140
6	665.6	-130
7	716.8	-120
8	742.4	-110
9	768.0	-100
10	793.6	-90
11	832.0	-80
12	844.8	-70
13	883.2	-60
14	921.6	-50
15	972.8	-40
16	998.4	-30
17	1024.0	-20
18	1049.6	-10
19	1088.0	0
20	1113.6	10
21	1139.2	20
22	1177.6	30
23	1241.6	30
24	1267.2	20
25	1292.8	10
26	1318.4	0
27	1356.8	-10
28	1433.6	-20
29	1561.6	-30
30	1702.4	-25
31	1779.2	-30
32	1830.4	-40
33	1868.8	-50
34	1894.4	-60
35	1920.0	-70
36	1945.6	-80
37	1996.8	-90
38	2086.4	-95
39	2176.0	-90
40	2252.8	-80
41	2432.0	-70
42	2508.8	-60
43	2585.6	-50
44	2739.2	-40
45	2841.6	-30
46	2931.2	-20
47	3123.2	-10
48	3430.4	0

END CF FILE

LINE 2 Data describing the aerial traverse.

	Distance from origin-metres	Anomaly gamma
1	0.0	-38
2	1590.4	-40
3	1846.4	-50
4	2000.0	-60
5	2102.4	-70
6	2204.8	-80
7	2256.0	-90
8	2307.2	-100
9	2435.2	-150
10	2588.8	-200
11	2665.6	-150
12	2768.0	-100
13	2793.6	-90
14	2819.2	-80
15	2832.0	-70
16	2921.6	-60
17	2998.4	-60
18	3075.2	-70
19	3152.0	-80
20	3228.8	-90
21	3280.0	-100
22	3395.2	-110
23	3433.6	-120
24	3472.0	-130
25	3484.8	-140
26	3548.8	-150
27	3587.2	-160
28	3612.8	-170
29	3753.6	-170
30	3779.2	-160
31	3817.6	-150
32	3881.6	-100
33	3920.0	-90
34	3945.6	-80
35	3996.8	-70
36	4035.2	-60
37	4176.0	-55

END OF FILE

LINE 3 Data describing the aerial traverse

Distance from Anomaly  
origin-metres gamma

1	0.0	-42
2	80.0	-40
3	1979.2	-30
4	2811.2	-30
5	3220.8	-40
6	3707.2	-50
7	3899.2	-60
8	3988.8	-60
9	4052.8	-50
10	4168.0	-50
11	4244.8	-60
12	4296.0	-70
13	4347.2	-80
14	4552.0	-90
15	4833.6	-100
16	5012.8	-110
17	5140.8	-115
18	5281.6	-110
19	5704.0	-110
20	5998.4	-120
21	6292.8	-130
22	6484.8	-120
23	6638.4	-110
24	6702.4	-100
25	6858.0	-50
26	6932.8	0
27	7035.2	50
28	7150.4	100
29	7188.8	110
30	7227.2	120
31	7265.6	130
32	7318.8	140
33	7393.6	150
34	7624.0	155
35	7680.0	150
36	8110.4	140
37	8340.8	130
38	8622.4	120
39	8878.4	110
40	9236.8	100
41	9492.8	90

END OF FILE



LINE 4 Data describing the aerial traverse

	Distance from origin-metres	Anomaly gamma
1	0.0	-49
2	209.2	-40
3	1621.2	-30
4	4053.2	-30
5	4834.0	-40
6	5333.2	-50
7	5384.4	-60
8	5448.4	-70
9	5525.2	-80
10	5576.4	-90
11	5602.0	-100
12	5678.8	-110
13	5730.0	-120
14	5768.4	-130
15	5806.8	-140
16	5832.4	-150
17	5909.2	-150
18	5934.8	-140
19	5973.2	-130
20	6024.4	-120
21	6114.0	-110
22	6242.0	-110
23	6318.8	-120
24	6370.0	-130
25	6395.6	-140
26	6421.2	-150
27	6498.0	-200
28	6562.0	-250
29	6615.2	-300
30	6677.2	-350
31	6754.0	-400
32	6856.4	-400
33	6958.8	-350
34	7010.0	-300
35	7086.8	-250
36	7112.4	-240
37	7150.8	-230
38	7240.4	-220
39	7368.4	-210
40	7496.4	-210
41	7650.0	-215
42	7776.0	-210
43	7854.8	-210
44	7957.2	-180
45	8034.0	-150
46	8187.6	-100
47	8290.0	-50
48	8443.6	0
49	8546.0	50
50	8622.8	100
51	8661.2	110
52	8725.2	120
53	8776.4	130
54	8840.4	140
55	8891.6	150
56	9006.8	160
57	9314.0	170
58	9749.2	160
59	9902.8	150
60	10018.0	140
61	10146.0	130
62	10312.4	120
63	10517.2	110
64	10594.0	105

ENC CF FILE

LINE 5 Data describing the aerial traverse

	Distance from origin-metres	Anomaly gamma
1	0.0	-30
2	356.8	-30
3	779.2	-40
4	1114.0	-48
5	1265.6	-40
6	1580.8	-30
7	1457.6	-40
8	1483.2	-50
9	1565.6	-80
10	1662.4	-100
11	1688.0	-110
12	1752.0	-112
13	1816.0	-110
14	1867.2	-100
15	1918.4	-80
16	1969.6	-70
17	2059.2	-70
18	2110.4	-90
19	2148.8	-100
20	2187.2	-110
21	2212.8	-120
22	2251.2	-130
23	2289.6	-140
24	2315.2	-150
25	2430.4	-200
26	2507.2	-225
27	2635.2	-250
28	2673.6	-275
29	2763.2	-300
30	2993.6	-350
31	3275.2	-360
32	3582.4	-250
33	3736.0	-230
34	3851.2	-200
35	3940.8	-180
36	4043.2	-150
37	4120.0	-130
38	4222.4	-100
39	4324.8	-50
40	4476.4	0
41	4542.4	50
42	4619.2	100
43	4670.4	150
44	4734.4	170
45	4798.4	200
46	4913.6	230
47	5016.0	250
48	5092.8	260
49	5259.2	260
50	5348.8	250
51	5464.0	230
52	5566.4	210
53	5630.4	200
54	5784.0	180
55	5912.0	160
56	6001.6	150
57	6193.6	130
58	6449.6	110
59	6603.2	100
60	6808.0	90
61	7115.2	80

ENC CP FILE

LINE 6 Data describing the aerial traverse

	Distance from origin-metres	Anomaly gamma
1	0.0	-30
2	932.4	-30
3	1380.4	-40
4	1495.6	-40
5	1521.2	-30
6	1649.2	-30
7	1777.2	-40
8	1854.0	-50
9	1905.2	-60
10	2058.8	-70
11	2186.8	-80
12	2263.6	-90
13	2314.8	-100
14	2366.0	-110
15	2404.4	-120
16	2442.8	-130
17	2468.4	-140
18	2506.8	-150
19	2545.2	-160
20	2570.8	-170
21	2596.4	-180
22	2622.0	-190
23	2647.6	-200
24	2750.0	-230
25	2814.0	-250
26	2942.0	-300
27	3070.0	-325
28	3210.8	-300
29	3326.0	-250
30	3415.6	-200
31	3518.0	-150
32	3594.8	-125
33	3658.8	-100
34	3761.2	-90
35	3812.4	-80
36	3978.8	-70
37	4286.0	-70
38	4490.8	-50
39	4580.4	0
40	4631.6	50
41	4682.8	100
42	4721.2	150
43	4798.0	200
44	4874.8	250
45	4951.6	280
46	5028.4	290
47	5079.6	300
48	5207.6	300
49	5271.6	290
50	5361.2	280
51	5412.4	270
52	5450.8	260
53	5489.2	250
54	5540.4	240
55	5591.6	230
56	5642.8	220
57	5694.0	210
58	5732.4	200
59	5770.8	190
60	5822.0	180
61	5873.2	170
62	5924.4	160
63	5988.4	150
64	6078.0	140
65	6167.6	130
66	6270.0	120
67	6410.8	110
68	6602.8	100
69	6820.4	90
70	7166.0	80

